

Title	重合初期段階における不均一系チーグラマー・ナッタ触媒の物理・化学的变化
Author(s)	Sumant, Dwivedi
Citation	
Issue Date	2014-06
Type	Thesis or Dissertation
Text version	ETD
URL	http://hdl.handle.net/10119/12229
Rights	
Description	Supervisor: 寺野 稔, マテリアルサイエンス研究科, 博士

**PHYSICAL AND CHEMICAL TRANSFORMATION IN
HETEROGENEOUS ZIEGLER-NATTA CATALYST AT
THE INITIAL STAGE OF POLYMERIZATION**

June 2014

SUMANT DWIVEDI

School of Materials Science

Japan Advanced Institute of Science and Technology

**PHYSICAL AND CHEMICAL TRANSFORMATION
IN HETEROGENEOUS ZIEGLER-NATTA
CATALYST AT THE INITIAL STAGE OF
POLYMERIZATION**

by

SUMANT DWIVEDI

**Submitted to
Japan Advanced Institute of Science and Technology
In partial fulfillment of the requirements
For the degree of
Doctor of Philosophy**

Supervisor: Professor Dr. Minoru Terano

School of Materials Science

Japan Advanced Institute of Science and Technology

June 2014

Referee-in-chief: **Professor Dr. Minoru Terano**
Japan Advanced Institute of Science and Technology

Referees: **Professor Dr. Masayuki Yamaguchi**
Japan Advanced Institute of Science and Technology

Associate Professor Dr. Toshiaki Taniike
Japan Advanced Institute of Science and Technology

Associate Professor Dr. Tatsuo Kaneko
Japan Advanced Institute of Science and Technology

Professor Dr. Koh-hei Nitta
Kanzawa University

Preface

The present dissertation is the result of the studies under the direction of Professor Dr. Minoru Terano during 2011-2014. The purpose of this dissertation is to understand the physical and chemical transformations in heterogeneous Ziegler-Natta (ZN) stopped-flow propylene polymerization responsible for the origin of macroscopic kinetics. The first chapter is consisted of general introduction to lead the objective of this research. Understanding chemical and physical transformations of ZN catalyst at initial stage of propylene polymerization kinetics: Key role of alkylaluminium in catalyst activation process represents the chapter 2. Role of external donor and hydrogen at the initial stage of Ziegler-Natta propylene polymerization has been discussed in chapter 3. Initial morphology and kinetics development in Ziegler-Natta catalyst studied through stopped-flow ethylene/propylene and 1-hexene/propylene copolymerization has been clarified in chapter 4. Finally, last chapter summarizes the general conclusions from this study.

Sumant Dwivedi

Terano Laboratory,

School of Materials Science,

Japan Advanced Institute of Science and Technology

May 2014

Contents

Chapter 1 General introduction	1
1.1 Polyolefin and Ziegler-Natta catalyst	2
1.2 History and development of stereospecific catalysts	4
1.3 Catalysts: Structure and Chemistry	8
1.3.1 $\text{TiCl}_4/\text{MgCl}_2$ Catalysts	8
1.3.2 Activator Chemistry	11
1.3.3 Catalyst Activator Interaction	13
1.3.4 Lewis Base Effects	15
1.4 Active sites and Polymerization Chemistry	18
1.4.1 Metal-Carbon Bond Formation	25
1.4.2 Regioselectivity	25
1.4.3 Chain Termination	26
1.4.4 Polymer Morphology	27
1.4.5 Copolymerization	30
1.5 Polymerization kinetics	31
1.6 Objective of this study	38

References	40
Chapter 2 Understanding chemical and physical transformation of Ziegler-Natta catalyst at initial stage of propylene polymerization kinetics: Key role of alkylaluminium in catalyst activation process	50
2.1 Introduction	51
2.2 Experimental	55
2.2.1 Materials	55
2.2.2 Catalyst synthesis	56
2.2.3 Propylene polymerization	56
2.2.4 Polymer analyses	58
2.3 Results and discussion	59
2.4 Conclusions	74
References	75
Chapter 3 Role of external donor and hydrogen at the initial stage of Ziegler-Natta propylene polymerization	79
3.1 Introduction	80
3.2 Experimental	83
3.2.1 Materials	83
3.2.2 Catalyst synthesis	83

3.2.3 Propylene polymerization	84
3.2.4 Polymer analyses	85
3.3 Results and discussion	85
3.4 Conclusions	94
References	95
Chapter 4 Initial morphology and kinetics development in Ziegler-Natta catalyst studied through stopped-flow ethylene/propylene and 1-hexene/propylene copolymerization	98
4.1 Introduction	99
4.2 Experimental	102
4.2.1 Materials	102
4.2.2 Catalyst synthesis	102
4.2.3 Homo- and co-polymerization	103
4.2.4 Polymer analyses	104
4.3 Results and discussion	105
4.4 Conclusions	117
References	118
Chapter 5 General conclusions	121

Achievements	vi
Acknowledgments	ix
Minor research theme	xi

Chapter 1
General Introduction

1. Introduction

1.1 Polyolefin and Ziegler-Natta catalyst

The great potential of polyolefin materials is confirmed by the fact that 80 years after their discovery, more than 100 Mt of this material have been produced in 2011 and catalyzed processes account for 70–80% of that total.^[1] The catalysts used for the olefin polymerization are chemically and physically complex structures. The active site upon which the polymer chains grow is most commonly obtained from a metal chloride (e.g. TiCl_4) in the case of Ziegler–Natta (ZN) catalysts^[2], a metal oxide (CrO_x) in the case of Phillips catalysts^[3], or a metallocene catalyst (metal linked to one or two cyclopentadienyl rings)^[4]. The molecular precursors can be used in solution to polymerize olefin, but are more often deposited on a highly porous solid support (typically MgCl_2 for ZN catalysts, or silica for the others)^[5], and the supported catalyst is often activated by the addition of an activator (e.g. alkylaluminium)^[6].

Polypropylenes, as well as polyethylene, are increasingly replacing other materials because of their versatile properties, low cost, reduced environmental impact, and easy recycling. The world demand for polypropylene jumped from 6.4 million metric tons in 1983 to 38.6 metric tons in 2004, with a growing rate as high as 5.8% from 2004 to 2009.^[7] Recent analyses predict that the world annual polypropylene production will increase from 52 metric tons in 2008 to 69.1 metric tons in 2013, and forecast an annual increase on polypropylene world demand by 3.7 % in the 2010-2013 timeframe.^[8] More than 90% of polypropylene has been produced by ZN catalysts.^[9]

ZN catalyst can be defined as a transition metal compound bearing a metal-carbon bond able to carry out a repeated insertion of olefin units. Usually, though not necessarily, the catalyst

consists of two components (i.e., transition metal salt (most frequently halide) and a main group metal alkyl (activator) which serves the purpose of generating the active metal-carbon bond.^[10]

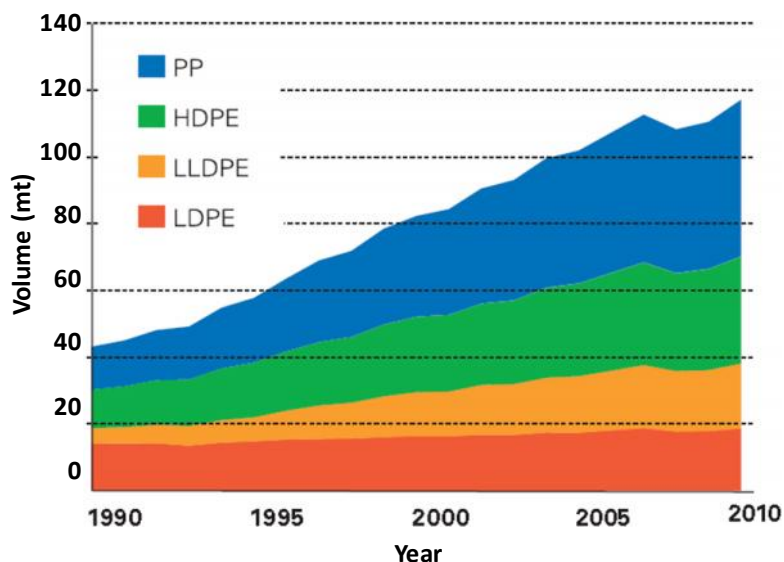


Figure 1 World polyolefin production.

It was Natta in 1954 who, following the previous discovery of Ziegler of the ability of $\text{TiCl}_4/\text{AlR}_3$ mixtures to polymerize ethylene, first succeeded in preparing polypropylene (PP) having an isotactic content around 30 to 50 % by using the same catalyst system.^[11] Natta realized that much higher isotactic yields (80 % to 90%) could be obtained by using crystalline TiCl_3 modification instead of soluble TiCl_4 .^[12] Since then the “isotactic” PP has become most important polyolefin plastics, and a huge amount of work has been done in both the industrial and the academic worlds to develop ever more efficient catalyst systems, as well as to elucidate the mechanisms by which the stereospecific polymerization is governed.

The aim of this chapter is to provide a short exhaustive description of the different catalysts which have been or are currently used for PP manufacturing as well as of the fundamental aspects related to the polymerization mechanisms, stereochemistry and kinetics.

1.2 History and development of the stereospecific catalysts

The development of various stereospecific catalysts is tremendous since the invention of the ZN catalysts. The exhaustive list can be broadly classified in six-generations.

1.2.1 First Generation Catalysts

The $\text{TiCl}_3/\text{AlEt}_2\text{Cl}$ catalyst used in the earlier industrial processes for the PP production showed low productivity and stereospecificity (i.e., the isotactic polymer or isotactic index (II in wt%)) being around only 90%.^[13] Consequently, both removal of the catalytic residues (deashing) and separation of the atactic polymer fraction were required.^[14]

Considering that in TiCl_3 only the surface Ti atoms, which represents only a small fraction of total Ti, were likely to be accessible to the alkylaluminium and thus available for making the active polymerization sites, several efforts were soon started to improve its efficiency. Three main approaches appear to have actually been followed to increase the fraction of the accessible Ti atoms:

- a. Reduction of the size of the catalytic microparticles (crystallites).
- b. Dispersion of Ti compounds on the high surface carriers,
- c. Use of soluble transition metal compounds.

1.2.2 Second Generation Catalysts

These catalysts, usually referred as “Solvay” TiCl_3 (development by Solvay), can be considered as the first example of the second generation catalysts for PP.^[15] These catalysts have much higher surface area than the usual AA- TiCl_3 (where AA stands for Al-reduced and activated), a five-fold productivity and an II around 95 %.^[16]

1.2.3 Third Generation Catalysts

Attempts to develop supported catalysts started very early in the 60's by making use of conventional high surface area supports bearing surface functional groups able to chemically anchor the transition metal compound. These attempts, however, though leading in some cases to highly active catalysts for polyethylene (PE), were not very successful for the PP (because of their low activity) until the discovery of the catalysts based on the “activated” MgCl_2 were active for PE as well for PP.^[17] Due to the low II the use of this catalyst was limited to the PE only. However, this problem was overcome by the addition of the appropriate Lewis base which made it possible to obtain highly active and stereospecific catalysts by co-milling MgCl_2 , TiCl_4 and a Lewis base, usually referred to as “internal donor” (D_i)^[18], combined with the alkylaluminium as activator and second Lewis base, usually called “external donor” (D_e)^[19].

MgCl_2 -supported and donor modified catalyst is the parent of a large family of catalysts which have been called the third generation. Though sufficiently active to avoid the need for deashing, these catalysts still required the removal of the atactic polymer which varies from 6 % to 10 %.^[20]

1.2.4 Fourth Generation Catalysts

The highly active and stereospecific catalysts known as super high activity catalysts (SHAC), which, though still making use of benzoic acid esters as electron donors, were claimed to display a superior productivity and the isotacticity.^[21] In the early of 80's, the high level of isotacticity was achieved by discovery of new combination of electron donors, namely alkylphthalates as D_i and alkoxy silane (or silyl ethers) as D_e, able to afford much better productivity and isotacticity balance than the benzoic acid esters.^[22] These catalysts are known as fourth generation catalysts.

1.2.5 Fifth Generation Catalysts

In the second half of 80's, a new type of the electron donor was discovered (1, 3-diethers) which, if used as internal components, provided extremely high activities and isotacticities without the need of any external Lewis base.^[23] These catalysts, though not yet brought into the industrial use, potentially form the new class of catalysts for the PP production and known as fifth generation catalysts.

1.2.6 Sixth Generation Catalysts-Metallocenes

The approach to the homogeneous stereospecific catalysts, which has proved disappointing for many years, began to advance with the discovery of stereorigid metallocenes of transition metals, such as Zr and Hf, when combined with methylaluminoxane (MAO), were able to polymerize PP with high yields and stereoregularity.^[24] The discovery aroused an enormous

interest in both industrial and academic worlds, not only because of its scientific value but also because it appears to open the way to materials with unprecedented properties. These classes of catalysts can be classified as the sixth generation of catalysts.

These generations of catalysts can be summarized as shown in the Table 1.

Table 1 Various generation of ZN catalysts and their characteristics.

Generation	Composition	Activity ^a (Kg•PP/g Cat)	II (wt%)	Morphology control	Process requirements
1 st	-TiCl ₃ 0.33AlCl ₃ + DEAC	0.8-1.2	90-94	not possible ^b	deashing + atactic removal
2 nd	-TiCl ₃ + DEAC	3-5 (10-15)	94-97	possible	Deashing
3 rd	TiCl ₄ /Ester/MgCl ₂ + AlR ₃ /Ester	5-10 (15-30)	90-95	possible	Atactic removal
4 th	TiCl ₄ /Diester/MgCl ₂ + TEA/Silane	10-25 (30-60)	95-99	possible	-
5 th	TiCl ₄ /Diether/MgCl ₂ + TEA	25-35 (70-120)	95-99	possible	-
6 th	Zirconocene + MAO	(5-9•10 ³) (Zr) ^c	90-99 ^d	to be achieved	-

a

Polymerization: hexane slurry, 70 °C, 0.7 MPa, 4 h, H₂ for molecular weight (MW) control (values in bracket are for bulk polymerization for 2h at 70 °C with hydrogen).

^b Only possible with alkylaluminium reduced TiCl₃, at 200-300 m size level.

^c 1 h polymerization time

^d mmmm % (by ¹³ C NMR)

1.3 Catalysts: Structure and Chemistry

We will primarily discuss the catalyst structure and chemistry of the MgCl_2 -based ZN catalyst due to their great importance in industry as well as in academia.

1.3.1 $\text{TiCl}_4/\text{MgCl}_2$ Catalysts

MgCl_2 is used as the support in ZN catalyst because it has similar crystal structure with TiCl_3 , which makes it easy to bear the catalyst site on its surface. There are two crystalline structures are known for MgCl_2 , the commercial α -form and the less stable β form. According to Natta, the violet α , β and γ modifications display a layer structure arising from regular stacking of structural Cl-Ti-Cl triple layers containing Ti atoms between two layers of Cl ions.^[25] The three modifications differ in the mode of Cl packing, which is hexagonal in α form and cubic in the β form.^[26] On the other hand, the γ form displays a random succession of the hexagonal and cubic close packing.^[27] The brown δ modification, on the contrary, exhibits a fibre like structure. Similar to the β - TiCl_3 , the α -form has a layer structure of the CdCl_2 type and shows a cubic close-packed stacking (ABC...ABC...) of double chlorine layers with interstitial Mg^{2+} ions in six-fold coordination.^[28] The β -form, on the contrary, shows a hexagonal close packing like that of α - TiCl_3 .^[26] However, in the catalysts we are concerning to, MgCl_2 exists in the “highly activated” form, namely γ - MgCl_2 , which exhibits a disordered structure arising from the translation and rotation of the structural Cl-Mg-Cl layers with respect to one another.^[29] As a consequence, the X-ray spectrum shows a gradual disappearance of the (104) reflection and its replacement by a broad “halo” centered at $d = 2.65 \text{ \AA}$ (i.e., in an intermediate position between the cubic (2.56 \AA) and the hexagonal (2.78 \AA) close packing). Zannetti *et al.* proposed the

models to explain for the structural disorder of MgCl_2 , based on a stochastic succession of structural layers still remaining a close parking of the Cl ions.^[30] In these models, the sequence between two structural layers was described by three probability numbers: P_{cub} , P_{hex} and $P_{\text{rot}}(+/-60)$ (their sum being 1). The crystallite sizes along the crystallographic directions were also expressed with three parameters: N_a , N_b , N_c . These facts were in line with the experimental evidences and reveals that the extremely activated MgCl_2 could be considered as made up of very small lamellae with a thickness close to just one structural layer ($N_c \sim 1$)

A typical $\text{TiCl}_4/\text{MgCl}_2$ catalyst is prepared in four main temperature-controlled steps: digestion, activation, washing, and drying. The digestion step includes the reaction of an organo-magnesium, $\text{Mg}(\text{OR})_2$, compound, TiCl_4 , and an internal electron donor in a chlorinated organic solvent; TiCl_4 is dispersed in the precursor porous surface, forming MgCl_2 crystals and $\text{TiCl}_3 \cdot (\text{OR})$. In the activation step, $\text{TiCl}_3 \cdot (\text{OR})$ is removed by further addition of TiCl_4 and solvent. The formed catalyst is washed with a volatile organic solvent in the washing step. Finally, hot nitrogen is used in the drying step to evaporate the solvent, obtaining a free-flowing $\text{TiCl}_4/\text{MgCl}_2$ powder.^[31] Electron donors control the TiCl_4 distribution on the (100) and (110) faces of the MgCl_2 surface.^[32] Ti_2Cl_8 species coordinate with the (100) faces through dinuclear bonds to form the isospecific polymerization sites, while the electron donor molecules tend to coordinate with the non-stereospecific and more acidic sites on the (110) faces. When aromatic monoesters and diesters are used as internal donors, the addition of alkylaluminums (alkylation) results in the partial removal of the internal donor; therefore, external donors are needed to maintain high stereoselectivity. During catalyst preparation, there is also a chance of the internal donor to coordinate with the (100) face, but it has been reported that, in the case of ethyl benzoate, TiCl_4 is able to remove the donor from the (100) stereospecific face during the

titanation step.^[33] However, when 1, 3-diethers are used as internal donors, they coordinate strongly with the (110) faces and cannot be removed by alkylaluminum.[34] As a consequence, ZN catalysts with excellent isospecificity are obtained with diether internal donors in the absence of external donors.

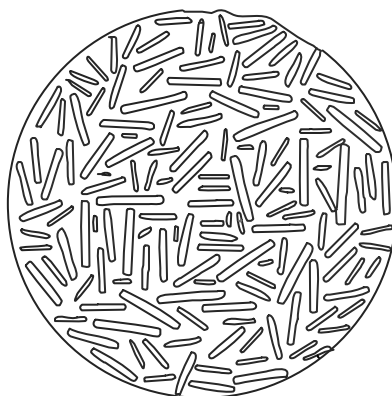


Figure 2 Model for lamellae structure of MgCl_2 supported ZN catalyst.

The illustration of catalyst structure is presented in Figure 2. The highly activated MgCl_2 usually displays very small crystallite size. Though this increases to some extent, owing to recrystallization, during hot treatment with TiCl_4 , it remains very low in the catalyst. High surface areas and pore volume are thus expected, and are actually observed, in MgCl_2 -supported catalysts.

Catalytically active surface are low-index planes that expose unsaturated Mg^{2+} ions with the (104) and (110) lateral planes have long considered as representative ones.^[29,30] These two lateral cuts, for electroneutrality reasons, contain coordinatively unsaturated Mg^{2+} ions, with coordination number of 4 on the (110) cut and 5 on the (104) cut and will be discussed in later

section with details. Busico *et al.*, by using dispersion-corrected density functional theory calculation, withdrew that the surface energy of (104) plane is much lower than that of the (110) plane, leading to the equilibrium crystallographic morphology with a predominance of the more stable (104) lateral surface.^[35] These authors also suggested that the less stable (110) lateral surface can exist in the activated MgCl_2 as a result of non-equilibrium, or equilibrium shifted in the presence of adsorbates such as TiCl_4 or Lewis bases. Mori *et al.* observed mechanically activated MgCl_2 with high-resolution transmission electron microscope and found an equivalent existence of both (104) and (110) surfaces.^[36] Andoni *et al.* also reported an equal growth of MgCl_2 crystal along both [104] and [110] directions when phthalate-based internal donor was employed, however when the 1,3-diether was applied, the crystal growth preferentially occurred along the [110] direction.^[37] Recent DFT calculations by Cavallo *et al.* exactly pointed out the shifted equilibrium, where the (110) lateral surface predominated the (104) surface in the presence of ether electron donor.^[38]

1.3.2 Activator Chemistry

The activators used with the MgCl_2 -supported catalysts are invariably trialkylaluminum, triethylaluminum (TEA) and tri*iso*-butylaluminum (TiBA) being by far the most preferred ones.^[39] Chlororalkylaluminum was employed for the early generations of ZN catalyst, but in fact, afford a much poorer performance and can be used only in combination with trialkyls.

On the other hand, the external donor can be used appears to be dependent on the type of internal donor. Most of the literature deals with the interaction between TEA or TiBA and aromatic monoesters, whose chemistry has recently reviewed by several authors. According to

most of the findings, the interaction involved first the formation of an acid-base complex through the carbonyl oxygen, as demonstrated by the shift of the infrared C=O stretching frequency from $\sim 1725 \text{ cm}^{-1}$ in the free ester to 1655 cm^{-1} to 1670 cm^{-1} in the AlR_3/D_e mixture.^[40] The complex is most often assumed to exist in 1:1 ratio, but on the basis of spectroscopic evidence and calorimetric studies, complexes involving two moles of AlR_3 per mole of D_e also have been hypothesized.

In the case of alkoxy silanes, the formation of a 1:1 complex between TEA and silane has been indicated by means of ^{13}C NMR spectroscopy.^[41] The complex seems to have oxygen atom from only one OR group, irrespective of the number of OR groups attached to the Si.

The above complexes can undergo a further reaction, especially in the presence of excess of AlR_3 as is usual for the polymerization. Silyl ethers, in turn, can undergo an exchange reaction with the alkylaluminium, with the formation of alkylated silylethers and dialkylaluminium alkoxides. The reaction rate is appreciable for silanes containing three or four OR groups and at high concentrations of the alkylaluminium.^[42] Under the much more diluted polymerization conditions, however, the reaction is much slower. The reaction is even slower and sometimes absent for the dialkoxysilanes and practically absent for the monoalkoxysilanes.^[43]

In conclusion, it can be stated that all types of external donor easily form complexes with the free AlR_3 activator. These complexes are rather stable for silanes, whereas in the case of aromatic esters, they further react, leading to destruction of ester and its replacement with the significantly less stereoregulating products.^[44]

1.3.3 Catalyst-Activator Interaction

MgCl₂-supported catalysts are much more complex systems than the TiCl₃-based ones, not only because of the presence of Lewis bases which can interact with both the catalyst and activator, but also owing to the different type of Ti compound used, which is normally in the tetravalent state and prone to undergo reduction upon interaction with alkylaluminium. The aim of this section is to review the modifications occurring in the catalyst composition and structure when it is put into contact with the activator mixture, as these changes are likely to be closely related to the polymerization performance. Two aspects are mainly considered: the transformations concerning the catalyst composition and the change in the oxidation state of the Ti component.

a. Change in catalyst composition

Catalysts involving aromatic monoesters as both D_i and D_e have recently been reviewed by Barbe *et al.*^[45] Their findings were subsequently confirmed by other authors, were that in the absence of any D_e the following modifications takes place in the catalyst through exchange equilibria with the activator.

- extensive removal of the D_i due to complexation or reaction with alkylaluminium,
- incorporation of substantial amounts of alkylaluminium, and
- slight loss TiCl₄.

As far as phthalates and alkoxy silanes as D_i/D_e are concerned, much less experimental data are available. Nonetheless, the reported results suggest a qualitatively similar behavior. Some remarkable quantitative differences, however, appear to hold:

- The initial rate by which the content of D_e in the catalyst increases as a function of the D_e/TEA ratio is much higher for silanes, though the level attained at the high ratios is higher for the aromatic monoesters, and

- The silanes appear to favor the removal of the internal donor (phthalate), whereas the contrary is, to some extent, observed with the D_i and D_e systems of monoesters.

This finding, confirmed by many authors as well, has been explained by assuming silanes coordinate more strongly to $MgCl_2$ than TEA, whereas the opposite is true for the benzoic acid esters.^[46] On the other hand, it has also been reported that D_i/D_e exchange is much easy when cross combination of the above donors are considered.^[47]

Practically nothing has been reported about how the external base, incorporated into the catalyst through above exchange, is linked to the solid. However, according to results obtained by the authors by means of FTIR and NMR, the Lewis base appears to be almost exclusively bonded to Mg in the same way like the internal donor.^[48] Bulky alkoxy-Ti chlorides also can arise from the reaction between esters and Ti-H bonds coming from the chain transfer with H_2 , whereas in the case of silanes the possible exchange reaction products, Ti-O-R contain small alkoxy groups and thus would be easily re-alkylated by the AlR_3 .^[49] On the other hand a reaction between Ti-polymer bonds and silanes has been excluded on the basis of the ^{13}C enriched silanes.^[50]

b. Ti oxidation state

It is generally accepted that the interaction of alkylaluminium with the catalyst facilitates the reduction of Ti^{4+} oxidation state to Ti^{3+} . The literature reports are often contradictory, owing to

the different catalysts and analytical methods used. Actually a reduction of both Ti^{3+} (20 %) and Ti^{2+} (80 %) has been reported by Kashiwa *et al.* for a $TiCl_4/EB$ (ethyl benzoate)/ $MgCl_2$ catalyst after 2 h treatment with TEA at 60 °C and $Al/Ti = 50$.^[51] With the similar catalyst even at milder reaction conditions (10 min., 50 °C, 3:1 TEA/ D_e as activator), Chien *et al.* observed that 85 % of the initial Ti^{4+} was reduced to Ti^{3+} and 15 % to Ti^{2+} .^[52] With the same catalyst Weber found, after contact with TEA at 25 °C, 70 % of Ti^{3+} and 30 % of Ti^{2+} were detected.^[53] From the above results despite the different catalysts and conditions investigated, it seems reasonable to conclude that under polymerization conditions a considerable reduction of Ti takes place, not only to Ti^{3+} but to the Ti^{2+} as well.

1.3.4 Lewis Base Effects

It seems quite clear that to obtain high stereospecificity, Lewis base must be added to either or both the catalyst and activator system. Especially in the fourth generation catalyst a precise combination of D_i and D_e holds the key to control the stereospecificity and activity. Within each donor pair, the D_e/Ti ratio is without doubt the most critical parameter determining the catalyst performance in terms of productivity and stereospecificity. The structure of internal donor appears to be the factor which determines the need for the external base and the type to be used. In detail it can be envisaged as follows:

a. If D_i is highly reactive towards the activator, it usually tends to be displaced from the catalyst. If, in addition, it is highly stereoregulating, as are aromatic monoesters, stereospecificity becomes lower as the donor extraction proceeds. Two possibilities are then opened to preserve the stereospecificity^[54], either

a(1). The D_i extraction is prevented, as for instance by lowering activator concentration or by using hindered Al-alkyls^[55], or

a(2). An equally effective external base is required to replace the internal one in the catalyst thus preserving its stereospecificity. On the other hand, if D_i is not so stereoregulating, as for instance phthalates, the use of a highly efficient external donor able to selectively replace it on the catalyst is absolutely required. This is the clear case for the silanes.^[56]

b. If, on the contrary, D_i possesses high stereoregulating ability and no little reactivity toward activator, it cannot be removed from the catalyst, thus no external donor is required. This appears to be the case of 5th generation catalysts.[57]

Table 2 ZN catalyst performances with different D_i/D_e for propylene polymerization

D_i	D_e	Invented	Productivity (kg-PP/g-cat)	Isotacticity (wt%)	MWD (M_w/M_n)
Benzoate	Benzoate	1971	15-30	93-96	8-10
Phthalate	Alkoxysilane	1980	40-70	95 - 99	6-8
Diether	-	1988	100-130	95-98	4-5
Diether	Alkoxysilane	1988	70-100	98 - 99	4-5
Succinate	Alkoxysilane	1999	40-70	95-99	10-15

The widely used combination of D_i and D_e are EB/aromatic monoesters and phthalate/alkoxy silanes. In both systems, the increase of the D_e/Al molar ratio brings progressive increase of isotactic index (II). The increment in catalyst performance found to be more dominant for the phthalate/alkoxy silane systems as function of D_i/D_e ratio. The phthalate/alkoxy systems show much better performance at lower D_e consumption than the latter.^[58]

In all systems the polymer properties appear to depend to some extent on the amount of external donor. In general, it has been observed that the addition of alkoxy silane based external donor cause increase in MW in absence of H_2 . The effect is less clear for the MWD, for which either no effect or most a slight broadening of isotactic fraction has been reported.^[59]

The structure of external donor appears to have a significant effect on the catalyst performance, as well as on the polymer structure. According to Proto, Sachhi, Seppala and Harkonen, the performance of silanes are greatly affected by the number and size of alkoxy group as well as the bulkiness of the moiety attached to the Si.^[60] Generally, two small OR (methoxy or ethoxy) groups are required for high catalyst performance. The MWD and silane structure possess no correlation. On the other hand the MW is generally reported to increase with the steric hindrance of the silanes. In the terms of microtacticity of the heptane insoluble fraction it was found that their performance increases with the increment in the bulkier alkyl part of alkoxy silane structure.^[61] Okano *et al.* found that both electronic and steric factors are important for the contribution by external donor in deciding the overall catalyst performance.^[62] Highly commercialized dialkyldialkoxy silane based external donors are cyclohexylmethyl dimethoxy silane or dicyclopentadienyl dimethoxy silane.

1.4 Active sites and Polymerization Chemistry

It has been regarded that in heterogeneous ZN catalysts there are at least two kinds of active sites associated with isotactic and atactic polymeric fractions is well known; however this simplified picture was inadequate to explain the following experimental data:

- a. The broad distribution of tacticity and MW even for the polymer fraction insoluble in xylene, and
- b. The compositional heterogeneity of propylene copolymers both with ethylene and higher-olefins.

The relative proportion of two active sites (isospecific and aspecific) varies with the nature of catalyst; the fraction of highly isospecific centers increases with the isotactic index of the polymer.^[63] The MWD of PP produced with MgCl₂ supported ZN catalysts is broad and falls in the ranges of 3 to 8. Monomer diffusion limitation through the polymer layer as a cause of MWD broadening has been accommodated for long.^[64] The presence of various kinds of active sites on the surface of catalyst possessing different values of apparent chain propagation constant has been suggested as reason as source of MWD broadening. Kashiwa *et al.* explained the change in the shape of GPC curve of isotactic fraction from monomodal to bimodal upon addition of the electron donor, suggested the formation of new active centers modified by the donor.^[65]

The outstanding progresses in enhancing the heterogeneous catalyst performance have not been accompanied by equal progress in the knowledge of the structure of the active sites and of some steps of the polymerization reaction. However, recent advances in the knowledge of the true nature of active centers in homogenous metallocene-based catalyst allowed the successful application to these sites of the same mechanism of enantioselectivity suggested for the

hypothetical sites in heterogeneous catalysts, thus explaining many experimental results.^[66] However the precise nature and state of each active sites and polymerization behavior are still ambiguous. In this section we will briefly discuss the various proposed olefin polymerization models and mechanism.

A great number of models for explaining the polymerization mechanism by the active centers of ZN catalysts have been proposed. Natta, for the first time, proposed that the steric control is due to the structure of the active site located on the borders of the crystal layers of TiCl_3 .^[67] Electron microscopy observations of the polymer growth on the well formed -TiCl_3 crystals led to the conclusion that the active sites are not present on the basal surfaces. Arlman and Cossee proposed that the active centers are located on the lateral crystal surfaces which, in -TiCl_3 , corresponds to (110) planes. The proposed Cossee polymerization mechanism is as shown in the Figure 3.^[68]

It shows that the single bonded Cl-atom substituted by an alkyl group, giving Ti-C bond. It contains two steps: co-ordination to monomer at the vacant octahedral coordination site with the double bond parallel to the Ti-C bond, and chain migratory insertion of the coordinated monomer with the migration of the growing chain to the position previously occupied by the coordinated monomer; the transition state is assumed to be a four membered ring of Ti, the last carbon atom of the growing chain and the two carbon atoms forming the double bond of the monomer. Stereochemistry is assumed only if before a further insertion, the chain skips back to the position occupied before the insertion.

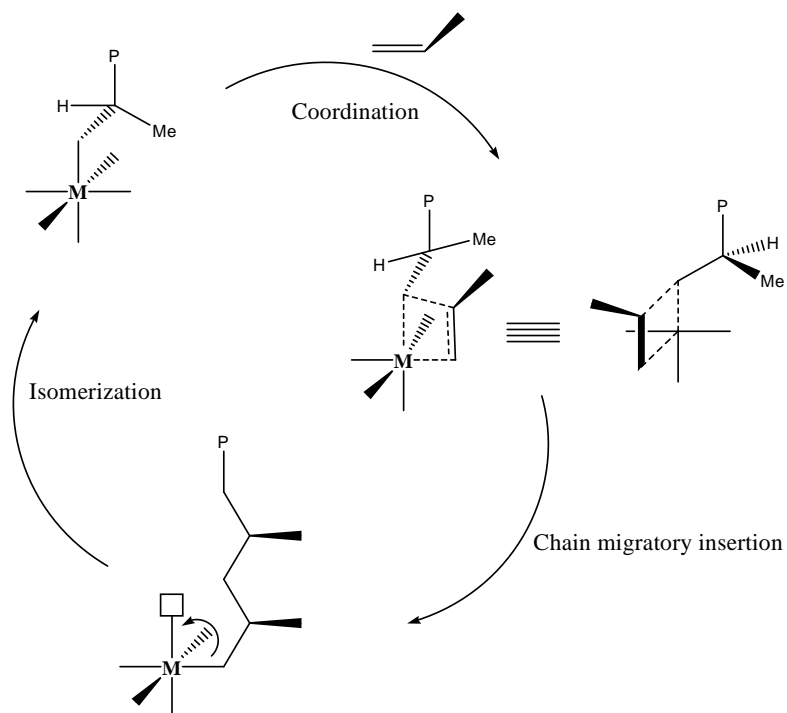


Figure 3 The Cossee-Arlman polymerization mechanism

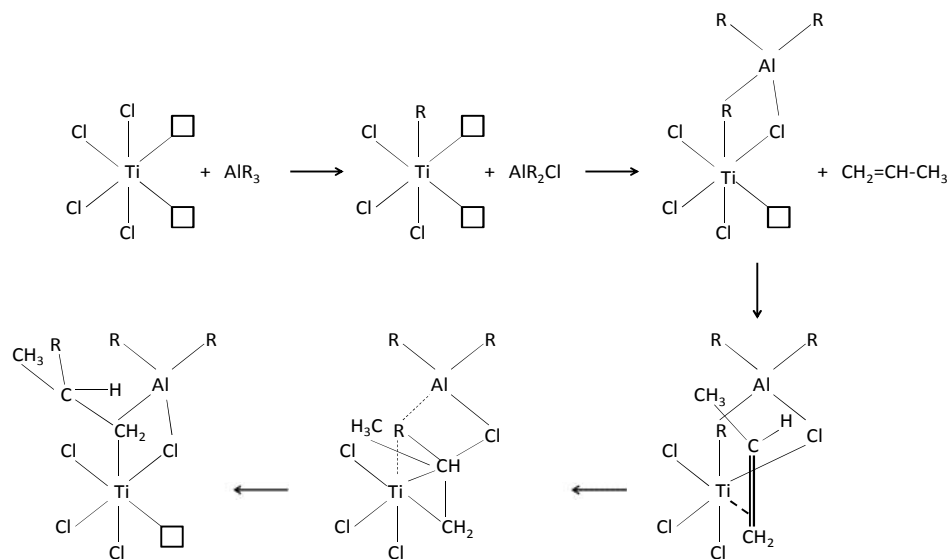


Figure 4 Bimetallic polymerization mechanism by Rodriguez and Van Looy.

The surface model proposed by Allegra obviates the necessity of the back skip step to assure the stereoselectivity because a C_2 symmetry axis locally relates the atoms relevant to the non-bonded interactions with the monomer and the growing chain.^[69] Corradini *et al.* on the basis of some evaluation of the non-bonded interactions for the Cossee and Allegra models, suggest that the chiral environment of the metal atom imposes a chiral orientation of the first C-C bond of the chain, and this orientation has been identified as crucial for determining the stereospecificity.^[70] Bimetallic catalytic centers have been proposed by Patat and Sinn, Natta and Rodriguez. In these models, a ligand (Cl or alkyl group) and the last carbon of the growing chain link Ti and Al through double bridge. In the mechanism suggested by the Rodriguez, which is similar to the Cossee mechanism, the double bridge represents the driving force to shift back at its initial position the bridged alkyl group of growing chain after the migratory insertion step.^[71]

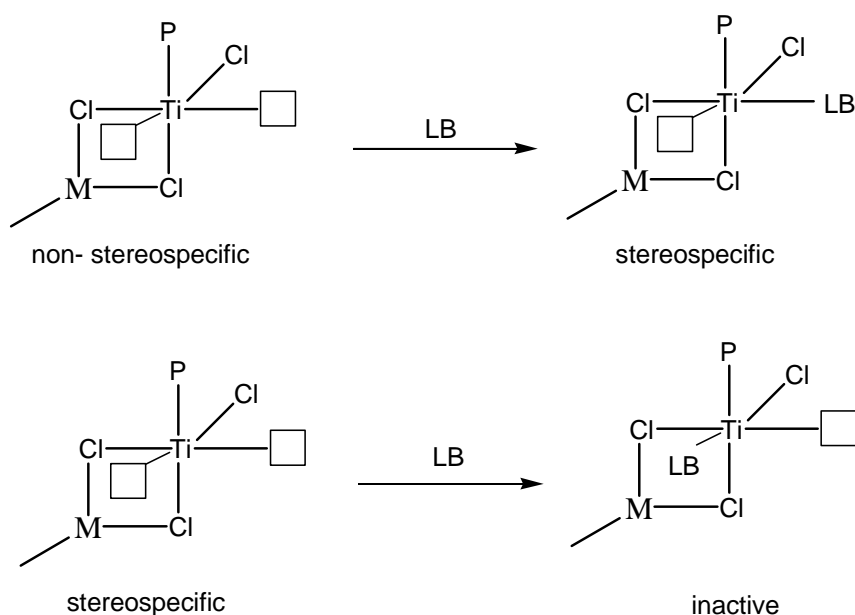


Figure 5. Active site model proposed by Soga *et al.* in the presence of Lewis Base (LB).

The presence of Lewis base is essential to improve the stereospecificity of the MgCl_2 -supported catalysts. A number of experiments have shown that the existence of equilibria between the Lewis base present on the surface of the catalyst and Lewis base complexed in solution with alkylaluminium.^[72] The aspecific sites would be deactivated preferentially with respect to the isospecific ones, owing to their stronger Lewis acidity. The enhanced productivity of stereoregular polymer observed when the polymerization is carried out in the presence of donor has been explained by assuming that aspecific sites having two coordination vacancies are converted to single vacancy isospecific sites by complexation with the donor.^[73] Unfortunately, complexes of the donor with the transition metal have never been unambiguously reorganized on the catalyst surface. The spectroscopic studies have shown that that donor have complexation with the MgCl_2 ; however the concentration of these complexes are very low.

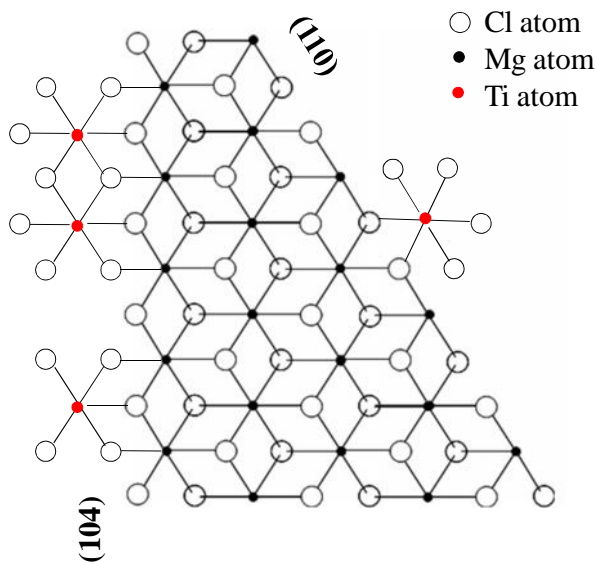


Figure 6 Model of mono and dinuclear TiCl_4 species with different MgCl_2 faces (104) and (110).

Busico *et al.* showed that reduced TiCl_4 on the (100) MgCl_2 crystal face has two vacant sites and the (110) face has only one site.^[74] Vacant sites are necessary for polymerization, but sites with more than one vacancy are aspecific. Dimerized TiCl_3 on the (100) face are believed to be stereospecific sites.^[75] Chirality of metal ion is thought to be responsible for the inherent stereospecificity of the catalyst. Based on the microstructural and stereochemical analysis of atactic PP produced from various types of heterogeneous Ti-based catalysts, Doi *et al.* proposed a reversible interconversion between isospecific and syndiospecific stereoblocks.^[76] The stereoblock characteristics was also found in PP prepared from the donor-free $\text{TiCl}_4/\text{MgCl}_2$ -TEA catalyst system by Xu *et al.*^[77] They suggested the existence of equilibrium between monometallic sites and bimetallic sites in terms of reversible complexation with TEA. In these models both monometallic and bimetallic active sites coexists.

Corradini and Busico *et al.* established a three-site model in terms of equilibrium interconversion between three kinds of stereospecific active sites namely highly isospecific, poorly isospecific and syndiospecific sites to explain the stereoblock characteristics of the synthesized PP with MgCl_2 supported ZN catalysts within the last decade.^[78] The difference in the substitution of the two most important coordination positions (defined as L_1 and L_2) were postulated to be crucial. The model is illustrated in Figure 5.

Terano *et al.* established that the steric hindrance need not always arise from a donor molecule by using Busico model to propose structures for stereospecific active sites in the donor free ZN catalyst system, where high stereospecificity can arise by co-ordination of the Al alkyl adjacent to the active Ti.^[79] Terano *et al.* stated that the formation of active site with highest stereospecificity strongly depends upon the interaction of catalyst and activator without any monomer as a pretreatment by classifying the active sites into aspecific and three kinds of

isospecific sites in the ZN catalysts.^[80] The isospecificity of active sites strongly depends upon the bulkiness of the ligand positions for construction of asymmetry and chirality of active sites and steric hindrance.

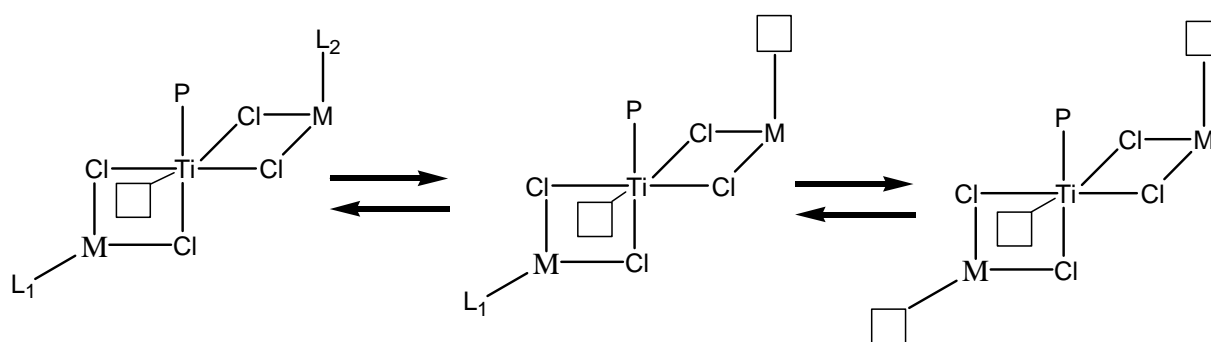
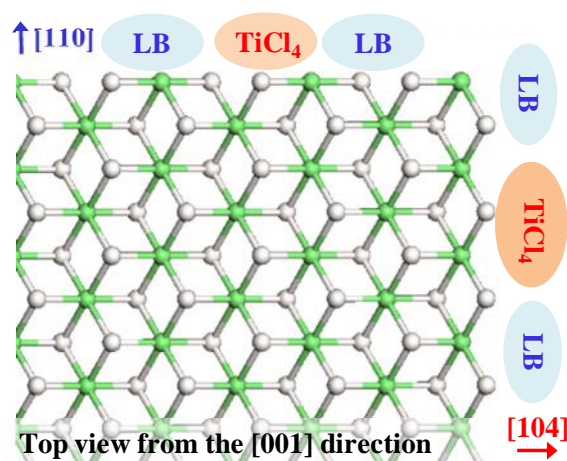


Figure 7 Three-site model of active Ti species for highly isospecific (a), poorly isospecific (b), and syndiospecific (c). M = Ti, Mg, or Al, $L_{1,2}$ = donor or Cl, \square = vacant site, and P = growing polymer chain.



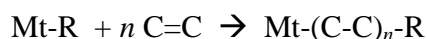
Courtesy: prepared by Professor Dr. Toshiaki Taniike

Figure 8 Coadsorption model of Ti species and electron donor on $MgCl_2$ surface

Recently, Taniike *et al.* reported the plausible coadsorption states of EB (D_i) with Ti mononuclear species on the $MgCl_2$ (110) and (100) surface.^[81] They concluded that EB coadsorbed energetically favorably with the Ti species on the two surface with increase of electron density of Ti species, selectively, on (110) surface, suggesting that coadsorption on (110) is electronically more favorable and significant. Many models have been proposed, but, the precise behavior of the Lewis bases and their interaction with the plausible active sites in ZN catalysts is still not known clearly.

1.4.1 Metal-Carbon Bond Formation

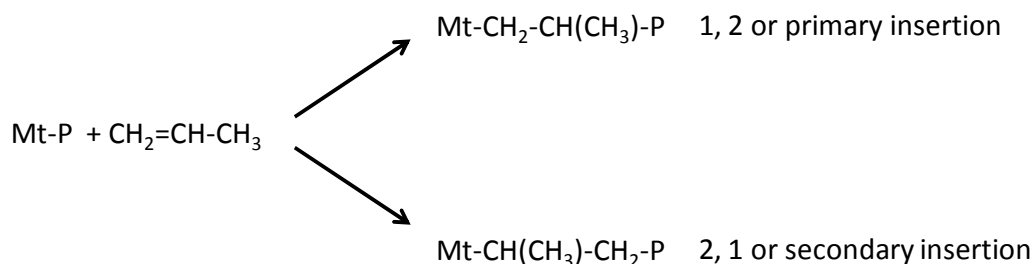
In terms of polymerization mechanism it is unanimously assumed that olefin polymerization with ZN catalysts involves a stepwise insertion of the monomer into transition metal-carbon^[82] (Mt-C) as follows:



The coordination of the monomer to the transition metal before the insertion step is generally assumed. The above mechanism is supported by various spectroscopic and radioactive isotopic labeling based experimental evidences.^[83] Therefore, there is no doubt that polymerization occurs by insertion of the olefin-double bond into transition metal-carbon bond.

1.4.2 Regioselectivity

The insertion of an α -olefin in the metal-carbon bond may take place in two different ways:



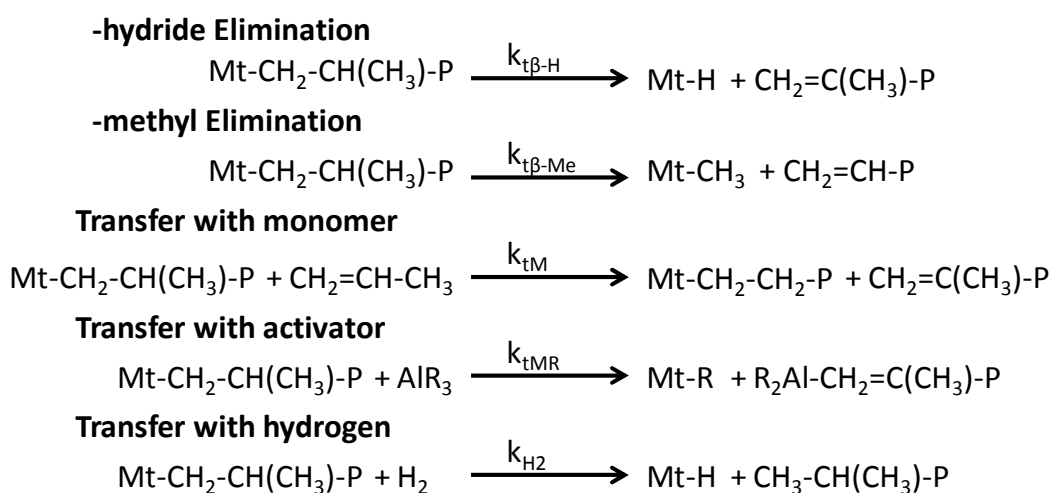
where Mt and P denote the transition metal and polymer chain, respectively.

It is unambiguously proved, by the chain end group analysis, that the 1, 2 insertion mode is working in isospecific polymerization of olefins. On the contrary the 2, 1 insertion mode prevails in syndiospecific propylene polymerization with $\text{VCl}_4/\text{Et}_2\text{AlCl}$ catalyst at low temperature.^[84] Regioregularity is extremely high in isotactic polymers obtained by heterogeneous catalysts; head-to-head and tail-to-tail enchainments are sufficiently few as to be undetectable by IR and NMR spectroscopy.^[85] However it has also been reported that occasional 2, 1 insertion is possible at isospecific centers in heterogeneous catalysts but this irregular prevents any further monomer insertion. The content of regioirregularities depends on kind of ligands to the metal center, polymerization temperature and monomer concentration. In general, regioirregularity are mainly of 2, 1 type when activity of the catalyst is very high.^[86]

1.4.3 Chain Termination

Polymer chain termination occurs mostly through the below mentioned reactions. The relative importance of the different chain transfer reactions depends on the catalyst system used and on the process conditions. Chain transfer by β -hydride elimination is not considered

important in propylene polymerization with traditional and MgCl_2 -supported heterogeneous catalysts. In the absence of hydrogen and under normal polymerization conditions, transfer with monomer is the most important chain termination process in propylene polymerization heterogeneous catalysts.^[87]



In propylene polymerization the chain transfer with the activator plays a secondary role. Transfer with hydrogen is, in all cases, the most efficient chain terminating process.^[88] Hydrogen does not influence the MWD of the polymer.

1.4.4 Polymer Morphology

The precise control of polymer morphology is highly desirable for PP manufacturing in the terms of the process economics and viability. The possibility of controlling to some extent the polymer shape, size and particle size distribution through the catalyst has been known since the

very early industrial PP manufacturing. It is based on the fact that the polymer usually tends to duplicates, on larger scale, the physical characteristics of the catalyst. This phenomenon is called replication.^[89] Though the particle growth mechanism has not yet been completely understood but a large number of evidences demonstrate that following phenomena usually takes place:

- a. As soon as polymerization starts, the catalyst grain begins to disrupt into huge number of small fragments. According to recent findings, this process is very fast and proceeds to the crystalline dimensions or even smaller.
- b. The catalyst fragments, though no longer in contact with each other, are kept together and uniformly dispersed in polymer.
- c. The fragments are spread outward as the particle grows. This implies that the polymer growth occurs around each fragment.

A fast and extensive catalyst fragmentation and a uniform polymer growth rate across the particle seem to be key feature for faithful replication. As far as catalyst is concerned, a proper balance between reactivity and mechanical properties are desired such as high surface area and porosity, high enough inter-particle mechanical strength but should not be very low, homogeneous distribution of active sites and no diffusion limitations.^[90]

The particle growth, which, according to Goodall, can be called the “expanding universe model” appear to be not only supported by the experimental evidence but also by the mathematical modeling. The most popular among such models is “multigrain model” (MGM).^[91] MGM is simplified and quantitative version of the “expanding universe model”. It assumes that;

- Catalyst fragmentation is already completed at time zero;
- Catalyst fragmentation are of uniform size; and
- The polymer grows as a spherical globular microparticle around each catalyst fragmentation.

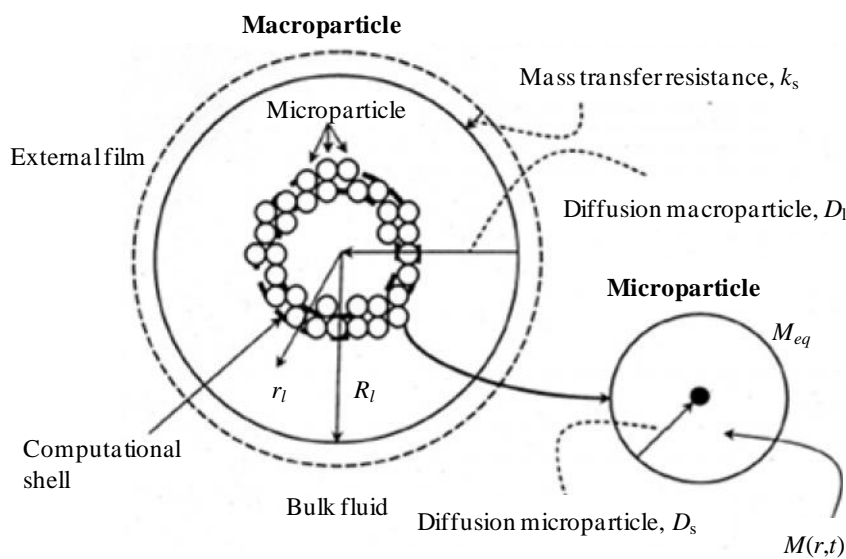


Figure 8 Schematic representation of MGM model.

Two limiting modes of the fragmentation of porous catalyst carriers observed experimentally are shown in the Figure 3. Kosek *et al.* recently reported that the generalized discrete element model of growing catalyst/polymer particle based on force and mass transport interactions among micro-elements are demonstrated on and extended to the “shrinking core” and “continuous bisection” fragmentation mode.^[92]

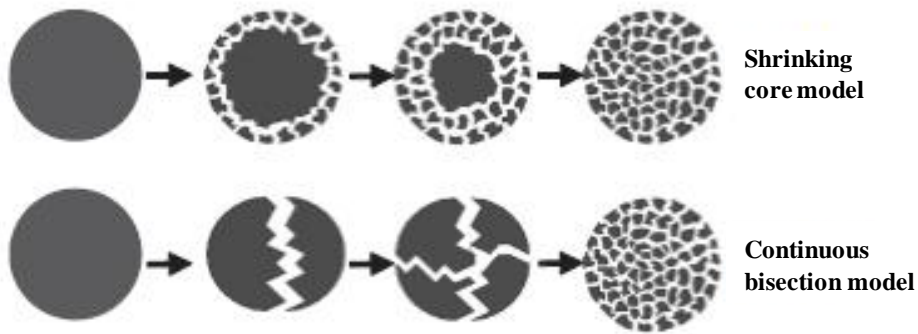


Figure 9 Fragmentation mode representation proposed by Kosek *et al.*

In propylene polymerization serious mass transfer limitation and thus concentration profiles across the particle are likely to occur only in a very early stage of the polymerization stage as a result of either a bad catalyst design, such as large size and low porosity, or a high polymerization temperature.^[93] Hutchinson demonstrated that these drawbacks can be overcome or strongly decreased by prepolymerization. The prepolymerization has the effect of decreasing the polymerization rate per unit particle volume and increasing at the same time the surface area available for the monomer diffusion.^[94]

Both the experimental finding and the modeling results confirm that a satisfactory control of polymer morphology through replication process is possible with precise catalyst design and maintaining initial polymerization kinetics.

1.4.5 Copolymerization

It was observed that when copolymerization of propylene with small amounts of ethylene causes an increase in polymerization rate.^[95] This behavior may be accounted for by assuming

that propylene insertion in Ti-C bond is easier when ethylene is bonded to the transition metal or that ethylene insertion after regioirregular (2, 1) propylene insertion reactivates the dormant site.^[96] It was found that the comonomer reactivity decreases with the increasing the steric hindrance around the double bond in the following order:

Ethylene > Propylene > 1-Butene > linear 1-olefins > branched 1-olefins.

The copolymers prepared by MgCl₂ supported ZN catalyst comprises broad composition distribution by nearly and equally broad stereoregularity and molecular weight distribution and seem to be originated from various kinds of active sites having different stereospecificity as well as reactivity towards (co)monomers.^[97]

1.5 Polymerization Kinetics

Kinetic investigations of propylene polymerization with heterogeneous ZN catalysts are very useful in the industrial development of the reaction but have given a limited contribution to the understanding of the polymerization mechanism. The heterogeneous nature of the catalyst, presence of different kinds of active sites, the chemical transformation of the components of catalyst during the time, and the procedure of contact of catalyst components in the rate and stereospecificity of polymerization of the polymerization make it difficult to study the kinetics of polymerization with these catalysts.

Heterogeneous ZN catalyst can possess several stages in the polymerization kinetics which can be broadly classified in three-classes i.e. 1. induction period, 2. constant-rate period and, 3. decay period.^[98] The induction period believed to comprise several events such as metal alkyl and transition metal react to form active centers, polymerization (quasi-living up to 0.2 s) and

followed by the catalyst fragmentation. The temperature in the vicinity of the active center can become much higher than the reaction medium and may lead to chemical and physical changes in the catalyst.^[99] The uncontrolled induction period may provide bad polymer morphology and/or early-decaying kinetics.^[100] This shows that the induction period is not only possessing active site activation but also controls the catalyst activation to regulate the constant-rate period. The reason(s) for the origin of polymerization kinetics through catalyst activation have been rarely discussed in literature. The precise understanding of catalyst activation allows the development of highly functional olefin polymerization catalyst with long-lasting kinetics as well as good polymer morphology.

The constant-rate period believed to be achieved with acquiring steady state (or stationary state) polymerization rate, the system attains an equilibrium state, that is, the number of active centers remained constant. This region represents the completion of most-possible catalyst fragmentation. Longer constant-rate period offers better polymerization kinetics.

Decay period represents region the stage of polymerization kinetics in which rate curves reaches a maximum and then continues to decline. The decay rate depends on number of factors. A wide range of plausible mechanisms have been proposed as a reason for the catalyst decay during polymerization. Some researchers assume that the rapid rate decrease could be caused by a physical phenomenon based on a monomer flux diffusion limitation due to the encapsulation of the catalyst in the polymer layer.^[101] On the contrary, Keii *et al.*, Yoon *et al.* and Mori *et al.* obtained results indicating that the monomer diffusion through the polymer is not responsible for the catalyst decay. They proposed the explanation based on the presumption that the deactivation occurs independently of the presence of a monomer, and is caused by the interaction of the catalyst with an alkylaluminium compound via over reduction.^[102] A novel insight into the

catalyst deactivation was presented by Lim and Choung. They assumed that the catalyst deactivation was caused by a combination of chemical and physical phenomena, such as active sites reduction and monomer diffusion resistance.^[103] Recently, Terano *et al.* reported a plausible protective effect on the active sites by coordinating monomers and growing polymer chains. They suggest that the growing polymer chain, always present on the active center during the polymerization, prevents it from further reaction with TEA compound and thus protects it from deactivation.^[104] These elegant studies especially by Terano *et al.* and Keii *et al.* revealed that active site activation as well as deactivation seems to be deeply related with alkylaluminium.^[105]

Many kinetic models have developed to describe the ZN olefin polymerization. Tait *et al.* consider a competitive reversible adsorption reaction of monomers and alkylaluminium with the active sites.^[106] This kinetic model is described by Langmuir-Hinshelwood isotherm.^[107] The overall polymerization rate can be given as:

$$R_p = \frac{K_p[C^*]K_M[M]}{1 + K_M[M] + K_A[A]}$$

where K_p represents the propagation rate constant, C^* is the concentration of active sites, $[M]$ and $[A]$ represents the bulk equilibrium concentrations of monomer and alkylaluminium, K_M and K_A are the equilibrium adsorption constants for the respective adsorption equilibria.

The kinetic model proposed by Bohm includes Cossee model^[108], describes the catalytic process by the Rideal mechanism^[109], and the complexation of the active transition metal center

by the monomer represents the most important step. The polymerization rate can be given as follows:

$$R_p = \frac{K_a K_p [M]}{K_p + K_d} \times \left[[C^*] / \left[1 + \left(\frac{b}{a} \right) + \left(\frac{c}{a} \right) \right] \right]$$

with the rate constants K_a and K_d for the formation and dissociation of the active center-monomer complex, the rate constant K_p for the insertion of the complexed monomer into the transition metal-carbon bond, and the term $1/1 + (b/a) + (c/a)$ for the influence of alkylaluminium adsorption and monomer co-ordination on active centers.

Various mathematical models were successful in predicting the polymerization kinetic behavior and explaining the observed polymer properties in terms of molecular weight or chemical composition distribution.^[110] The polymerization kinetics was the result of a delicate interplay between number of factors such as kind of catalyst, temperature, pressure, monomer concentration, presence or absence of donor or/and hydrogen etc. But these studies were either applicable to some specific kind of ZN catalyst or/and cannot explain the precise polymerization mechanism. Especially the reason for the origin of the polymerization kinetics has not been intensively studied, which as discussed, holds key for providing long lasting kinetics.

MgCl₂-supported Ziegler catalysts have achieved a spectacular success in improving the activity and stereospecificity of the catalyst for olefin polymerization. The elucidation of numerous unanswered questions with respect to olefin ZN polymerization is still an intense research in both industry and academia. ZN catalyst contains multiple components and generates

large heterogeneity as well as complexity for understanding the multiple simultaneous chemical and physical phenomena. The following subjects are of particular interest such as the formation and transformation of active sites, correlation between the nature and performance of active sites in terms of activity, stereospecificity and catalyst morphology development.^[111] These factors play crucial roles in determining the catalyst performance but the comprehension of these fundamental matters has progressed more slowly than the empirical development of the industrial catalysts. Deeper understanding of these basic aspects will lead to further development in this area.

The stopped-flow method for heterogeneous ZN olefin polymerization was first developed by Keii and Terano to evaluate specific kinetic parameters.^[112] Compared with a homogeneous stopped-flow polymerization system connected with a spectroscopic detector, this polymerization system is heterogeneous, and the catalyst particles can facilitate the mixing process in slurry flow conditions. The major feature of this technique is its ability to precisely control the polymerization time (*ca.* 0.03 s) for extremely short period (*ca.* 0.2 s) which is much less than the average lifetime of the growing polymer chains, and the states of the active sites are constant without time-dependent changes and occurrence of chain-transfer reactions, indicating that a quasi-living polymerization can be performed.^[113] Furthermore, the information concerning the active sites and the polymerization procedures was obtained by direct analysis of the polymer produced at the initial polymerization stage.^[114]

Figure 4 shows the apparatus for the two vessel SF polymerization. Vessels A and B are special glass vessels equipped with water jackets and magnetic bead. Catalyst slurry and activator solution saturated with monomer are placed in vessels A and B respectively. Flask C contains acidic ethanol as quenching solution. After both the slurry and solution attained

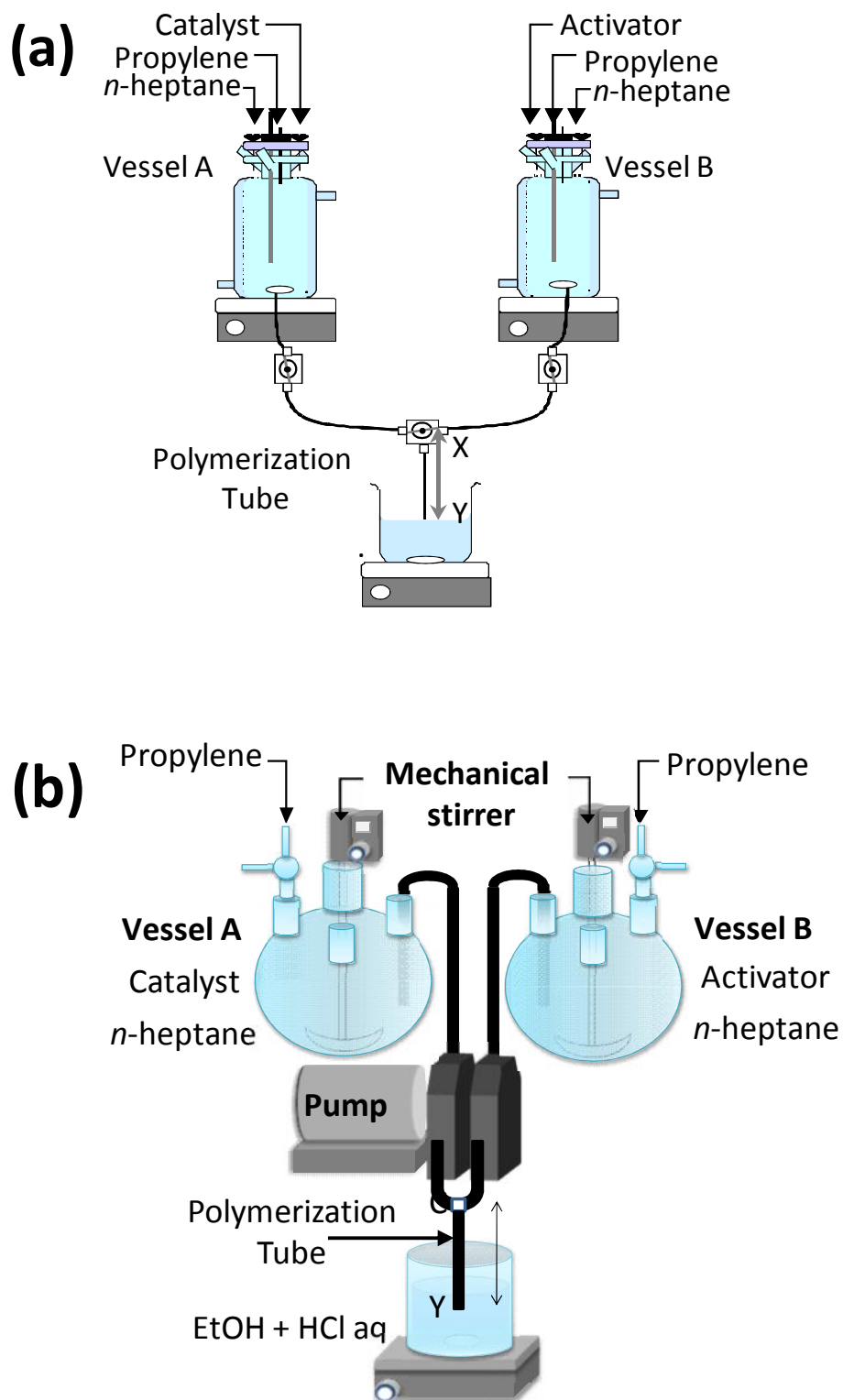


Figure 10 (a) SF apparatus and, (b) LSF apparatus.

stationary conditions, they are forced to flow simultaneously through a Teflon tube from vessels A and B into flask C under a small pressure of nitrogen. Polymerization occurs in the Teflon tube from point X to Y.

The SF polymerization has been mainly studied up to quasi-living region and able to explain not only the polymerization mechanism in terms of nature and state of active sites but also for catalyst/polymer particle morphology development. However, the SF kinetics of constant activity is different from the macroscopic kinetics for the ZN olefin polymerization. The induction period represents the region comprising both the quasi-living region and catalyst activation period. It is obvious to conclude that some unknown changes in the catalyst might occur during the polymerization which can be hold responsible for the catalyst activation and useful for connecting bridge between ZN macroscopic and SF kinetics. The understanding of the origin for the overwhelming ZN macroscopic kinetics demands prolonged SF studies to observe the kinetic transition from constant activity to catalyst activation stage. But the conventional SF system has few limitations for prolonged polymerizations such as poor mixing of the catalyst/activator solution in polymerization tube, tube plugging due to viscosity development with polymerization and improper flow rate. These issues were well considered and Taniike *et al.* developed an improved SF system called large-scale stopped flow (LSF).^[115] The LSF has overcome the drawbacks of the conventional SF system. Figure 5 represents the LSF apparatus. The LSF consist pump to offer controlled flow rate and wider polymerization tube to eradicate the viscosity problems and homogenizer for instant solution quenching by providing very high rate of agitation (12,000 rpm). These crucial developments in the improvement of the SF system makes it more powerful tool and can be employed for conducting the prolonged polymerization for the understanding of the origin of kinetics.

1.6 Objective of this Study

In current era, the PP has acquired impressive maturity and no aim appears too ambitious for it. The performance of PP production and its applications are constantly under the limelight. The production of PP has grown from around 1.5 million tons in 1970's to about 50 million tons in 2011.^[116] However, the exponential progress by industry for polymer production and properties improvements are much ahead of general understanding of catalyst responsible for its production. The major reason is the large heterogeneity of active sites, simultaneous interaction between multiple components and moisture sensitive nature of the ZN catalyst. Although many remarkable studies has been done but still many questions related to ZN polymerization mechanism are unanswered such as precise role of alkylaluminium/donor/hydrogen/comonomer in ZN catalysis and their correlation with polymerization kinetics development are still key questions to be encountered.

In ZN catalysts, it is widely accepted that the use of an alkylaluminium as an activator is vital for the olefin polymerization.^[117] The alkylaluminium participates in active site activation, deactivation and conversion of the active site behavior during polymerization in combination with other chemical entities such as donors. Besides this, active sites nature also varies in the presence of chain transfer agents, such as H₂. Simultaneously, the polymer formation over the catalyst generates hydraulic stress in the pores and causes fragmentation. The fragmentation exposes hidden active sites for polymerization and start after attaining few g-polymer/g-cat.^[118] These parallel phenomena decide kinetic behaviors of ZN catalyst in a complicated way.

The initial stage of the polymerization is known to exert crucial influences on the polymerization kinetics and particle morphology development,^[100] where the polymerization

Chapter 1
General Introduction

conditions as well as the kind of polymer formed can strongly affect the particle morphology.^[94,119] McKenna *et al.* found that the initial instants of the polymerization are, perhaps, the most important of the reaction because in this phase heat and mass transfer resistances can be very significant and critical to decide the polymerization kinetics.^[111] The delicate interplay of various chemical entities and catalyst/polymer particle growth (physical processes) with the polymerization kinetics development needs to be unfolded for better understanding of ZN catalysis.

The objective of this study is to understand the role of alkylaluminium/donor/chain-transfer agent/comonomer in terms of chemical and/or physical processes occurring in the ZN catalyst and their correlation with the early stages of polymerization kinetics with stopped-flow technique. The dissertation consists of five chapters. The first chapter is consisted of general introduction to lead the objective of this research. Understanding chemical and physical transformations of ZN catalyst at initial stage of polymerization kinetics: Key role of alkylaluminium in catalyst activation process represents the chapter 2. Role of external donor and hydrogen at the initial stage of Ziegler Natta propylene polymerization has been addressed in chapter 3. Initial morphology and kinetics development in Ziegler-Natta catalyst studied through stopped-flow ethylene/propylene and 1-hexene/propylene copolymerization has been discussed in chapter 4. Finally, chapter 5 summarizes the general conclusions from this study.

References

- [1] P. S. Chum, K. W. Swogger, *Prog. Polym. Sci.*, **2008**, 33, 797.
- [2] (a) J. Boor Jr., *ZN Catalysts and Polymerizations*, Academic Press, New York **1979**, p. 21.
(b) K. Ziegler, H. Breil, H. Martin, E. Holzkamp, *German Patent 973626* **1953**.
- [3] (a) M. P. McDaniel, *Adv. Catal.* **1985**, 33, 47. (b) Y. Fang, B. Liu, M. Terano, *Kinet. and Catal.* **2006**, 47(2), 295. (c) K. Tonosaki, T. Taniike, M. Terano, *Macromol. React. Eng.* **2011**, 5, DOI: 10.1002/mren.201000053.
- [4]. K. Soga, T. Shiono, *Prog. Polym. Sci.* **1997**, 22, 1503.
- [5] E. P. Moore, Jr., *The Rebirth of Polypropylene: Supported catalysts*, Hanser publishers, Munich, **1998**. (b) M. P. McDaniel, D. C. Rohlfing, E. A. Benham, *Polym. React. Eng.* **2003**, 11, 101.
- [6] (a) Montedison, *British Patent 1286867* **1968**. (b) Shell Oil, *U. S. Patent 4414132* **1979**.
- [7] Alberta Poly(propylene) Market Study, *CMAI*, September **2004**.
- [8] NEDO, *World Demand of Polyolefins*, April **2007**.
- [9] P. Galli, P.C. Barbe, L. Noristi, *Angew. Makromol. Chem.* **1984**, 120, 73.
- [10] (a) Montecatini, *Italian Patent 535712* **1954**. (b) C. Vasile, Ed., *Handbook of Polyolefins*, Marcel Dekker: New York **2000**.
- [11] Montecatini, *Italian Patent 537425*, **1954**.
- [12] Montecatini, *Italian Patent 526101*, **1954**.

Chapter 1
General Introduction

- [13] Anderson Chem. Co., *Division of Staffer Chem. Co.: Technical Bulletin Titanium Trichloride Anhydrous*, August, **1959**.
- [14] C. E. Tornqvist, C. C. W. Seelback, A. W. Langer, Jr., N. J. Nixxon, *U. S. Patent* 3128252, **1964**.
- [15] J. P. Hermans, P. Henriouille, *U. S. Patent* 3769233, **1973**.
- [16] Z. W. Wilchinsky, R. W. Looney, E. G. M. Tornqvist, *J. Catal.* **1973**, 28, 351.
- [17] Mitsui Petrochemicals, *JP Patent* 1031698 **1968**.
- [18] Montedison, *Belgian Patent* 785332 **1972**.
- [19] Montedison and Mitsui Petrochemicals, *German Patent* 2643143 **1977**,.
- [20] B. L. Goodall, R. P. Quirk (Ed.), *Transition Metal Catalyzed Polymerizations*, Harwood Academic Publishers, New York, *Alkenes and Dienes* **1983**, Part A, p. 355.
- [21] J. R. Severn, J. C. Chadwick (Eds.), *Tailor-Made Polymer: Via Immobilization of Alpha-Olefin Polymerization Catalysts*, Wiley-VCH, Berlin, **2008**.
- [22] Montedison, *European Patent* 45977 **1982**.
- [23] HIMONT Incorporated, *U. S. Patent* 4971937 **1990**.
- [24] H. Sinn, W. Kaminsky, H. J. Vollmer, R. Woldt, *Angew. Chem. Int. Ed.*, **1980**, 92, 396.
- [25] G. Natta, *Chim. Ind. (Milano)* **1960**, 42(11), 1207.
- [26] I. W. Bassi, F. Polato, M. Calcaterra, J. C. J Bart, *J. Crystallogr.* **1982**, 159, 297.
- [27] G. Natta, A. Zambelli, I. Pasquon, G. M. Giongo, *Chi. Ind. (Milano)* **1966**, 48, 307.

- [28] J. Boor, *Ziegler-Natta Catalysts and Polymerizations*, Academic Press, New York, **1979**.
- [29] U. Giannini, *Makromol. Chem., Suppl.* **1981**, 5, 216.
- [30] R. Zannetti, C. Marega, A., Marigo, A., Martorana, *J. Polym. Sci., Part B: Polym. Phys.*, **1988**, 26, 2399.
- [31] M. Chang, X. Liu, P. J. Nelson, G. R. Munzing, T. A. Gegan, Y. V. Kissin, *J. Catal.* **2006**, 239, 347.
- [32] J. C. Chadwick, G. M. M. van Kessel, O. Sudmeijer, *Macromol. Chem. Phys.* **1995**, 196, 1431.
- [33] V. Busico, P. Corradini, L. De Martino, A. Proto, V. Savino, E. Albizzati, *Makromol. Chem.* **1985**, 186, 1279.
- [34] L. Barino, R. Scordamaglia, *Macromol. Theory Simul.* **1998**, 7, 407.
- [35] V. Busico, M. Causa, R. Cippulo, R. Credendino, F. Cutilo, N. Friederichs, R. Lamanna, A. Segre, V. V. A. Castelli, *J. Phys. Chem. C*, **2008**, 112, 1081.
- [36] H. Mori, M. Sawada, T. Higuchi, K. Hasebe, N. Otsuka, M. Terano, *Macromol. Rapid Commun.* **1999**, 20, 245.
- [37] (a) A. Andoni, J. C. Chadwick, J. W. Niemantsverdriet, P. C. Thune, *Macromol. Rapid Commun.*, **2007**, 28, 1466. (b) A. Andoni, J. C. Chadwick, J. W. Niemantsverdriet, P. C. Thune, *J. Catal.*, **2008**, 257, 81.
- [38] R. Credendino, J. T. M. Pater, A. Correa, G. Morini, L. Cavallo, *J. Phys. Chem. C*, **2011**, 115, 13322.

- [39] Shell Oil, *U. S. Patent 4393182* **1979**.
- [40] R. Spitz, J. L. Lacombe, M. Primet, *J. Polym. Sci. Part A: Polym. Chem.* **1984**, 22, 2611.
- [41] J. J. A. Dusseault, C. C. Hsu, *J. Macromol. Sci., Rev. Macromol. Chem. Phys.* **1993**, C33, 103.
- [42] E. Vahasarja, T. T. Pakkanen, T. A. Pakkanen, E. Iiskola, *J. Organomet. Chem.* **1987**, 25, 3241.
- [43] E. Albizzati, M. Galimberti, U. Giannini, G. Morini, *Macromol. Chem. Makromol. Symp.* **1991**, 48/49, 223.
- [44] J. C. W. Chien, J. C. Wu, *J. Polym. Sci. Part A: Polym. Chem.* **1982**, 20, 2445.
- [45] P. C. Barbe, C. Cecchin, L. Noristi, *Adv. Polym. Sci.*, **1986**, 81, 3.
- [46] M. C. Sacchi, I. Tritto, C. Shan, R. Mendichi, L. Noristi, *Macromol.* **1991**, 24, 6823.
- [47] Mitsui P. C., *European Patent 086288* **1986**.
- [48] E. Iiskola, A. Pelkonen, H. J. Kakkonen, J. Pursianen, T. A. Pakkanen, *Makromol. Chem. Rapid Commun.* **1993**, 14, 133.
- [49] A. Zambelli, L. olive, P. Ammendola, *Gazz. Chem. It.* **1986**, 116, 259.
- [50] V. Busico, P. Corradini, L. DeMartino, A. Proto, E. Albizzati, *Makromol. Chem.* **1986**, 187, 1115.
- [51] N. Kashiwa, J. Yoshitake, *Makromol. Chem.* **1984**, 185, 1133.
- [52] J. C. W. Chien, J.C. Wu, *J. Polym. Sci. Part A: Polym. Chem.* **1982**, 20, 2461.
- [53] S. Weber, J. C. W. Chien, Y. Hu, *J. Polym. Sci. Part A: Polym. Chem.* **1989**, 27, 1499.

- [54] R. Spitz, J. L. Lacombe, A. Guyot, *J. Polym. Sci. Part A: Polym. Chem.* **1984**, 22, 2625.
- [55] Montedison, *U. S. Patent 4315836* **1980**.
- [56] A. W. Langer, T. J. Burkhardt, J. J. Steger, *Polym. Sci. Technol.* **1983**, 19, 225.
- [57] T. J. Burkhardt, A. W. Langer, D. Barist, W. G. Funk, T. Gaydos, R. P. Quirk (Ed.), *Transition Metal Catalyzed Polymerizations, ZN and Metathesis Polymerizations*, Cambridge University Press **1988**, p. 227.
- [58] N. Kashiwa, S. Kojoh, *Macromol. Symp.* **1995**, 89, 27.
- [59] J. C. Chadwick, A. Miedema, O. Sudmeijer, *Makromol. Chem.* **1994**, 195, 167.
- [60] (a) A. Proto, L. Oliva, C. Pellecchia, A. J. Sivak, L. A. Cullo, *Macromol.* **1990**, 23, 2904. (b) M. C. Sacchi, F. Forlini, I. Tritto, R. Mendichi, G. Zannoni, L. Noristi, *Macromol.* **1992**, 25, 5914. (c) J. V. Seppala, M. Harkonen, L. Luciani, *Makromol. Chem.* **1989**, 190, 2535. (d) M. Harkonen, L. Kuutti, J. V. Sepala, *Makromol. Chem.* **1992**, 193, 1413.
- [61] (a) Idemitsu, *European Patent Appl. 452916* **1991**. (b) Amoco, *European Patent Appl. 419249* **1991**.
- [62] T. Okano, K. Chida, H. Furuhashi, A. Nakano, S. Ueki, T. Keii, K. Soga (Eds.), *Catalytic Olefin Polymerization*, Kodansha, Elsevier **1990**, p. 177.
- [63] M. Kakugo, T. Miyatake, Y. Naito, K. Mizunuma, *Macromol.* **1988**, 21, 314.
- [64] S. Floyd, T. Heiskanen, T. Taylor, T. W. Taylor, *J. Appl. Polym. Sci.* **1987**, 33, 1021.
- [65] N. Kashiwa, J. Yoshitake, *Polym. Bull.* **1984**, 12, 99.

Chapter 1
General Introduction

- [66] (a) J. A. Ewen, *J. Am. Chem. Soc.* **1984**, 106, 6355. (b) A. Zambelli, P. Ammendola, A. Grassi, P. Longo, A. Proto, *Macromol.* **1986**, 19, 2703.
- [67] G. Natta, *J. Inorg. Nucl. Chem.* **1958**, 8, 589.
- [68] E. J. Arlman, P. Cossee, *J. Catal.* **1964**, 3, 99.
- [69] G. Allegra, *Makromol. Chem.* **1971**, 145, 235.
- [70] P. Corradini, V. Busico, G. Guerra, G. C. Eastmann, A. Ledwith, S. Russo, P. Sigwalt, (Eds.), *Comprehensive Polymer Science*, , Pergmon Press **1989**, 4, p. 2950.
- [71] (a) P. Patat, H. Sinn, *Angew. Chem.* **1958**, 70, 96. (b) G. Natta, G. Mazzanti, *Tetrahedron* **1960**, 8, 86. (c) L. A. Rodriguez, H. M. van Looy, *J. Polym. Sci. A1* **1966**, 4, 1971.
- [72] U. Giannini, G. Giunchi, E. Albizzati, P. C. Barbe, M. Fontanille, A. Guyot (Eds.), *Recent Advances in Mechanistic and Synthetic Aspects of Polymerization, NATO ASI Sect. 215, D. Reidel Publishing Co.* **1987**, p. 473.
- [73] E. Albizzati, U. Giannini, G. Morini, C. A. Smith, R. Ziegler, G. Fink, R. Mulhaupt, H. H. Brintzinger, *Ziegler Catalysts, Springer Verlag* **1995**, p. 413.
- [74] V. Busico, P. Corradini, A. Ferraro, L. DeMartino, A. Proto, V. Savino, E. Albizzati, *Makromol. Chem.* **1985**, 186, 1279.
- [75] P. Corradini, U. Barone, R. Fusco, G. Guerra, *Gazz. Chem. Ital.* **1983**, 113, 601.
- [76] Y. Doi, *Makromol. Chem. Rapid Commun.* **1982**, 3, 635.
- [77] J. Xu, L. Feng, S. Yang, *Macromol.* **1997**, 30, 2539.

- [78] V. Busico, R. Cipullo, G. Monaco, G. Talarico, M. Vacatello, *Macromolecules* **1999**, 32, 4173.
- [79] H. Mori, K. Hasebe, M. Terano, *Polym.* **1999**, 40, 1389.
- [80] B. Liu, T. Nitta, H. Nakatani, M. Terano, *Macromol. Chem. Phys.* **2003**, 203, 2412.
- [81] T. Taniike, M. Terano, *J. Catal.* **2012**, 293, 39.
- [82] G. Natta, P. Pino, E. Mantica, F. Danusso, G. Mazzanti, M. Peraldo, *Chim. Ind. (Milan)* **1956**, 38, 24.
- [83] A. Zambelli, P. Locatelli, M. C. Sachhi, I. Tritto, *Macromol.* **1982**, 12, 831.
- [84] A. Zambelli, P. Longo, C. Pellicchia, A. Grassi, *Macromol.* **1987**, 20, 2035.
- [85] V. Busico, P. Cipullo, P. Corradini, *Makromol. Chem. Rapid Commun.* **1992**, 13, 15.
- [86] A. Toyota, T. Tsutsui, N. Kashiwa, *J. Mol. Catal.* **1989**, 56, 237.
- [87] V. A. Zakharov, G. D. Bukatov, Y. I. Yermakov, *Adv. Polym. Sci.* **1983**, 51, 61.
- [88] G. Guastalla, U. Giannini, *Makromol. Chem. Rapid Commun.* **1983**, 1, 519.
- [89] (a) M. N. Berger, B. M. Grievesson, *Makromol. Chem.* **1965**, 83, 80. (b) W. H. Buls, T. L. Higgins, *J. Polym. Sci. Part A. Polym. Chem.* **1970**, 8, 1025.
- [90] L. Noristi, E. Marchetti, G. Baruzzi, P. Sgarzi, *J. Polym. Sci. Part A. Polym. Chem.* **1994**, 32, 3047.
- [91] S. Floyd, T. Heiskanen, T. W. Taylor, *J. Polym. Sci. Part A. Polym. Chem.* **1987**, 33, 1021.
- [92] (a) Z. Grof, J. Kosek, M. Marek, *AIChE J.*, **2005**, 51, 2048. (b) Z. Grof, J. Kosek, M. Marek, *Ind. Eng. Chem. Res.*, **2005**, 44, 2389.

- [93] R. A. Hutchinson, W. H. Ray, *J. Appl. Polym. Sci.* **1987**, 34, 657.
- [94] R. A. Hutchinson, C. M. Chen, W. H. Ray, *J. Appl. Polym. Sci.* **1992**, 44, 1389.
- [95] J. G. Wang, H. Chen, B. T. Huang, *Makromol. Chem.* **1993**, 194, 1807.
- [96] (a) K. Soga, T. Ouzumi, J. R. Park, *Makromol. Chem.* **1990**, 191, 2853. (b) H. N. Cheng, M. Kakugo, *Macromol.* **1991**, 24, 1724.
- [97] J. F. Ross, *J. Macromol. Sci. Chem.* **1984**, A21, 453.
- [98] J. Boor Jr., *ZN Catalysts and Polymerizations*, Academic Press, New York **1979**, p. 468.
- [99] T. F. L. McKenna, *Macromol. Symp.*, **2007**, 260, 65.
- [100] A. Di. Martino, G. Weickert, T. F. L. McKenna, *Macromol. React. Eng.* **2007**, 1, 165.
- [101] C. Przbyla, B. Tesche, G. Fink, *Macromol Rapid Commun.* **1999**, 20, 328.
- [102] (a) T. Keii, E. Suzuki, M. Tamura, M. Murata, Y. Doi, *Makromol. Chem.* **1982**, 183, 2285. (b) J. S. Yoon, W. H. Ray, *Ind. Eng. Chem. Res.* **1987**, 26, 415. (c) N. M. Ostrovskii, F. Kenig, *J. Chem. Eng.* **2005**, 107, 73. (d) H. Mori, K. Hasebe, M. Terano, *Polym.* **1999**, 40, 1389.
- [103] S. Y. Lim, S. Choung, *J. Appl. Catal. A, Gen.* **1997**, 153, 103.
- [104] (a) H. Mori, M. Yamahiro, M. Terano, M. Takahashi, T. Matsukawa, *Macromol. Chem. Phys.* **2000**, 201, 289. (b) N. Murayama, B. Liu, M. Terano, *Polym. Int.* **2004**, 53, 723. (c) B. Liu, N. Murayama, M. Terano, *Ind. Eng. Chem. Res.* **2005**, 44, 2382.
- [105] T. Keii, K. Soga, M. Terano (Eds.), *Catalyst Design for Tailor-Made Polyolefins*, Kodansha-Elsevier, Amsterdam London New York Tokyo **1994**, 89, 1.
- [106] D. R. Burfield, I. D. Mc Kenzie, P. J. T. Tait, *Polym.* **1972**, 13, 302.

- [107] T. Keii, *J. Res. Inst. Catal. Hokkaido Univ.* **1980**, 28(3), 243.
- [108] L. L. Bohm, *Polym.* **1978**, 19, 545.
- [109] A. K. Ingberman, I. G. Levine, R. J. Turbett, *J. Polym. Sci. Part A. Polym. Chem.* **1966**, 4, 2781.
- [110] P. J. T. Tait, *Coordination Polymerization, Academic Press* **1975**, p. 155.
- [111] (a) T. Keii, E. Suzuki, M. Tamura, Y. Doi, *Makromol. Chem.* **1994**, 195, 167. (b) F. Machado, E. L. Lima, J. C. Pinto, T. F. Mckenna, *Polym. Eng. Sci.* **2011**, 51, 302.
- [112] T. Keii, M. Terano, K. Kimura, K. Ishii, *Makromol. Chem. Rapid Commun.* **1987**, 8, 583.
- [113] T. Keii, M. Terano, K. Kimura, K. Ishii, W. Kaminsky, H. Sinn (Eds.), *Transition Metals and Organometallics as Catalyst for Olefin Polymerization*, Springer Verlag, Berlin **1988**.
- [114] B. Liu, H. Matsuoka, M. Terano, *Macromol. Rapid. Commun.* **2001**, 22, 1.
- [115] T. Taniike, S. Sano, M. Ikeya, V. Q. Thang, M. Terano, *Macromol. React. Eng.* **2012**, 6, 275.
- [116] C. Vasile (Ed.), *Handbook of Polyolefins, Marcel Dekker, New York* **2000**.
- [117] (a) H. Schneko, W. Dost, W. Kern, *Makromol. Chem.* **1969**, 121, 159. (b) K. Seenivasan, A. Sommazzi, F. Bonino, S. Bordiga, E. Groppo, *Chem. Eur. J.* **2011**, 17, 8648.
- [118] (a) P. Galli, J. C. Haylock, *Prog. Polym. Sci.* **1991**, 16, 443. (b) A. Dashti, S. A. A. Ramazani, Y. Hiraoka, S. Y. Kim, T. Taniike, M. Terano, *Macromol. Symp.* **2009**, 285, 52.

Chapter 1
General Introduction

[119] (a). E. J Nagel, V. A. Kirilov, W. H. Ray, *Ind. Eng. Chem.* **1980**, 19, 372. (b) T. F. L. Mckenna, R. Spitz, D. Cockljat, *AIChE.* **1999**, 45, 2393. (c) T. F. Mckenna, J. B. P. Soares, *Chem. Eng. Sci.* **2001**, 56, 3931.

Chapter 2

Understanding chemical and physical transformations of Ziegler-Natta catalyst at initial stage of propylene polymerization kinetics: Key role of alkylaluminium in the catalyst activation process

2.1 Introduction

One of the most interesting and significant discoveries in the 20th century in the field of plastics is the invention of the Ziegler-Natta (ZN) catalyst.^[1] The basis of state-of-the-art high-activity ZN catalyst lay in the discovery of “activated” MgCl₂, which support TiCl₄ and give high catalyst activity for both ethylene and propylene polymerization.^[2] The excellent plant operability demands controlled kinetics as well as good polymer morphology from the view point of process economics and viability.^[3] The high activity ZN catalyst is generally formulated by synthesizing spherical supports.^[4] A variety of synthetic routes have been developed to obtain better solid pro-catalyst^[5] or pre-polymerized catalyst^[6] for controlling the kinetics and polymer morphology. However the reason for the origin of over-whelming ZN propylene polymerization kinetics is still unknown. Deeper understanding of basic aspects for polymerization kinetics will lead to further development in this area.

ZN olefin polymerization involves a series of physical and chemical phenomena. The polymerization initiates with alkylation and reduction of TiCl₄ by alkylaluminium as an activator.^[7] The polymer formation tends to progress on the surfaces of more accessible pores and build up stress in the pores to induce the pore breakage called fragmentation of catalyst particles. The catalyst fragmentation into sub-particles exposes less accessible or hidden TiCl₄, leading to the formation of new active sites.^[8] The deactivation of active sites also takes place in polymerization due to over-reduction of Ti species with alkylaluminum.^[9] One of the major stumble blocks for the precise understanding of ZN polymerization kinetics is the large heterogeneity of active sites. The nature and the state

of active sites in heterogeneous ZN catalyst largely vary due to the multiple interactions between various chemical components. These parallel phenomena decide kinetic behaviors of ZN catalyst in a complicated way.

A number of studies have been conducted to understand kinetic and morphological aspects of heterogeneous ZN olefin polymerization. Co-grinding MgCl₂-based ZN catalyst in propylene polymerization possess decay type kinetics and associated with the chemical factors *i.e.* deactivation of active sites by the over reduction of Ti- species.^[10] The empirical development in industrial ZN catalyst synthesis leads to the formation of spherical porous MgCl₂-supported ZN catalyst, which possess not only chemical but also physical characteristics responsible for the polymerization kinetics. Although many reports have been published on the catalyst deactivation [xxx] and fragmentation behavior of the catalyst cluster during polymerization but less attention has been paid to the catalyst activation and polymerization kinetics development. Many groups laid emphasis on the catalyst/polymer morphology development.^[11] Elegant morphological study of ZN catalyst for olefin polymerization was performed by Kakugo *et al.* using electron microscopy.^[12] They demonstrated that original catalyst clusters broke into small particles which are dispersed throughout the resulting polymer. Pater *et al.*^[10] carried out ZN propylene polymerization kinetics and morphological studies at extremely low reaction rates. They found that the polymerization rate drop significantly with increasing prepolymerization yield. They proposed these observations of polymerization kinetics to the change in catalyst/polymer morphology. Noristi *et al.* examined the particle growth mechanism in propylene polymerization with a spherical ZN catalyst, and showed that homogenous

Chapter 2

Understanding chemical and physical transformations of Ziegler-Natta catalyst at initial stage of propylene polymerization kinetics: Key role of alkylaluminium in catalyst activation process

polymer growth throughout the catalyst particles (essential to facilitate homogeneous fragmentation) should be attained by uniform distribution of active sites.^[13] In similar lines, Nooijen^[14] and Zheng *et al.*^[15] found that uniform diffusion of an activator throughout the catalyst particles is required to attain homogeneous fragmentation with controlled particle morphology. Nooijen also found that the maximum activity of a catalyst depends on the diffusion of an activator. In this way, previous studies have accumulated a collection of knowledge, directly as well as indirectly on the ZN polymerization kinetics and morphology development through different techniques and perspectives. However, the satisfactory cooperation of simultaneous physical and chemical phenomena based systematic discussion was lacking for the precise understanding of the ZN catalyst activation.

It is widely known that an initial stage of the polymerization exerts crucial influences on the polymerization kinetics and particle morphology development,^[16] where the polymerization conditions as well as the kind of polymer formed can strongly affect the particle morphology.^[17] McKenna *et al.* found that the initial instants of the polymerization are, perhaps, the most important of the reaction because in this phase heat and mass transfer resistances can be very significant and critical to decide the polymerization kinetics and particle morphology.^[18] The degree of the catalyst activation at an initial stage is also important: In industry, the catalyst activation is well controlled by pre-polymerization, which is a polymerization step performed under mild conditions to achieve gentle fragmentation leading to controlled particle morphology and superior kinetics.^[19] Taniike *et al.* tracked the initial particle morphology development using a SF technique and found

that spatial distribution of macropores in catalyst particles have significant participation in triggering catalyst particle fragmentation.^[20] The understanding of the catalyst activation behavior, especially in the early stages of olefin polymerization, represents an important research task, aiming at a controlled kinetics and good polymer particle morphology.

The importance of early stage of polymerizations was quite evident for thorough understanding of the kinetics and morphology development. The precise control of the polymerization time to trace the initial instants of polymerization can be achieved with SF method. Elegant studies by Terano *et al.*^[21], Keii *et al.*^[22], Mckenna *et al.*^[23] and Soga *et al.*^[24] have proved the efficacy of SF technique for elucidating the kinetic mechanism, real time information of active sites/intermediates and other kinetics parameters in quasi-living region (<0.2 s) for heterogeneous ZN olefin polymerization. The technique can also be employed for the morphological studies.^[25] Recently, SF technique has been greatly improved by Taniike *et al.*^[26] and termed it as large-scale stopped-flow (LSF) polymerization because of its ability to produce more amount of polymer per batch of polymerization. The LSF has successfully eradicated the viscosity development issues with polymerization as observed in conventional SF systems. Due to this, LSF can be employed for carrying the prolonged polymerization i.e. beyond quasi-living period. The ability of SF to conduct kinetic as well as morphological studies makes it a powerful tool to analyze the initial kinetics for understanding both the chemical as well as physical phenomenon simultaneously. To understand the series of phenomenon's in the order/fraction of seconds, the stopped-flow (SF) olefin polymerization technique can be used.

Chapter 2

Understanding chemical and physical transformations of Ziegler-Natta catalyst at initial stage of propylene polymerization kinetics: Key role of alkylaluminium in catalyst activation process

The window of possibilities for prolonged SF experiments was remained unexplored for understanding the catalyst activation. The objective of the present study is to make a systematic investigation for understanding the catalyst activation in ZN propylene SF prolonged polymerizations (0.1 – 5.0 s) in the terms of catalyst/polymer particle growth (physical transformations) and active site nature variation (chemical transformations). Role of activator in ZN catalysis is significant for deciding the fate of polymerization kinetics by its very initial activation capability for the polymerization. In current study, the concentration of activator has been varied in polymerization to observe the difference in the catalyst activation degree. The catalyst/polymer particle morphology was analyzed by using scanning electron microscope (SEM). The number average molecular weight (M_n) of polymers was acquired by gel permeation chromatography (GPC). The bivariate distribution of polymer molecular weight and the crystallinity were achieved by cross fractionation chromatography (CFC).

2.2 Experimental

2.2.1 Materials

Triisobutyl aluminum (TiBA, donated by Tosoh Finechem Co.), titanium tetrachloride (TiCl_4) and dehydrated tetrahydrofuran (THF) were used as delivered. *n*-Heptane and toluene were used after being passed through a column of 4A molecular sieve and bubbling with dry N_2 overnight. Diisobutylphthalate (DiBP) was dehydrated by molecular sieves 4A before being used as an internal donor. Propylene (kindly donated by Japan Polypropylene Co. and Sumitomo Chemical Co., Ltd.) was used as delivered.

2.2 Catalyst synthesis

A TiCl₄/DiBP/MgCl₂ catalyst was prepared from synthesized spherical Mg(OEt)₂ based on a patent^[27] with minor modifications^[28]. Briefly, 10 g of Mg(OEt)₂ and 80 ml of toluene were charged in a 200 ml flask equipped with a mechanical stirrer under N₂. Thereafter, 20 ml TiCl₄ was injected in the flask, and the mixture was heated to 90 °C followed by the addition of 2.7 ml of DiBP and reacted at 115 °C for 2 h. After that, the mixture was washed twice with 100 ml of toluene at 90 °C. The mixture was again reacted with newly added 20 ml of TiCl₄ in 80 ml of toluene at 115 °C for 2 h. Thus obtained catalyst was washed ten times with 200 ml of heptane at 40 °C. The Ti and DiBP contents in the catalyst were determined as 2.6 and 12 wt% respectively.

2.2.3 Propylene polymerization

In this study, a recently developed LSF apparatus illustrated in Figure 1 was employed. The idea of the LSF polymerization is quite similar to that for conventional SF polymerization: Catalyst slurry contained in a vessel (Vessel A) and activator solution contained in a separate vessel (Vessel B) are simultaneously transferred in tubes and then contacted at a T junction point to initiate the polymerization. The polymerization is carried out in a tube from C to D, until the polymerization mixture is cast to a quenching solution. The most important advantage of the SF polymerization is the capability to precisely control the polymerization time by adjusting either the tube length from C to D or the transfer rate of the polymerization slurry. In the LSF polymerization, the catalyst slurry

Chapter 2

Understanding chemical and physical transformations of Ziegler-Natta catalyst at initial stage of propylene polymerization kinetics: Key role of alkylaluminium in catalyst activation process

and activator solution agitated by a mechanical stirrer are transferred with the aid of a tubing pump at a pre-calibrated pumping speed, which facilitates not only greatly improved flow stability but also the reaction scalability in comparison with the conventional one. Especially, the high flow stability allows a constant transfer rate independently of the slurry viscosity, which gradually increases as the polymerization progresses. This feature of the LSF system has made it possible to apply a SF technique for prolonged polymerization like several-10 s with the time resolution of 0.03 s, while the polymerization time was at maximum around 1.0 s in the conventional system.

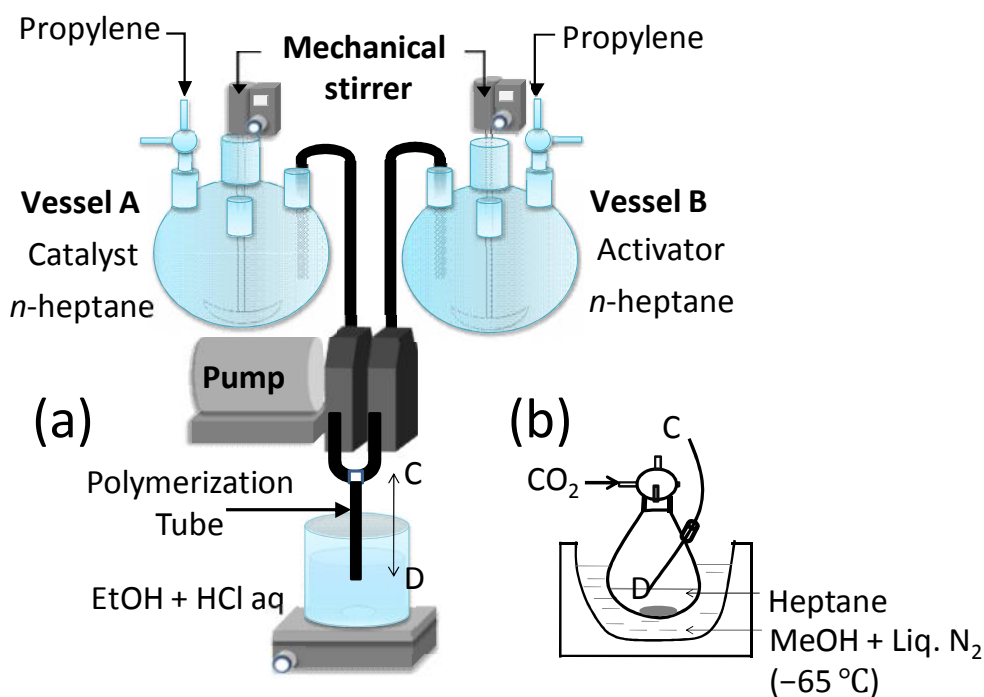


Figure 1 LSF apparatus

Catalyst slurry (8.5 mg/ml) and activator solution (70, 35, or 17.5 mM) in *n*-heptane were respectively prepared under N₂. A series of SF polymerizations from 0.1 s to 5.0 s were carried out at 1 atm and 30 °C by varying the TiBA concentration (70, 35 and 17.5 mM), while the catalyst concentration was kept constant. Monomer saturated slurry and solution were pumped out for polymerization at a pre-calibrated rate of 10 ml/s from each vessel. The polymerization was quenched by casting the polymerization mixture in excess acidic ethanol under high agitation (12,000 rpm). The polymer slurry was washed, dried and re-precipitated to obtain the polymerization kinetics.

In order to examine the morphology of catalyst/polymer particles, a special quenching method was adopted as shown in Figure 1 (b).^[22] The polymerization was quenched under CO₂ atmosphere in heptane at -65 °C. To improve the stability of particles in air, anhydrous THF (THF/Ti: 200/1 (mol/mol)) was added to the heptane. After the removal of upper solvent, the particles were dried and transferred to a vial under N₂ atmosphere.

2.2.4 Polymer analysis

Morphology observation

The surface and bulk morphologies of catalyst/polymer particles were observed by scanning electron microscopy (SEM, Hitachi S-4100). The bulk morphology was examined after the particles were randomly cut by a razor under N₂. The samples were coated with Pt-Pd for 100 s through an ion sputter (Hitachi E-1030) and finally transferred into the SEM equipment. Representative images for the morphologies were assured by measuring each sample twice and acquiring at least five images at each measurement.

GPC measurement

The molecular weight distribution of the obtained PP was determined by GPC (HT-GPC 350, Viscotek) at 140 °C in *o*-dichlorobenzene (ODCB) containing 0.03 wt% of butylated hydroxytoluene (BHT) as an antioxidant. The samples were subjected to hot filtration prior to the measurements.

Cross fractionation chromatography

The molecular weight and crystallinity distribution of polymer was simultaneously determined by CFC (T150A, Sumitomo Chemical Co., Ltd.) with ODCB as solvent. The instrument first fractionates the polymer according to the elution temperature by following the temperature rising elution fractionation (TREF) process, and the resultant fractions were injected in a stepwise manner to a GPC unit equipped with an infra-red (IR) detector.

2.3 Results and discussion

Polymerization kinetics

The spherical Mg(OEt)₂-based ZN catalyst is one of the most widely used industrial catalyst and known to exhibit mild activation behavior, where the activity gradually rises up along the polymerization time and maintains a plateau activity for a long time, *i.e.* build-up type kinetics.^[24, 25] On the other hand, previous SF studies on the ZN polymerization dictated that the polymer yield develops proportionally to the polymerization time with the activity kept at constant at the very initial stage.^[18] The continuity and discrepancy

between the increasing activity at the time scale of minutes and the constant activity at the time scale of a fraction of seconds have not yet been addressed.

The kinetic profile of the propylene polymerization was studied by a series of SF experiments from 0.1 s to 5.0 s at three different activator concentrations, while the catalyst concentration was kept constant. In Figure 2a, it was observed that the activator concentration critically affected the initiation of the kinetic profiles. At $[Al] = 70$ mM, the yield developed in a linear way (up to 0.5 s) with the time, where the zero intercept indicates the instantaneous active-site formation in accordance with previous studies. In the case of lower activator concentrations, the yields also developed almost proportionally to the time, but the yield levels became lower with the appearance of an induction period. The induction time was longer for $[Al] = 17.5$ mM (*ca.* 0.8 s) than for $[Al] = 35$ mM (*ca.* 0.4 s). It was also found that a higher activator concentration leads to a higher level of the yield, most plausibly because of a larger active-site concentration. Note that $TiCl_4$ itself is not active for the olefin polymerization, and needs to be reacted with alkyl aluminum.

Chapter 2

Understanding chemical and physical transformations of Ziegler-Natta catalyst at initial stage of propylene polymerization kinetics: Key role of alkylaluminium in catalyst activation process

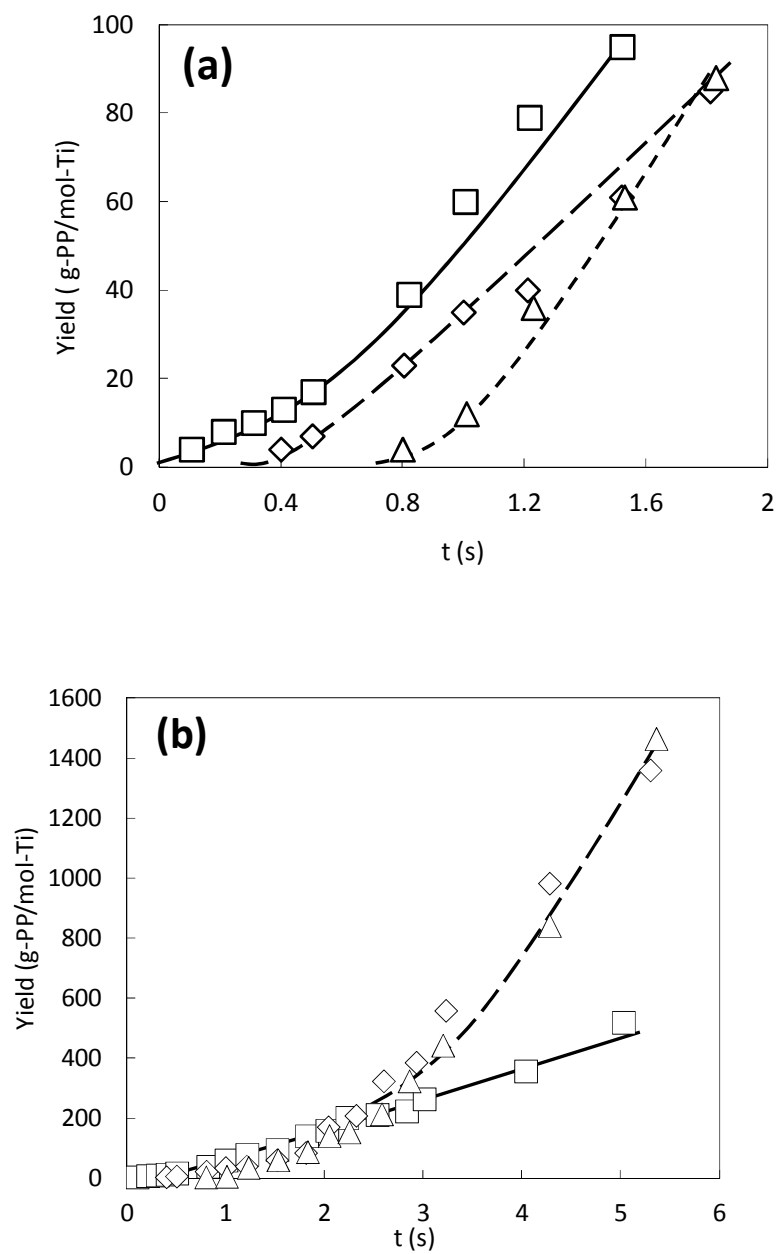


Figure 2 Polymerization kinetics trend at activator concentrations 17.5 mM (), 35 mM () and, 70 mM (), (a) up to *ca.* 1.8 s and (b) up to *ca.* 5.0 s.

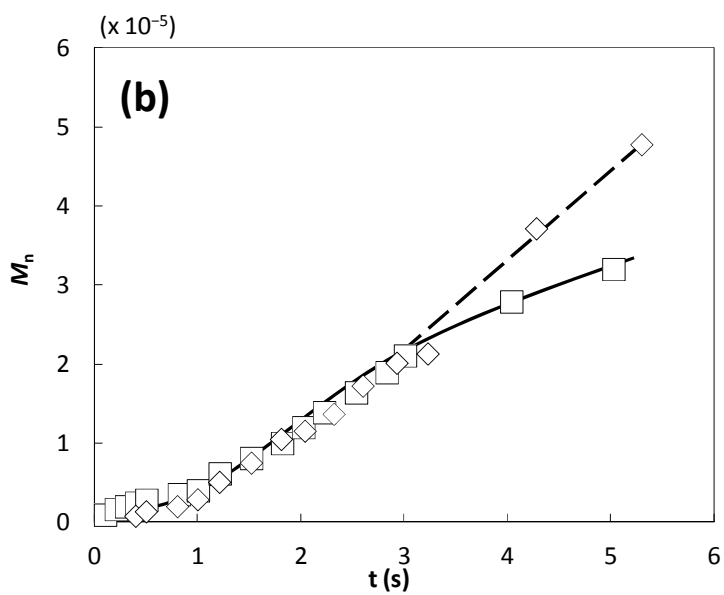
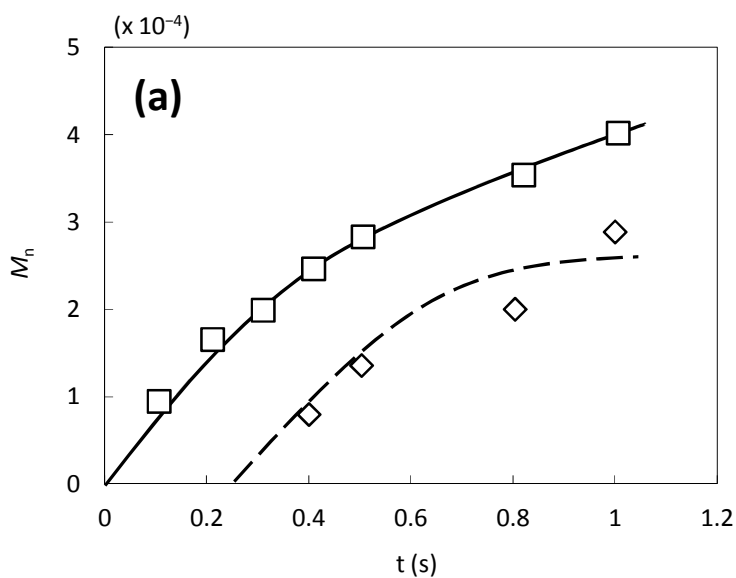


Figure 3 M_n v/s polymerization time at activator concentrations 35 mM () and, 70 mM (), (a) up to *ca.* 1.0 s and (b) up to *ca.* 5.0 s respectively.

Figure 2b shows the kinetic profiles up to 5.0 s. So far, the SF polymerization had been applied up to *ca.* 1.2 s^[29] due to the above-mentioned viscosity problem, and this was the first for the SF technique to be applied up to *ca.* 5.0 s. At [Al] = 70 mM, the linear yield increment up to about 0.5 s was followed by a non-linear rise up in the yield up to 5.0 s, where the catalyst activity given as the gradient of the yield monotonically increased along the time. This behavior corresponds to the build-up part of the kinetics, and we have successfully observed how the linear yield increment in the typical SF polymerization is continued to the build-up kinetics in the nominal polymerization. Similar trends were observed at lower activator concentrations ([Al] = 35, 17.5 mM): the kinetic profiles led to non-linear increments at *ca.* 0.8 s for [Al] = 35 mM and *ca.* 1.2 s for [Al] = 17.5 mM. The most noteworthy is that a higher activator concentration gave a higher yield in the linear region, but the yield became higher for a lower activator concentration due to a greater curvature. Thus, it was found that the activator concentration critically affected not only the initiation of the polymerization but also the continuing kinetic profiles in the build-up region, whose origin is examined later.

The origin of the linear yield increments is well known as a consequence of constant propagation rate constant and active-site concentration. In other words, the nature and number of active sites are kept unchanged after the formation. Accordingly, the observed build-up kinetics suggests both/either gradual increases in the active-site concentration and/or in the propagation rate constant. The polymer molecular weight (M_n) was obtained by GPC in order to address the origin of the build-up kinetics (Figure 3). At [Al] = 70 mM, a linear M_n increment corresponding to quasi-living polymerization was observed up to

about 0.4 s, while it showed a converging behavior up to about 1.0 s due to an increasing contribution of chain transfer reactions.^[30] Beyond 1.0 s, M_n started to linearly increase again but much more rapidly, indicating the increase in the propagation rate constant. At *ca.* 3.0 s, M_n again exhibited a convergent behavior. In the case of $[Al] = 35$ mM, a linear M_n increment was observed up to about 0.8 s, beyond which the M_n curve once showed a convergent behavior and again linearly developed from *ca.* 1.0 s with an enhanced curvature, similarly to the case of $[Al] = 70$ mM. Differently from $[Al] = 70$ mM, M_n continued a linear development over *ca.* 3.0 to 5.0 s. This difference over 3.0 s between the two activator concentrations is plausibly attributed to the frequency of the chain transfer reaction with alkyl aluminum. The molecular weight distribution was gradually broadened from around 3 to 6 with the progress of the polymerization.

In Figure 3, M_n showed a stepwise growth behavior, which can be roughly divided into three steps along the time: 1) a linear increment, 2) a saturating behavior, and 3) another linear increment at a higher rate than the first step. The steps 1) and 2) resulted from quasi-living polymerization and an increasing contribution of chain transfer reactions, respectively.^[30] On the other hand, the step 3) can be understood in terms of the ageing of active sites due to interaction/reaction with activator. It is known that a pretreatment of ZN catalyst with activator not only enhances the propagation rate constant of active sites but also prolong the lifetime of a growing chain.^{[31],[32]} In this context, it is plausible that the larger increment at the step 3) arose from active sites, whose nature was altered by activator during the polymerization.

In considering the origin of the observed transition in polymerization kinetics from

Chapter 2

Understanding chemical and physical transformations of Ziegler-Natta catalyst at initial stage of propylene polymerization kinetics: Key role of alkylaluminium in catalyst activation process

linear to build-up (Figure 2), the M_n development was compared with the yield development at different activator concentrations. In other words, we attempted to ascribe the kinetic transition either to an increase in the propagation rate constant or to an increase in the active site concentration. It was found that the yields built up in a non-linear way after the transition, while M_n increased always linearly or in a convergent way. Moreover, the magnitudes of the M_n increments were much smaller than those of the yields and hardly depended on the activator concentration, while the kinetic transition strongly depended on it. These considerations strongly suggested that the build-up kinetics was not relevant to the propagation rate constant, but from an increasing active site concentration. Thus, it was presumed that the exposure of hidden $TiCl_4$ with catalyst fragmentation play a major role for building up the polymerization rate. In order to get deeper understanding on the activation, we have separately studied plausible physical and chemical transformations by SEM and CFC in the subsequent sections, respectively.

Physical transformation

The role of physical transformations in the kinetic transition has been examined using SEM at different activator concentrations, where a special quenching method was employed to preserve the catalyst/polymer particle morphologies. Figure 4a represents the surface and bulk morphologies of the employed catalyst. Catalyst macro particles were nearly spherical, composed by secondary agglomeration of lamellar-shaped building units. The agglomeration manner of the building units decides the catalyst inner structure, especially

for the spatial distribution of macropores formed as interspaces among the building units. The cross-sectional view of the catalyst (Figure 4a: B,C) shows that the catalyst inner structure was composed by three-layered structures according to the manner of the secondary agglomeration: A dense outermost layer followed by a porous layer with the loosely packed building units and finally a tightly packed core.^[22] The vacant space in the catalyst cross-sectional image indicates macropores, which were mainly located in the mid porous layer.

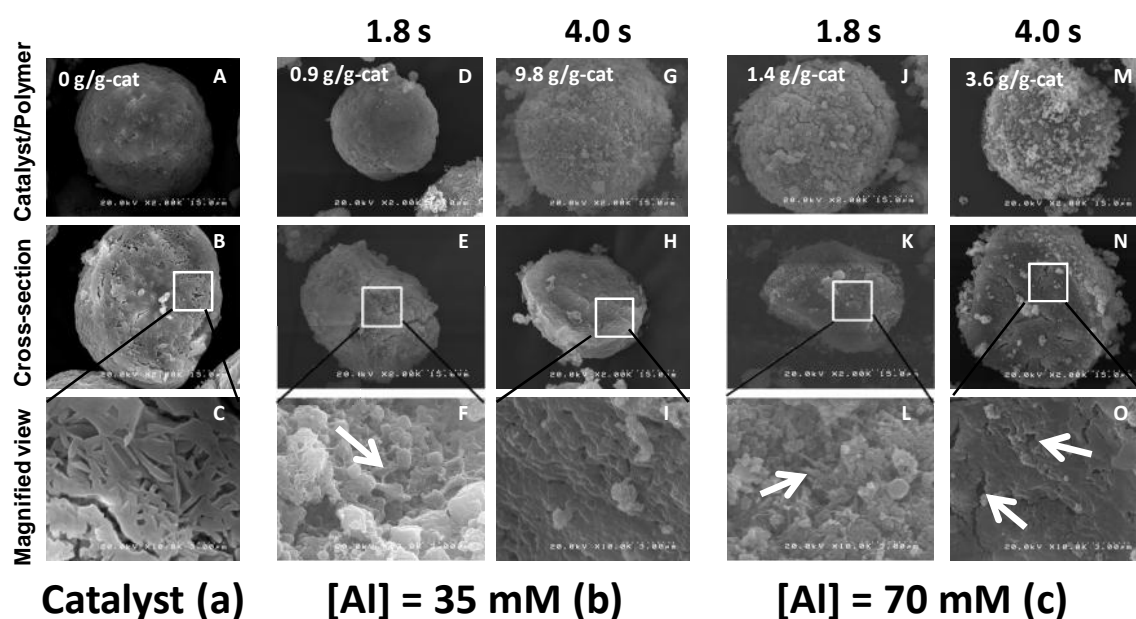


Figure 4 Surface and bulk SEM images of catalyst and catalyst/polymer particles at 1.8 s and 4.0 s for SF propylene polymerization at $[Al] = 35$ and 70 mM, respectively. The yield was mentioned in g-PP/g-cat to show the macroscopic phenomena of catalyst/polymer particle morphology development with polymerization kinetics.

Figure 4b,c shows SEM images for the catalyst/polymer particles obtained from the SF polymerization for 1.8 s and 4.0 s at two different activator concentrations: $[Al] = 35$ and 70 mM. At $[Al] = 35$ mM, the polymerization for 1.8 s (corresponding to 0.9 g-PP/g-cat) hardly changed the looking of particle surfaces (Figure 4b: D). However, on observing cross-sectional images (Figure 4b: E and F), it was found that the macropores of the particles were partially filled with the polymer, and some fibrillar structures were visible (pointed with arrows). It is widely accepted that such fibrillar structures result from the stretching of the formed polymer during the fragmentation of catalyst particles.^[25] With the progress of polymerization from 1.8 to 4.0 s (0.9 to 9.8 g-PP/g-cat), the particle surfaces became rougher by being covered by the formed polymer (Figure 4b: G). The cross-sectional view of the catalyst/polymer particles showed smooth texture to indicate that most of the catalyst macropores were filled with polymer (Figure 4b: H and I). At the higher activator concentration ($[Al] = 70$ mM), the morphological development for 1.8 s (Figure 4c: J,K and L) rather exhibits rough particle surfaces while the inner morphology of partial macropores filling and fibril formation was similar with lower activator concentration. On the other hand, significant differences were observed at 4.0 s (Figure 4c-M). Even producing a sufficient amount of polymer (3.6 g-PP/g-cat), the particle surfaces were not smooth but even became rougher than those at 1.8 s. The cross-sectional images clarified a thick polymer shell was formed on the particle periphery, while a relatively great part of macropores remained unfilled (pointed with arrows) and the layered structures were still clearly visible (Figure 4c, N and O). This fact indicated that the polymer was rather

selectively formed on the surfaces, and consequently the fragmentation inside the particles progressed less compared with the case of the lower activator concentration.

Thus, it was found that the difference in the activator concentration caused significant impact on the morphological development, and it must be directly related to the observed difference in the kinetics. Using a variety of activators, Nooijen concluded that the diffusion of an activator in the catalyst particles plays a critical role in determining the mode of the fragmentation at the initial stage of the polymerization.^[14] They observed that a less bulkier activator diffuses more deeply inside the catalyst particles, and thus causes the uniform fragmentation, while a bulkier activator exhibited retarded diffusion in the catalyst particles and results in non-uniform fragmentation. Zheng *et al.* also found that activator diffusion uniformly inside catalyst particles is a prerequisite for uniform fragmentation.^[33] Taniike *et al.* postulated that macropore filling is a critical step for initiating the catalyst fragmentation.^[20] On the other hand, it is widely accepted that polymer layer formed on catalyst surfaces can retard the diffusion of monomer or even alkylaluminum (*i.e.* the filter effect).^[34] At the lower activator concentration ($[Al] = 35$ mM), the macropores were almost fully filled at 1.8 s (Figure 4b: H and I). This fact could be considered as a result of uniform activator diffusion, as was seen in the uniform catalyst fragmentation at 4.0 s. On the other hand, the SF polymerization at the higher activator concentration (70 mM) facilitated the higher initial activity, thus forming a greater amount of polymer on accessible surfaces (Figure 4c: M). However, a greater amount of polymer on the surfaces must retard the diffusion of monomer and alkylaluminum, which could be confirmed by unfilled porosity at 1.8 s and a much smaller degree of the inner

fragmentation at 4.0 s. The observed great difference in the magnitude of the fragmentation at the two activator concentrations was believed as the origin of the different kinetics, especially in terms of the non-linear yield enhancement. It was envisaged that uniform fragmentation exposes a greater quantity of hidden surfaces, and polymerization on these newly exposed surfaces accelerate further fragmentation, which is believed as the origin of the sudden and non-linear kinetics.

Chemical transformation

In heterogeneous ZN olefin polymerization, the polymer structure, more or less, represents the average nature of active sites in the catalyst responsible for their formation. One of the most comprehensive ways to obtain the full definition of polyolefin structures is a measurement by two dimensional distribution in terms of polymer molecular weight and tacticity distribution by CFC. In order to examine chemical transformations in terms of the average nature of active sites, selected polymer samples (1.0, 1.8 and 4.0 s at $[Al] = 35$ and 70 mM) were subjected to CFC measurements. A general view of raw and differential CFC plots was as shown in Figure 5. The CFC contour plots are represented in Figure 6. CFC data are composed of three axes, namely, polymer elution temperature (T), polymer MW (LogMW), and polymer fraction at each T and Log MW ($P(T, \text{LogMW})$). The T value has direct correlation with the polymer stereoregularity *i.e.* active site stereospecificity.^[35]

In order to examine the chemical transformations three-polymer samples were selected from 1.0 s, 1.8 s and 4.0 s. The raw and differential contour CFC plots were

generated. The differential CFC plots were generated using Equation 1.

$$P = P_{t_2 \rightarrow t_1} = P_{t_2}(T, \text{LogMW}) - P_{t_1}(T, \text{LogMW}) \quad 1$$

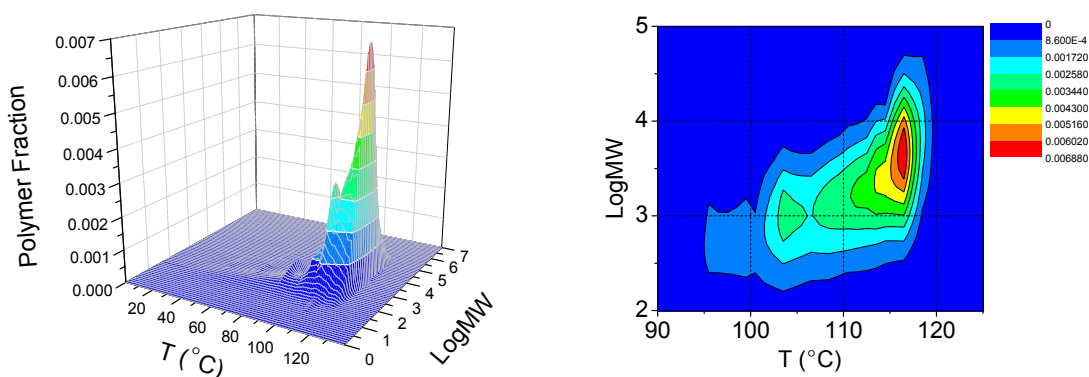


Figure 5 Representative 3D CFC plot with the corresponding contour plot showing the distribution of major polymer fraction.

Table 1 represents the center of mass for the observed change in polymer fraction with respect to T and LogMW for the differential CFC data.

Table 1 Differential CFC Data

[Al] (mM)	T (° C) (1.8 s – 1.0 s)	LogMW	T (° C) (4.0 s – 1.8 s)	LogMW	P _{1.0 → 1.8}	P _{1.8 → 4.0}
					(%)	(%)
35	20.2	1.1	5.8	1.4	9.7	17.4
70	17.9	0.9	18.3	0.9	9.3	14.0

Chapter 2

Understanding chemical and physical transformations of Ziegler-Natta catalyst at initial stage of propylene polymerization kinetics: Key role of alkylaluminium in catalyst activation process

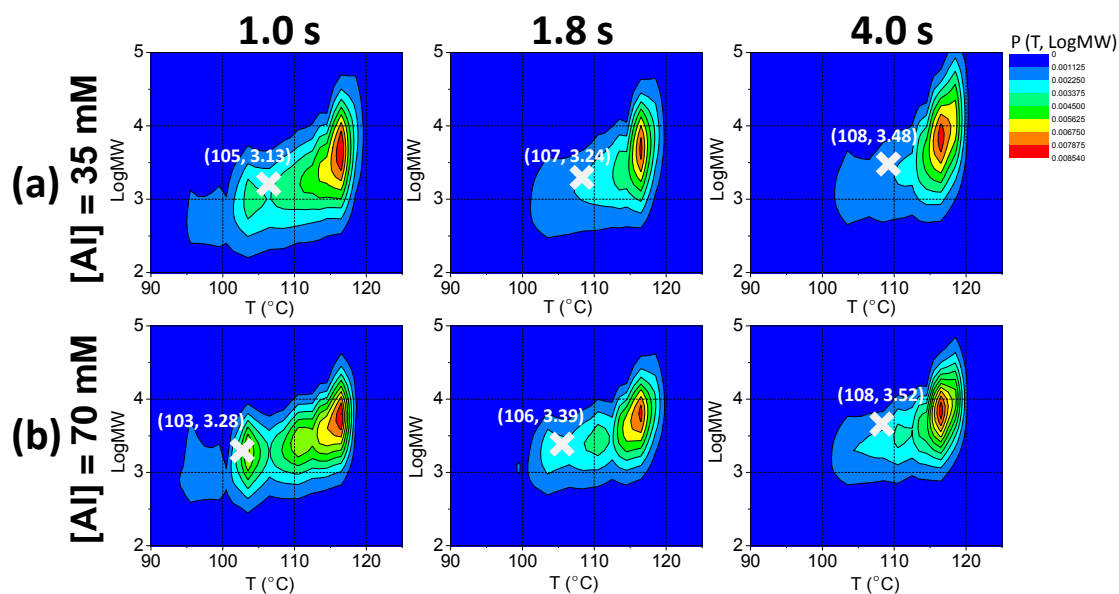


Figure 6 CFC contour plots for polymer at 1.0 s, 1.8 s and 4.0 s obtained with SF polymerization at (a) $[Al] = 35$ mM and (b) $[Al] = 70$ mM, respectively.

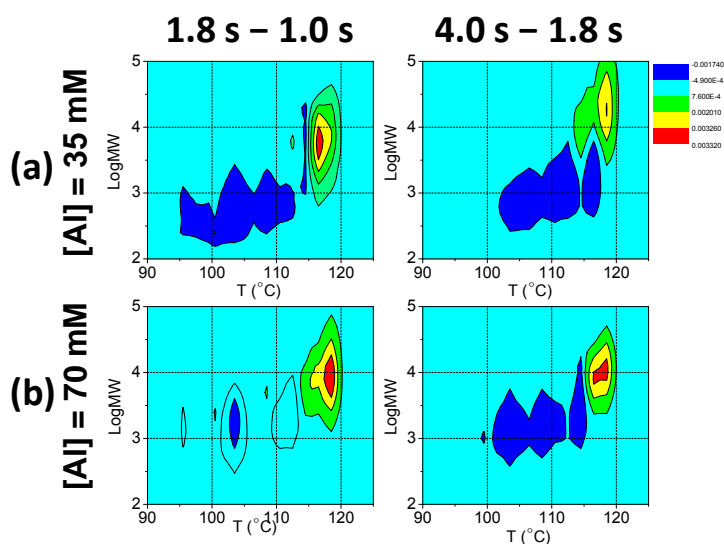


Figure 7 Differential CFC contour plots for polymer at 1.8 s – 1.0 s, 4.0 s – 1.8 s at (a) $[Al] = 35$ mM and (b) $[Al] = 70$ mM, respectively.

CFC contour plots appeared more or less similar as they all possessed most of polymer fraction concentrated at higher T and LogMW and a tail pointing towards lower T and LogMW. Figure 6a ([Al] = 35 mM), represents that at *ca.* 1.0 s the center of mass of the contour plot exists at co-ordinates (105, 3.13). The center of mass represents the average positioning of the polymer fractions along this sample. On increasing the polymerization time to 1.8 s, a shift in the polymer fraction was observed towards larger T and LogMW. The center of mass of the contour plot at 1.8 s exists at co-ordinates (107, 3.24). This shows that with the increment of polymerization time from *ca.* 1.0 s to 1.8 s the polymer possess dominantly higher stereoregularity i.e. formed by highly isospecific active sites. It is known that increase in polymer isotacticity accompany the increase of chain propagation capabilities of the active sites. It can be envisaged that during this region the chemical transformations possess variation in the nature of active sites, which were dominantly isospecific in nature. Thereafter at 4.0 s, a shift in the polymer fraction was observed towards larger T and LogMW. The center of mass of the contour plot at *ca.* 1.8 s exists at co-ordinates (108, 3.48). In Table 1, [Al] = 35 mM, the $P_{1.0 \rightarrow 1.8 s}$ represents that the differential area under the Figure 7a changes with +9.7 %. However the $P_{1.8 \rightarrow 4.0 s}$ show that the differential area was further increased by +17.4 %. These areas demonstrate the chemical transformations occurred in the ZN catalyst for the defined region. The increase in T was found to be slower as compared to LogMW. These results clearly demonstrate the nature of active sites on moving at *ca.* 4.0 s was governed by superior chain propagation capabilities.

In the Figure 6b ([Al] = 70 mM) similar contour plots were observed for 1.0 s and

Chapter 2

Understanding chemical and physical transformations of Ziegler-Natta catalyst at initial stage of propylene polymerization kinetics: Key role of alkylaluminium in catalyst activation process

1.8 s. It was observed that at *ca.* 4.0 s the polymer fraction distribution range was nearly similar as observed at 1.8 s. The center of mass of the contour plot at *ca.* 4.0 s exits at (108, 3.52). It shows that at *ca.* 4.0 s the polymer stereoregularity (active site isospecificity) increases accompanied with slower increase in LogMW. The suppression of the chain elongation due to enhanced chain transfer at 4.0 s can be attributed to the greater degree of active sites ageing with higher activator content. In Table 1, $[Al] = 70$ mM, the $P_{1.0 \rightarrow 1.8 s}$ represents that the differential area under the Figure 7b changes by +9.3 %. On the other hand the $P_{1.8 \rightarrow 4.0 s}$ show that the differential area was increased by 14.0 %. The $P_{1.8 \rightarrow 4.0 s}$ for $[Al] = 70$ mM was found to be smaller than the $[Al] = 35$ mM. These results clearly revealed that the nature of active sites in the two regions i.e. from 1.0 s to 1.8 s and 1.8 s to 4.0s, were changed but with quite slower pace and showing gradual transformation of the active sites. The results clearly exemplify that the higher activator concentration play major role for regulating the MW development with enhanced chain transfer capabilities.

In summary, it was found that the catalyst undergoes both physical and chemical transformations during the polymerization up to 5.0 s. However, catalyst fragmentation, *i.e.* the physical transformation, dominated the polymerization kinetics, whose detail was strongly dependent on the activator concentration. The location and amount of initially formed polymer on/in catalyst particles significantly regulated subsequent polymerization kinetics through the diffusion limitation. On the other hand, the chemical transformation was mainly based on the ageing of active sites with activator, which affected the chain growth behavior of the polymers.

2.4 Conclusions

An improved stopped-flow (SF) technique was employed to clarify the origin of kinetics in propylene polymerization with $\text{Mg}(\text{OEt})_2$ -based Ziegler-Natta catalyst. Polymerization in the range of 0.1-5 s exhibited kinetic transition from a linear development to a build-up-type development of the yield. It was found that a lower alkylaluminum concentration led to a lower yield in the linear regime, while the extent of the activation became greater in the build-up regime. The origin of these kinetic behaviors was studied using scanning electron microscopy (SEM) for catalyst/polymer particles and cross-fractionation analyses for polymer structures. It was found that the kinetic transition mainly arose from the fragmentation of the catalyst particles and resultant increase in the active-site concentration. The fragmentation manner strongly depended on the alkylaluminum concentration, which affected not only the amount but also the placement of initial polymer formation. The nature of active sites varied as a result of an aging effect with alkylaluminum: their stereospecificity, propagation rate constant and tolerance for chain transfer reactions increased as the polymerization progressed.

Chapter 2

Understanding chemical and physical transformations of Ziegler-Natta catalyst at initial stage of propylene polymerization kinetics: Key role of alkylaluminium in catalyst activation process

References

- [1] E. P. Moore, Jr., “*Polypropylene Handbook*”, 1st edition, Hanser Publishers, New York **1996**, p. 11.
- [2] (a) P. Galli, G. Vecellio, *J. Polym. Chem.* **2004**, 42, 396. (b) A. Correa, F. Piemontesi, G. Morini, L. Cavallo, *Macromol.* **2007**, 40, 9181. (c) V. Busico, M. Causa, R. Cipullo, R. Credendino, F. Cutillo, N. Freiderichs, R. Lamanna, A. Segre, A. V. V. Castelli, *J. Phys. Chem. C.* **2008**, 112, 1081.
- [3] (a) P. Galli, P. C. Barbe, L. Noristi, *Angew. Makromol. Chem.* **1984**, 120, 73. (b) G. Cecchin, E. Marchetti, G. Baruzzi, *Macromol. Chem. Phys.* **2001**, 202, 1987.
- [4] L. A. Almeida, M.D. F.V. Marques, *Macromol. React. Eng.* **2012**, 6, 57.
- [5] R. A. Jorgensen, M. A. Kinnan, M. D. Turner, S. M. Whited, L. L. Ban, B. E. Wagner, *US Patent 8173569 B2*, **2012**.
- [6] K. I. Pentti, P. Leskinen, *US Patent 5641721*, **1999**.
- [7] (a) P. Cosee, *J. Catal.* **1964**, 3, 80. (b) J. J. A. Dusseault, C. C. Hsu, *J. Macromol. Sci., Rev. Macromol. Chem. Phys.* **1993**, C33, 103.
- [8] G. Cecchin, E. Marchetti, G. Baruzzi, *Macromol. Chem. Phys.* **2001**, 202, 1987. (b) F. Machado, J. P. Broyer, C. Novat, E. L. Lima, J. C. Pinto, T. F. McKenna, *Macromol. Rapid Commun.* **2005**, 26, 1846.
- [9] (a) T. Keii, E. Suzuki, M. Tamura, M. Murata, Y. Doi, *Makromol. Chem.* **1982**, 183, 2285. (b) J. S. Yoon, W. H. Ray, *Ind. Eng. Chem. Res.* **1987**, 26, 415. (c) N. M. Ostrovskii,

- F. Kenig, *J. Chem. Eng.* **2005**, 107, 73. (d) H. Mori, K. Hasebe, M. Terano, *Polym.* **1999**, 40, 1389.
- [10] (a) N. Kashiwa, J. Yoshitake, *Makromol. Chem.* **1984**, 185, 1133. (b) V. Busico, P. Corradini, A. Ferraro, A. Proto, *Makromol. Chem.* **1986**, 187, 1125.
- [11] M. Abboud, P. Denifl, K. H. Reichert, *J. Appl. Polym. Sci.* **2005**, 98, 2191.
- [12] M. Kakugo, H. Sadatoshi, J. Sakai, “*Catalytic olefin polymerization*”, T. Keii, K. Soga, Eds., Kodansha-Elsevier, Tokyo, **1990**, p. 345.
- [13] L. Noristi, E. Marchetti, G. Baruzzi, P. Sgarzi, *J. Polym. Sci. A*, **1994**, 32:3047.
- [14] (a) G. A. H Nooijen, *Catal. Today* **1991**, 11, 35. (b) G. A. H. Nooijen, *Eur. Polym. J.* **1994**, 30, 11.
- [15] X. Zheng, M. Smit, J. C. Chadwick, J. Loos, *Macromol.* **2005**, 38, 4673.
- [16] A. Di. Martino, G. Weickert, T. F. L. Mckenna, *Macromol. React. Eng.* **2007**, 1, 165.
- [17] (a). E. J Nagel, V. A. Kirilov, W. H. Ray, *Ind. Eng. Chem.* **1980**, 19, 372. (b) R. A. Hutchinson, C. M Chen, W. H. Ray, *J. Appl. Polym. Sci.* **1992**, 44, 1389. (c) T. F. L. Mckenna, R. Spitz, D. Cockljat, *AIChE.* **1999**, 45, 2393.
- [18] F. Machado, E. L. Lima, J. C. Pinto, T. F. Mckenna, *Polym. Eng. Sci.* **2011**, 51, 302.
- [19] (a) M. T. J. Pater, G. Weickert, M. P. W. van Swaaji, *AIChE*, **2003**, 49, 180. (b) M. T. J. Pater, G. Weickert, M. P. W. van Swaaji, *J. Appl. Polym. Sci.* **2003**, 87, 1421.

Chapter 2

Understanding chemical and physical transformations of Ziegler-Natta catalyst at initial stage of propylene polymerization kinetics: Key role of alkylaluminium in catalyst activation process

- [20] T. Taniike, V. Q. Thang, N. T. Binh, Y. Hiraoka, T. Uozumi, M. Terano, *Macromol. Chem. Phys.* **2011**, 212, 723.
- [21] (a) T. Keii, M. Terano, K. Kimura, K. Ishii, *Makromol. Chem. Rapid Commun.* **1987**, 8, 583. (b) B. Liu, H. Matsuoka, M. Terano, *Macromol. Rapid Commun.* **2001**, 22, 1.
- [22] T. Keii, K. Soga, “*Catalytic Olefin Polymerization*”, Elsevier, Tokyo, **1989**, p. 166.
- [23] A. Di. Martino, J. P. Broyer, D. Schweich, C. D. Bellefon, G. Weickert, T. F. L. McKenna, *Macromol. React. Eng.* **2007**, 1, 284.
- [24] (a) M. Kaminaka, K. Soga, *Polym.* **1992**, 33, 1105. (b) M. Kaminaka, K. Soga, *Macromol. Chem. Phys. Rapid Commun.* **1991**, 12, 367.
- [25] V. Q. Thang, T. Taniike, M. Umemori, M. Ikeya, Y. Hiraoka, N. D. Nghia, M. Terano, *Macromol. React. Eng.* **2009**, 3, 467.
- [26] T. Taniike, S. Sano, M. Ikeya, V. Q. Thang, M. Terano, *Macromol. React. Eng.* **2012**, 6, 275.
- [27] M. Terano, K. Kimura, A. Murai, M. Inoue, K. Miyoshi, *JP Patent S62-158704*, **1987**.
- [28] A. Dashti, A. Ramazani, Y. Hiraoka, S. Y. Kim, T. Taniike, M. Terano, *Polym. Int.* **2008**, 58, 40.
- [29] H. Mori, M. Yamahiro, M. Terano, M. Takahashi, T. Matsukawa, *Macromol. Chem. Phys.* **2000**, 201, 289.

- [30] M. Ikeya, Y. Hiraoka, T. Taniike, M. Terano, *Current Trends Polym. Sci.* **2012**, 16, 101.
- [31] H. Mori, M. Yamahiro, M. Terano, M. Takahashi, T. Matsukawa, *Macromol. Chem. Phys.* **2000**, 201, 289.
- [32] T. Nitta, B. Liu, H. Nakatani, M. Terano, *J. Mol. Catal. A: Chem.* **2002**, 180, 25.
- [33] X. Zheng, J. Loos, *Macromol. Symp.* **2006**, 236, 249.
- [34] (a) S. [Floyd, K. Y. Choi; T. Taylor, W.H. Ray, *J. Appl. Polym. Sci.* **1986**, 32, 2935. (b) T. F. Mckenna, F. Barbotin, R. J. Spitz, *Appl. Polym. Sci.* **1996**, 62, 1835. (c) C. Przybyla,]B. [Tesche, G. Fink, *Macromol. Rapid Commun.* **1999**, 20, 328.] (d) M. S. Pimplapure, X. Zheng, J. Loos, G. Weickert, *Macromol. Rapid Commun.* **2005**, 26, 1155.
- [35] M. Kakugo; H. Sadatoshi; M. Yokoyama; K. Kojima, *Macromol.* **1989**, 22, 547.

Chapter 3

*Role of external donor and hydrogen at the
initial stage of Ziegler-Natta propylene
polymerization*

3.1 Introduction

Heterogeneous Ziegler-Natta (ZN) catalysts dominate most of the commercial polypropylene (PP) production processes worldwide.^[1] The spherical $\text{Mg}(\text{OEt})_2$ based ZN catalyst occupy prime industrial importance due to their mild activation stage followed by long lasting kinetics.^[2] The comprehension of role of various chemical entities present in the ZN catalyst with the development of polymerization kinetics is still an open question. This is primarily due to large heterogeneity in the active sites. Understanding the differences among the active site types present on heterogeneous Ziegler-Natta catalysts is an exigent task because of their simultaneous multiple interactions between alkylaluminium (activator), electron donors, hydrogen (H_2), MgCl_2 , TiCl_4 and sensitivity to poisons.^[3, 4] The deeper knowledge of ZN catalysis for development of the catalyst demands precise investigation of role of various chemical entities with the progress of polymerization.

$\text{Mg}(\text{OEt})_2$ based ZN catalysts comprises an internal donor which are typically used in combination with an activator and external donor added during polymerization. Nowadays, the catalyst which is most widely used in PP manufacture contain a diester (e. g. diisobutylphthalate) as internal donor and are used in combination with an alkoxy silane external donor of type $\text{RR}'\text{Si}(\text{OMe})_2$ or $\text{RSi}(\text{OMe})_3$.^[5] These catalyst systems are well commercialized for the PP production. External donor has been used to improve the catalyst stereospecificity.^[6] On the other hand, H_2 employed as standard molecular weight regulator in industrial polyolefin production by acting as a chain transfer agent. However, the precise understanding about the role of external donor and H_2 with the progress of polymerization is still not well known.

It is widely known that the external donor not only affects the polymerization rate but also the polymer tacticity and molecular weight distribution (MWD).^[7] The requirement for an external donor for the catalyst already containing an internal donor is due to the fact that external donor retains and/or improves the active site stereospecificity by compensating the loss of internal donor due to the reaction with activator.^[8] Regarding the mechanism of external donor action several hypothesis have been proposed and suggested that the selective coordination of the Lewis base with aspecific active sites can be considered as major reason for improving catalyst stereospecificity.^{[9],[10],[11],[12]} However, either these models were too simplified or very specific for their explanation and consequently unable to give clear picture of delicate interplay of chemical constituents with the development of polymerization kinetics.

Several researchers demonstrated that the addition of H₂ not only influences the chain transfer reactions but also increases the rate of propylene polymerization.^[13] The reason for the activity enhancement is generally considered as an effect of improved chain propagation with the increase in the number of active centers. Bukatov *et al.*, Parsons and Al-Turki proved these hypotheses experimentally by using ¹⁴C radio-labeling method.^[14] On the other hand, many researchers widely accepted explanation for the propylene polymerization activity enhancement by H₂ as result of the reactivation of dormant site formed as a result of regioirregular insertion of propylene into growing chain lead.^[15] Chadwick *et al.* observed that the magnitude of the chain transfer reactions was critically affected in the presence of external donor.^[16] Guastalla and Giannini studied the activity enhancement phenomena in the presence of H₂ and found that after 1 min of polymerization

the propylene polymerization rate increases dramatically.^[17] Mori *et al.* studied initial polymerization kinetics using stopped-flow (SF) technique and found that the H₂ did not affect the propagation rate constant, polymer molecular weight (MW) and the nature of active sites. Moreover, the pretreatment of catalyst with activator in the presence of H₂ exhibits lower activity due to formation of “dead-sites”. These dead sites were not reactivated even in the presence of H₂.^[18] However, the catalyst pretreatment with H₂ shows chain transfer reaction phenomena which was absent in the former one. Various studies were made in past for understanding the role of H₂ yet the real time comprehension for the change in the active sites nature with the progress of polymerization kinetics was hardly explored.

The understanding of the role of external donor and/or H₂ in ZN catalysis demands precise kinetics development analyses from the very initial stage of polymerization. The initial stage of propylene polymerization can be tracked through the SF technique which enables polymerization shorter than the life time of polymer chain.^[19] The most important advantage of this technique lies in its ability to control the polymerization time as low as 0.03 s. Many studies have been conducted by using SF technique to understand the nature and state of active sites at the very initial moments of the polymerization and proved the efficacy of the technique.^[10, 20] SF technique can conduct polymerization for several seconds using an improved apparatus which is known as large scale stopped flow (LSF).^{[21],[22]} The prolonged SF polymerization opens window of possibilities to explore the role of external donor and/or H₂ in ZN catalysts during polymerization.

In present study series of SF polymerizations were performed in the presence/absence of external donor and/or H₂ up to *ca.* 5 s. The obtained selected polymers were subjected to cross fractionation chromatography (CFC) analyses to clarify the average nature of active sites.

3.2 Experimental

3.2.1 Materials

Triisobutyl aluminum (TiBA, donated by Tosoh Finechem Co.) and titanium tetrachloride (TiCl₄) were used as delivered. *n*-Heptane and toluene were used after being passed through a column of 4Å molecular sieve and bubbling with dry N₂ overnight. Diisobutylphthalate (DiBP) was dehydrated by 4Å molecular sieves before being used as an internal donor. Cyclohexylmethyldimethoxy silane (CHMDMS) was used as an external donor with prior distillation. H₂ and propylene (kindly donated by Japan Polypropylene Co. and Sumitomo Chemical Co., Ltd.) were used as delivered.

3.2.2 Catalyst synthesis

A TiCl₄/DiBP/MgCl₂ catalyst was prepared from synthesized spherical Mg(OEt)₂ based on a patent^[23] with minor modifications^[24]. Same procedure was adopted as discussed in the chapter 2. The Ti and DiBP contents in the catalyst were determined as 2.6 and 12 wt% respectively.

3.2.3 Propylene polymerization

In this study, a recently developed LSF apparatus illustrated in Figure 1 was employed. The idea of the LSF polymerization is quite similar to that for conventional SF polymerization: Catalyst slurry contained in a vessel (Vessel A) and activator solution contained in a separate vessel (Vessel B) are simultaneously transferred in tubes and then contacted at a T junction point to initiate the polymerization. The polymerization is carried out in a tube from C to D, until the polymerization mixture is cast to a quenching solution.

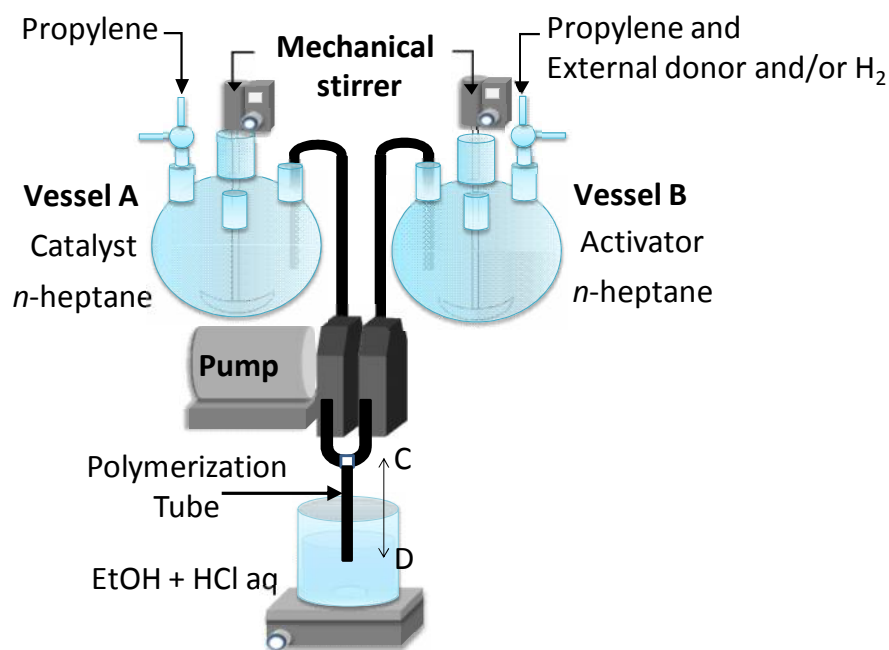


Figure 1 LSF Apparatus

Catalyst slurry (2l, 8.5 mg/ml) and the activator solutions (35 mM) in *n*-heptane were respectively prepared under N₂. A series of SF polymerizations from 0.1 s to 5.0 s were

carried out at 1 atm and 30 °C by adding CHMDMS (Si/Al =10 mol/mol) and/or H₂ in the activator solution only. The flow ratio of H₂:C₃H₆ (propylene) was monitored with mass flow meter (Kofloc Model D3810) and kept 200:800. Monomer saturated slurry and solution were pumped out for polymerization at a pre-calibrated rate of 10 ml/s from each vessel. The polymerization was quenched by casting the polymerization mixture in excess acidic ethanol under high agitation (12,000 rpm). The polymer slurry was washed, dried and re-precipitated to obtain the polymerization kinetics.

3.2.4 Polymer analysis

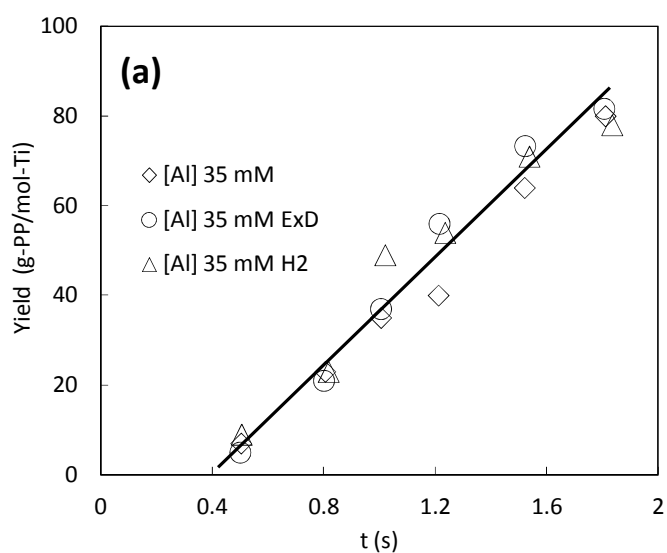
Cross fractionation chromatography

The molecular weight and crystallinity distribution of polymer was simultaneously determined by CFC (T150A, Sumitomo Chemical Co., *Ltd.*) with ODCB as solvent by following the same procedure as discussed in chapter 2.

3.3 Results and discussion

The spherical Mg(OEt)₂-based ZN catalyst are known to express mild activation behavior, where the activity gradually rises up along the polymerization time and maintains a plateau activity for a long time, *i.e.* build-up type kinetics.^[24, 25] In our previous study series of SF propylene polymerizations at various activator concentration were conducted. The continuity and discrepancy between the increasing activity at the time scale of minutes and the constant activity at the time scale of a fraction of seconds was addressed. It was found that the activator plays crucial role in catalyst activation to cause fragmentation firmly for

the catalyst/polymer particles which not only depends on the amount of polymer but also its location in and/or on the particle. However, nature of active sites with the activity development at initial stage of ZN propylene polymerization in presence of external donor and/or H_2 has not been yet discussed.



Chapter 3
 Role of external donor and hydrogen at the initial stage of
 Ziegler-Natta propylene polymerization

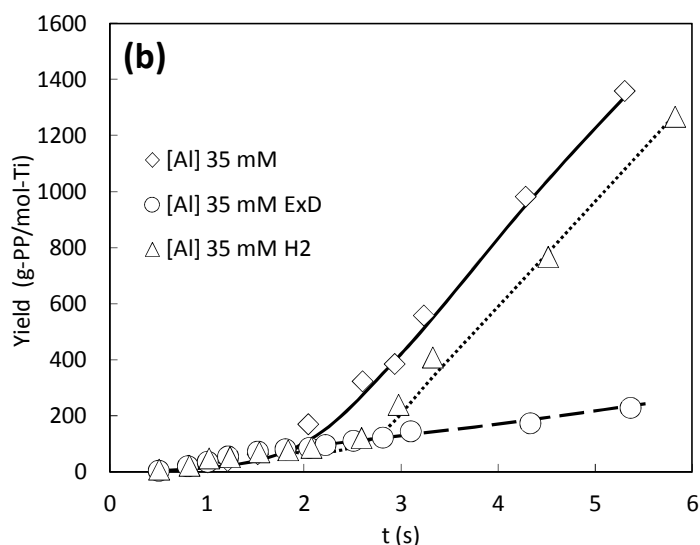


Figure 2 SF polymerizations kinetics at various conditions: absence of external donor and H_2 (), presence of external donor () and, presence of H_2 ().

The kinetic profile of the propylene polymerization was studied by a series of SF experiments from *ca.* 0.1 s to 5.0 s in the presence/absence of external donor and/or H_2 in the activator solution. Figure 2a represents the initial polymerization kinetics development up to *ca.* 1.8 s. It was observed that at 35 mM of activator concentration an induction period was observed and in accordance with our previous results. In general we found that the yield develops almost proportionally with the time with an appearance of induction period. The induction period was found to be independent of the presence/absence of external donor and/or H_2 , *ca.* 0.4 s. The linear yield development pattern up to 1.8 s shows constant number of active sites.

Figure 2b shows the overall polymerization kinetics up to *ca.* 5 s. It was found that in the absence of external donor and/or H₂ the activity develops gradually almost linearly with polymerization time until 1.8 s. Thereafter the yield starts to increase non-linearly with time up to *ca.* 5 s. Through our previous results the reason for the origin of build-up kind of kinetics was dominantly attributed to the catalyst fragmentation. In the presence of external donor it was found that the yield development behavior was almost linear without any noticeable non-linear increment. The lower yield in the presence of external donor can be attributed to the poisoning of active sites. While, in the presence of H₂ the non-linear yield development pattern was observed but slightly delayed (*ca.* 2.5 s) as compared to the polymerization kinetics in the absence of H₂ and external donor. The initial polymerization kinetics discrepancy resulted due to addition of external donor or H₂ can be attributed to be accompanied with variation in the active sites nature with the progress of polymerization. The active site nature variation has been discussed in the subsequent section.

Chemical transformation

As discussed in chapter 2, CFC data are composed of three axes, namely, polymer elution temperature (T), polymer MW (LogMW), and polymer fraction (P (T, LogMW)) measured by infra-red spectroscopy at each LogMW and T. The T has direct correlation with the polymer stereoregularity *i.e.* active site stereospecificity.^[25] In order to examine chemical transformations in terms of the average nature of active sites, selected polymer samples (1.0, 1.8 and 4.0 s at [Al] = 35 in the presence/absence of external donor and/or H₂) were subjected to CFC measurements.

The shape of all contour plots appears similar as they all possess most of polymer fraction concentrated at higher T and LogMW and a tail pointing towards lower T and LogMW. Figure 4 ([Al] = 35 mM), represents that at *ca.* 1.0 s the center of mass of the contour plot exists at co-ordinates (105, 3.13). The center of mass represents the average positioning of the polymer fractions along this sample. On increasing the polymerization time to 1.8 s, a shift in the polymer fraction was observed towards larger T and LogMW. The center of mass of the contour plot at 1.8 s exists at co-ordinates (107, 3.24). This shows that with the increment of polymerization time from *ca.* 1.0 s to 1.8 s the polymer possess dominantly higher stereoregularity *i.e.* formed by highly isospecific active sites. It is known that increase in polymer isotacticity accompany the increase of chain propagation capabilities of the active sites. It can be envisaged that during this region the chemical transformations possess variation in the nature of active sites, which were dominantly isospecific in nature. Thereafter at 4.0 s, a shift in the polymer fraction was observed towards larger T and LogMW. The center of mass of the contour plot at *ca.* 1.8 s exists at co-ordinates (108, 3.48). The increase in T was found to be slower as compared to LogMW. These results clearly demonstrate the nature of active sites on moving at *ca.* 4.0 s was governed by superior chain propagation capabilities.

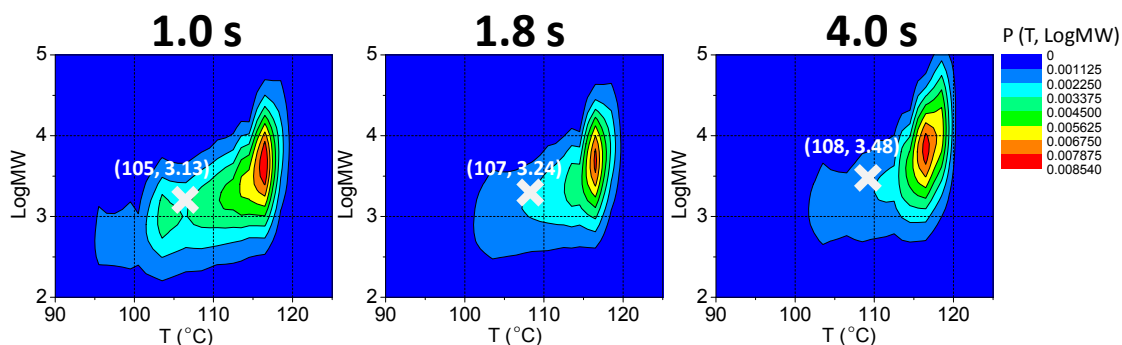


Figure 4 CFC contour plots for polymers SF propylene polymerization.

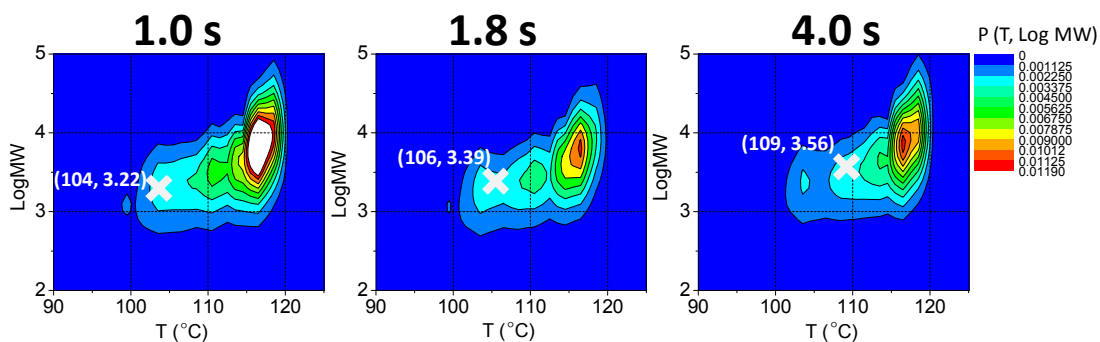


Figure 5 CFC contour plots for polymers obtained by SF propylene polymerization in presence of external donor.

Figure 5 represents the CFC contour plots for the polymers produced in the presence of external donor. At 1.0 s the center of mass of whole polymer fraction exists at (104, 3.22). With the progress of polymerization up to 1.8 s it was found that the polymer tacticity improves with polymer chain elongation with a shift in the center of mass of

polymer distribution to (106, 3.39). In other words the active sites at 1.8 s were highly isospecific with more ability for chain propagation capabilities. On increasing the polymerization time up to 4.0 s it was found that the active sites were predominantly isospecific and showing higher chain propagation capabilities with more shift in polymer center of mass (109, 3.56). It shows that in the presence of external donor active sites were becoming more isospecific with enhanced chain propagation capabilities.

Comparing the nature of active sites in the presence/absence of external donor, it was found that the nature of active sites in the presence of external donor comprised higher isospecificity with enhanced chain propagation. It is widely known that the structure of alkylaluminium is changed upon being complexed with alkoxy silane.^[26] These results suggest that the interaction/reaction of alkylaluminium-external donor complex with the active sites modulate their resistance towards the chain transfer reactions. On the hand, increase in active site isospecificity with the introduction of external donor can be attributed to the compensation by external donor at the cost of internal donor extraction by alkylaluminium. These results exemplify the action of external donor at the very initial stage of polymerization kinetics development. The active sites poisoning can be considered as a cause for the lower yield development.

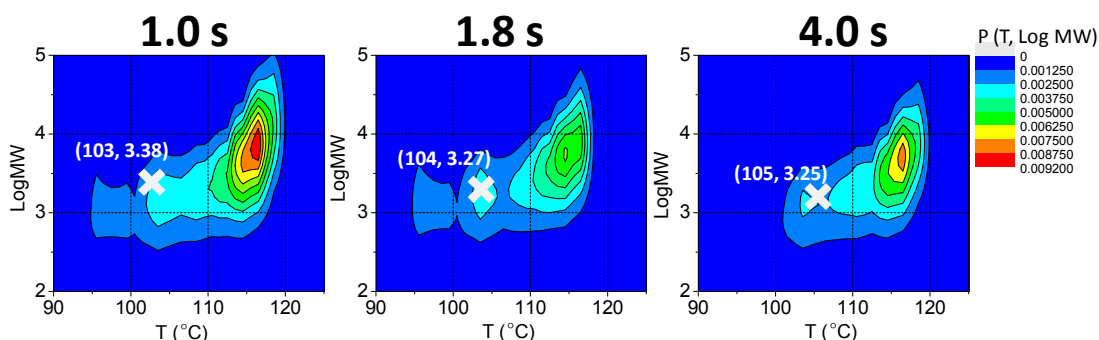


Figure 6 CFC contour plots for polymers obtained by SF propylene polymerization in presence of H_2 .

The active site nature variation as an effect of H_2 is represented with CFC contour plots in Figure 6. At 1.0 s it was observed that the center of mass of polymer fraction exists at (103, 3.38). On increasing the polymerization time up to 1.8 s it was observed that in the molecular weight of chain growth suppressed as a result of presence of H_2 which act as a chain transfer agent. It is widely known that the sensitivity to chain transfer to hydrogen is dependent on regio- and stereoselectivity, chain transfer after the occasional secondary insertion being particularly favored on account of relatively low reactivity 2, 1 inserted species in chain propagation.^[9] Later, Busico *et al.* proved that the polymeric chains become more regio-regular with the introduction of hydrogen as chain transfer agent.^[15] The higher polymer tacticity distribution corresponds towards the higher isospecificity of the active sites. At *ca.* 4.0 s of polymerization it was found that the active sites become more isospecific with shorter polymer chains. These results infer that the H_2 initiates to exhibit the chain transfer reactions dominantly from the initial stage of the build-up regime

Chapter 3
Role of external donor and hydrogen at the initial stage of
Ziegler-Natta propylene polymerization

of the polymerization kinetics. It is in knowledge that the pretreatment of catalyst and H₂ suppresses the chain growth. The obtained results suggest that the ageing of interaction and/or reaction of H₂ with active sites make them prone to faster chain transfer reactions. The results can be envisaged that the polymerization kinetics development bear ageing of interaction and/or reaction with H₂ lead to the formation of new active sites having better chain transfer capabilities.

In summary, it was found that the nature of active sites varies due to the ageing of interaction and/or reaction with the external donor or H₂ with the polymerization time. The nature of active sites in the presence of external donor was possessing greater chain propagation capabilities. While in the presence of H₂ the new active sites formed through ageing causes suppressed polymer chain growth.

3.4 Conclusions

The bridge between the initial constant activity stopped-flow region and build-up regime of the polymerization kinetics was firstly established for propylene polymerization in the presence of external donor and/or H₂ using an improved SF technique. In the absence of external donor and hydrogen the ageing of interaction and/or reaction of alkylaluminium and active sites alter their chain transfer capabilities. Yield development degree in the presence of external donor was found to be lowest and attributed to the active site poisoning. With the progress of polymerization, especially in the build-up region, active sites were found to be dominantly isospecific with higher chain propagation capabilities. On the other hand, in the presence of H₂, significant chain transfer behaviour appears to be active between *ca.* 1.0 to 4.0 s of polymerization.

References

- [1] P. S. Chum, K. W. Swogger, *Prog. Polym. Sci.* **2008**, 33, 797.
- [2] (a) M. Terano, K. Kimura, A. Murai, M. Inoue, K. Miyoshi, *JP Patent S62-158704*, **1987**. (b) A. Dashti, A. Ramazani, Y. Hiraoka, S. Y. Kim, T. Taniike, M. Terano, *Polym. Int.* **2008**, 58, 40.
- [3] E. P. Moore, Jr., “*Polypropylene Handbook*”, 1st edition, Hanser Publishers, New York **1996**, p. 11.
- [4] (a) J. B. P. Soares, *Chem. Eng. Sci.* **2001**, 56, 4131. (b) Y. V. Kissin, *Macromol. Symp.* **1995**, 89, 113.
- [5] (a) P. C. Barbe, G. Cecchin, L. Noristi, *Adv. Polym. Sci.* **1987**, 81, 1. (b) Eur. 45977 (1982), Montedison, invs: S. Parodi, R. Nocci, U. Giannini, P. C. Barb.; Chem. Abstr. 1982, 96, 181808v.
- [6] V. Busico, P. Corradini, L. external donor. Martino, A. Proto, V. Savino, E. Albizzati, *Makromol. Chem.* **1985**, 186, 1279.
- [7] J. C. Chadwick, G. Morini, G. Balbontin, I. Camurati, J. J. R. Heere, I. Mingozi, F. Testoni, *Macromol. Chem. Phys.* **2001**, 202, 1995.
- [8] (a) V. Busico, P. Corradini, L. D. Martino, A. Proto, E. Albizzati, *Makromol. Chem.* **1986**, 187, 1115. (b) M. Farina, C. Puppi, *J. Mol. Catal.* **1993**, 82, 3.

- [9] (a) J. C. Chadwick, G. Morini, G. Balbontin, I. Camurati, J. J. R. Heere, I. Mingozzi, F. Testoni, *Macromol. Chem. Phys.* **2001**, 202, 1995. (b) J. J. A. Dusseault, C. C. Hsu, *J. Macromol. Sci., Rev. Macromol. Chem. Phys.* **1993**, C33(2), 103.
- [10] B. Liu, H. Matsuoka, M. Terano, *Macromol. Rapid Commun.* **2001**, 22, 1.
- [11] V. Busico, R. Cipullo, G. Monaco, G. Talarico, M. Vacatello, *Macromolecules* **1999**, 32, 4173.
- [12] B. Liu, T. Nitta, H. Nakatani, M. Terano, *Macromol. Chem. Phys.* **2003**, 203, 2412.
- [13] W. K. Shaffer, W. H. Ray, *J. Appl. Polym. Sci.* **1997**, 65, 1053.
- [14] (a) G.D. Bukatov, V.S. Goncharov, V.A. Zakharov, *Macromol. Chem. Phys.* **1995**, 196, 1751. (b) I.W. Parsons, T.M. Al-Turki, *Polym. Commun.* **1989**, 30, 72.
- [15] (a) V. Busico, R. Cipullo, P. Corradini, *Macromol. Chem. Rapid Commun.* **1992**, 13, 15. (b) T. Tsutsui, N. Kashiwa, A. Mizuno, *Makromol. Chem. Rapid Commun.* **1990**, 11, 565. (c) J. C. Chadwick, A. Meedema, O. Sudmeijer, *Macromol. Chem. Phys.* **1994**, 195, 167.
- [16] J. C. Chadwick, J. J. R. Heere, O. Sudmeijer, *Macromol. Chem. Phys.* **2000**, 201, 1846
- [17] G. Guastalla, U. Giannini, *Makromol. Chem. Rapid Commun.* **1983**, 4, 519.
- [18] H. Mori, M. Endo, K. Tashino, M. Terano, *J. Mol. Catal. A: Chem.* **1999**, 145, 153.
- [19] T. Keii, M. Terano, K. Kimura, K. Ishii, *Makromol. Chem. Rapid Commun.* **1987**, 8, 583.

Chapter 3

Role of external donor and hydrogen at the initial stage of Ziegler-Natta propylene polymerization

[20] T. Keii, K. Soga, “*Catalytic Olefin Polymerization*”, Elsevier, Tokyo, **1989**, p. 166.

(b) A. D. Martino, J. P. Broyer, D. Schweich, C. D. Bellefon, G. Weickert, T. F. L. McKenna, *Macromol. React. Eng.* **2007**, 1, 284. (c) M. Kaminaka, K. Soga, *Polym.* **1992**, 33, 1105. (d) M. Kaminaka, K. Soga, *Macromol. Chem. Phys. Rapid. Commun.* **1991**, 12, 367.

[21] T. Taniike, S. Sano, M. Ikeya, V. Q. Thang, M. Terano, *Macromol. React. Eng.* **2012**, 6, 275.

[22] S. Dwivedi, T. Taniike, M. Terano, *Macromol. Chem. Phys.* **2014**, submitted.

[23] M. Terano, K. Kimura, A. Murai, M. Inoue, K. Miyoshi, *JP Patent S62-158704*, **1987**.

[24] A. Dashti, A. Ramazani, Y. Hiraoka, S. Y. Kim, T. Taniike, M. Terano, *Polym. Int.* **2008**, 58, 40.

[25] M. Kakugo; H. Sadatoshi; M. Yokoyama; K. Kojima, *Macromol.* **1989**, 22, 547.

[²⁶] J. Koivumaki, J. V. Seppala, L. Kutti, *Polym. Bull.* **1992**, 29, 185.

Chapter 4

Initial morphology and kinetics development

in Ziegler-Natta catalyst studied through

stopped-flow ethylene/propylene and

1-hexene/propylene copolymerization

4.1 Introduction

Ziegler–Natta (ZN) catalyst are predominant in the manufacture of polyolefins, accounting for about 110 million tons of polyolefin resins.^[1,2] Copolymers of propylene with other olefins are important commercial products. Mg(OEt)₂-based state-of-the-art ZN catalyst have acquired a great attention in industry as well as in academia because of their high overall activity despite of mild activation behavior. The excellent plant operability demands controlled kinetics as well as good polymer morphology from the view point of process economics and viability.^[3] However the understanding of the kinetics and morphological development in ZN copolymerization kinetics is still far from well known. Deeper comprehension of basic aspects for copolymerization kinetics will lead to further development in this area.

In Ziegler-Natta olefin polymerization, the enhanced development of polymerization kinetics by the addition of comonomer is well known as the comonomer effect.^[4] The comonomer effect has been well studied for copolymerization of ethylene with α -olefins and of propylene with ethylene/1-octene.^[5] A large pool of research accompanies the explanations for mechanistic aspects of comonomer effect in the terms of chemical and physical grounds.^[6] The chemical factors have been well studied and include the enhancement in chain propagation constant (through dormant site reactivation and/or higher comonomer reactivity). Physical factors include catalyst fragmentation which results increase in active site concentration.^[7] The physical factors (catalyst/polymer morphology development) come in action after attaining few g-polymer/g-cat. The physical factors are known to occupy an important position for controlling the polymerization kinetics.^[8] Systematic investigation of copolymerization kinetics from the view point of physical

Chapter 4

Initial morphology and kinetics development in Ziegler-Natta catalyst studied through stopped-flow ethylene/propylene and 1-hexene/propylene copolymerization

factors needs rigorous studies.

Many attempts were made for understanding the catalyst/polymer particle morphology development with polymerization. In industry to obtain better catalyst fragmentation control, a prepolymerization step, which is essentially a polymerization step, performed under mild conditions and at low reaction rates.^[9] The morphology of the catalyst particle changes, starting from the stage of being just a support material up to tiny fragments dispersed within the growing catalyst/polymer particle.^[10] Studies aimed at a better understanding of the morphology development during the early stages of polymerization were carried out by Kakugo *et al.* and Noristi *et al* and laid the basis of catalyst fragmentation.^[11] Soga *et al.* demonstrated that comonomer activation occurs only in cases in which homopolymerization produces a highly crystalline polymer.^[12] Cecchin *et al.* conducted propylene copolymerization with ethylene and 1-butene respectively. On the basis of obtained results, they projected a model to describe the catalyst/polymer particle growth that involves the features of both a dual grain and a polymeric flow system for conducting the catalyst/polymer fragmentation to sustain the reaction.^[13] Fink *et al.* proposed the easier diffusion of “small” monomer (ethylene) than 1-hexene through the polymer layer around the catalyst particle for promoting the polymerization to greater extent and termed as “filter effect”.^[14] Despite of tremendous research for observing the morphological development of ZN catalyst, the role of catalyst polymer morphology development in the origin of polymerization kinetics has been scarcely addressed.

In heterogeneous ZN olefin polymerization, the first few seconds in the life of the catalyst particles play a decisive role in the subsequent stages of polymerization. Under industrial conditions the process of fragmentation is completed within a few seconds^[15]

but it is not easy to follow the catalyst/polymer morphology development issue with polymerization kinetics. Terano *et al.* invented the “stopped-flow” method for the performing the polymerization shorter than the life time of polymer chain growth (<0.2 s) with very high time-precision.^[16] Studies by Terano *et al.*^[17], Keii *et al.*^[18], Mckenna *et al.*^[19] and Soga *et al.*^[20] proved the efficacy of SF technique for elucidating the kinetic mechanism, real time information of active sites/intermediates and other kinetics parameters for heterogeneous ZN olefin polymerization. Di Martino *et al.*^[21], Thang *et al.*^[22] and Taniike *et al.*^[23] proved the efficacy of SF apparatus for morphological studies successfully at the very initial moments of polymerizations. Recently, Taniike *et al.* employed SF method for the understanding of comonomer induced chemical and physical activation in ZN catalyst.^[24] They found at the very initial stage i.e. quasi-living region, the increment of propagation rate constant for propylene is dependent on the kind of comonomer (increased for ethylene and unchanged for 1-hexene). They proposed the existence of physical effects for the strong increment of polymer yield in continuously purged copolymerization. The experimental evidence for the physical activation in ZN catalyst demands prolonged SF polymerization.

The challenge associated with the objective of prolonged SF polymerizations is the viscosity development with progress of polymerization. Recently, this issue was well addressed and an improved SF apparatus was designed, known as large-scale stopped-flow (LSF) system.^[25] LSF has ability to conduct prolonged polymerization without any viscosity development issues up to several s with better flow rate and instantaneous quenching through time precision of 0.03 s. The LSF unlocks the door of prolonged copolymerization to observe the morphological aspects with kinetics development. In

Chapter 4

Initial morphology and kinetics development in Ziegler-Natta catalyst studied through stopped-flow ethylene/propylene and 1-hexene/propylene copolymerization

current study, prolonged propylene, ethylene/propylene and 1-hexene/propylene (co)polymerizations were conducted from *ca.* 0.1 to 5.0 s. The obtained polymerization kinetics was considered and selected catalyst/polymer samples were analyzed by scanning electron microscope (SEM) for understanding morphological aspects. Polymers x-ray diffraction (XRD) were employed to support the obtained conclusions.

4.2 Experimental

4.2.1 Materials

Triisobutyl aluminum (TiBA, donated by Tosoh Finechem Co.), titanium tetrachloride (TiCl₄) and dehydrated tetrahydrofuran (THF) were used as delivered. *n*-Heptane and toluene were used after being passed through a column of 4 Å molecular sieve and bubbling with dry N₂ overnight. Diisobutylphthalate (DiBP) and 1-hexene were purified by 4 Å molecular sieves. Ethylene and propylene (kindly donated by Japan Polypropylene Co. and Sumitomo Chemical Co., Ltd.) were used as delivered.

4.2.2 Catalyst synthesis

A TiCl₄/DiBP/MgCl₂ catalyst was prepared from synthesized spherical Mg(OEt)₂ based on a patent^[26] with minor modifications^[27]. Same procedure was adopted as discussed in the chapter 2. The Ti and DiBP contents in the catalyst were determined as 3.4 and 12 wt% respectively.

4.2.3 Homo- and co-polymerization

In this study, a recently developed LSF apparatus illustrated in Figure 1 was employed.

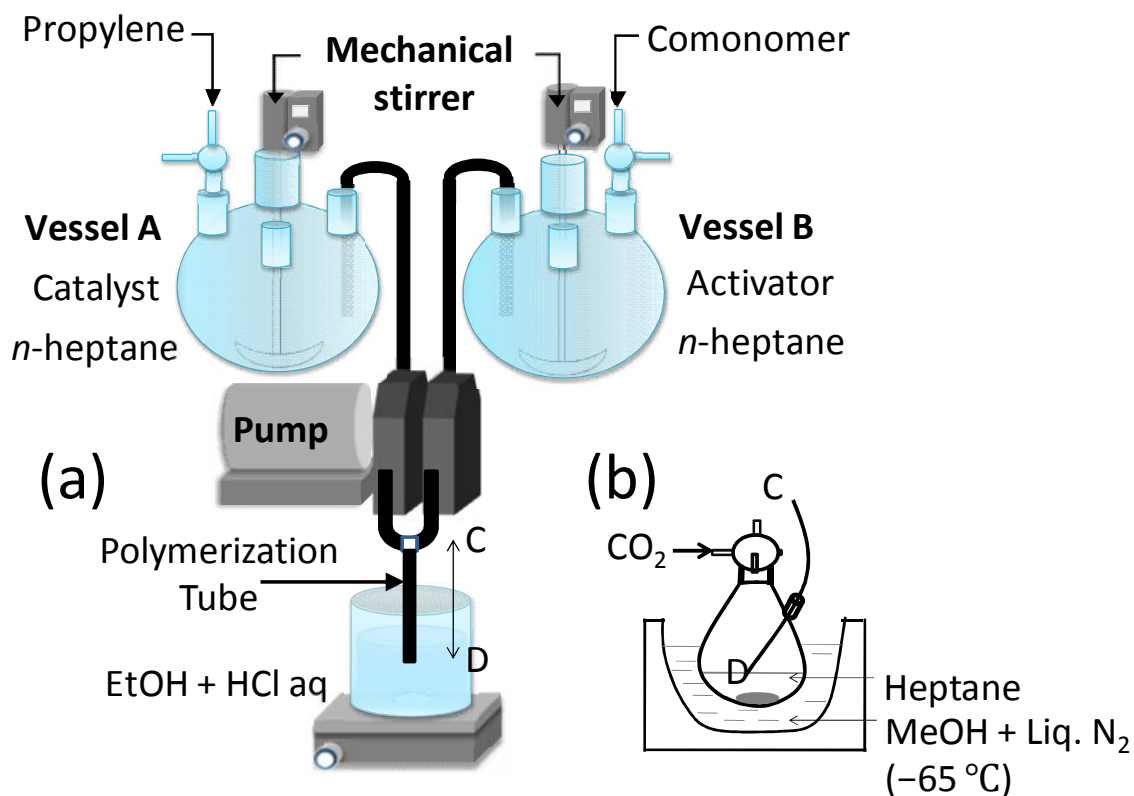


Figure 1 LSF Apparatus

The idea of the LSF polymerization is quite similar to that for conventional SF polymerization: Catalyst slurry contained in a vessel (Vessel A) and activator solution contained in a separate vessel (Vessel B) are simultaneously transferred in tubes and then contacted at a T junction point to initiate the polymerization. The polymerization is carried out in a tube from C to D, until the polymerization mixture is cast to a quenching solution.

Chapter 4

Initial morphology and kinetics development in Ziegler-Natta catalyst studied through stopped-flow ethylene/propylene and 1-hexene/propylene copolymerization

Catalyst slurry (8.5 mg/ml) and activator solution (35 mM) in *n*-heptane were respectively prepared under N₂. A series of SF polymerizations from 0.1 s to 5.0 s were carried out at 1 atm and 30 °C. Propylene saturated catalyst slurry and comonomer-activator solution were pumped out for polymerization at a pre-calibrated rate of 10 ml/s from each vessel. The polymerization was quenched by casting the polymerization mixture in excess acidic ethanol under high agitation (12,000 rpm). The polymer slurry was washed, dried and re-precipitated to obtain the polymerization kinetics.

In order to examine the morphology of catalyst/polymer particles, a special quenching method was adopted as shown in Figure 1 (b).^[22] The polymerization was quenched under CO₂ atmosphere in heptane at -65 °C. To improve the stability of particles in air, anhydrous THF (THF/Ti: 200/1 (mol/mol)) was added to the heptane. After the removal of upper solvent, the particles were dried and transferred to a vial under N₂ atmosphere.

4.2.4 Polymer analysis

Morphology observation

The surface and bulk morphologies of catalyst/polymer particles were observed by scanning electron microscopy (SEM, Hitachi S-4100). The bulk morphology was examined after the particles were randomly cut by a razor under N₂. The samples were coated with Pt-Pd for 100 s through an ion sputter (Hitachi E-1030) and finally transferred into the SEM equipment. Representative images for the morphologies were assured by measuring each sample twice and acquiring at least three images at each measurement.

XRD measurement

The polymer crystallinity was determined by powder X-ray Diffractometer (Rigaku, SmartLab) with Cu-K α radiation. Diffraction patterns were collected in reflection-mode geometry from 2° to $80^\circ 2\theta$ at the rate of $2^\circ 2\theta / \text{min}$.

4.3 Results and Discussion

A series of LSF polymerizations were conducted from *ca.* 0.1 to 5.0 s. The corresponding homo/copolymerization kinetics was represented in Figure 2.

In Figure 2a, at the early stage of propylene polymerization an induction period of *ca.* 0.3 s was observed followed by linear yield development up to *ca.* 1.8 s, these results were in line with our previous results.^[28] The constant activity region demonstrates no change in the number of active sites. It was found that ethylene/propylene copolymerization exhibits instantaneous active sites activation and linear activity increment until *ca.* 1.8 s. The instantaneous activation in ethylene/propylene copolymerization can be attributed to the higher reactivity of the ethylene as compared to propylene. The ethylene/propylene copolymerization exhibits higher activity as compared to the propylene polymerization.^[7] While, the 1-hexene/propylene copolymerization show similar induction period with propylene copolymerization. However, the subsequent 1-hexene/propylene copolymerization activity was constant but lower than both ethylene/propylene and propylene polymerization up to *ca.* 1.8 s, most probably due to the lower reactivity of 1-hexene than propylene and ethylene. These results represent the polymerization kinetics

Chapter 4

Initial morphology and kinetics development in Ziegler-Natta catalyst studied through stopped-flow ethylene/propylene and 1-hexene/propylene copolymerization

development at the very initial stage of polymerization with monomers possessing different reactivity.

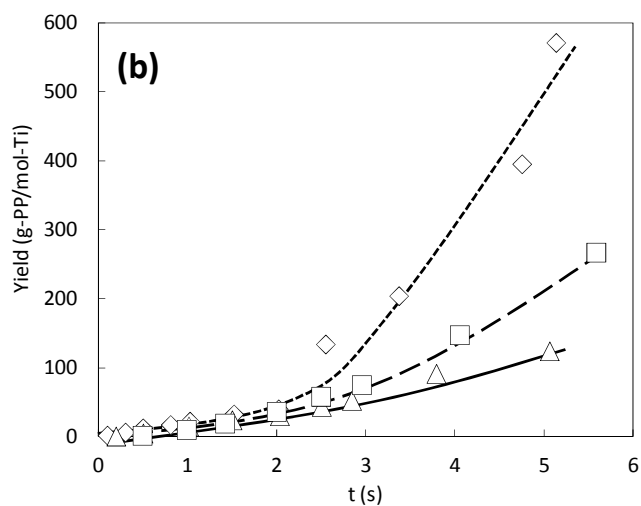
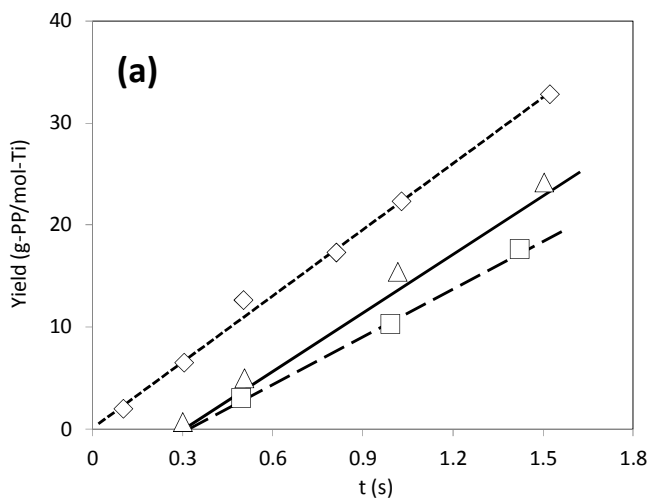


Figure 2 Kinetics for propylene (), ethylene/propylene () and, 1-hexene/propylene () SF homo/copolymerization.

Figure 2b represents the overall polymerization kinetics. The non-linear yield development expresses the build-up region of the polymerization kinetics. In general, it was observed that on increasing the polymerization time beyond *ca.* 1.8 s the catalyst activity increases non-linearly. The trend of yield enhancement for copolymerization were similar but of greater magnitude than propylene polymerization. Ethylene/propylene copolymerization show strongest transition followed by 1-hexene/propylene copolymerization. Comonomer activation is less pronounced in propylene/olefin copolymerization, but Jungling *et al.* observed a threefold increase in activity by adding a small quantity of 1-octene to propylene polymerization.^[5] They attributed the activity increment to the improved mass transfer in the growing catalyst/polymer particle. The non-linear increment yield increment either arose by the increase in the active site concentration and/or faster chain propagation. It is known for propylene polymerization that the origin of build-up kinetics is mainly the catalyst fragmentation.

In current study the observed transition of catalyst activity from linear to build-up region can be envisaged to the exposure of inner less accessible TiCl_4 for polymerization as result of catalyst particle disintegration with time. However, the trail of morphology development with copolymerization kinetics is still ambiguous and needed to be studied to explain the difference between the intensity of kinetic transition by introduction of different comonomer. The morphology development of selected catalyst/polymer particles (*ca.* 1.8 and 4.0 s) were traced by SEM and discussed in subsequent section.

Morphology development

The morphological aspects were examined using SEM for selected samples obtained through SF polymerization, where a special quenching method was employed to preserve the catalyst/polymer particle morphologies. Figure 3a represents the surface and bulk morphologies of the employed catalyst. Catalyst macro particles were nearly spherical, composed by secondary agglomeration of lamellar-shaped building units. The agglomeration manner of the building units decides the catalyst inner structure, especially for the spatial distribution of macroporosity formed as interspaces among the building units. The cross-sectional view of the catalyst (Figure3a: B,C) shows that the catalyst inner structure was composed by three-layered structures according to the manner of the secondary agglomeration: A dense outermost layer followed by a porous layer with the loosely packed building units and finally a tightly packed core.^[22] The vacant space in the catalyst cross-sectional image indicates macropores, which were mainly located in the mid porous layer.

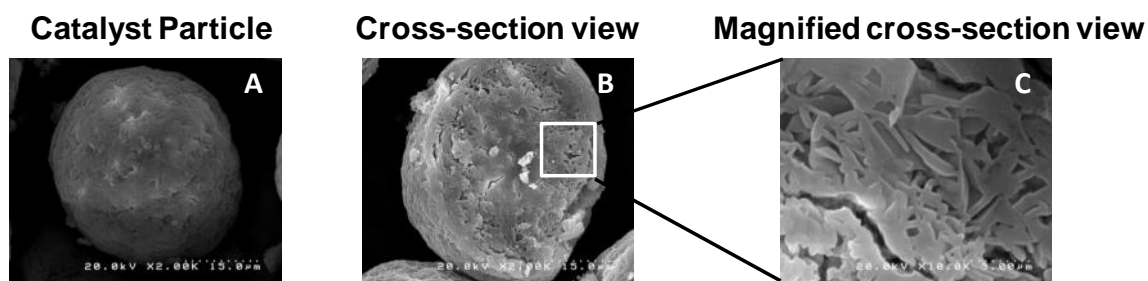


Figure 3a Catalyst images

It is known that the macropores possess key for triggering the catalyst fragmentation.^[23] Figure 3b,c and d shows the SEM images for the catalyst/polymer particles obtained at 1.8 s and 4.0 s from propylene, ethylene/propylene and 1-hexene/propylene SF homo/copolymerization, respectively. In propylene polymerization (Figure 3b) it was observed that the polymerization for 1.8 s (corresponding to 0.3 g-PP/g-cat) made particle surfaces slightly rougher, indicating the polymer formation on the surfaces (Figure 3b: D). On observing the cross-sectional image (Figure 3b: E,F) of the same catalyst/polymer particles, it was found that the macropores of the particle were partially filled with the polymer. With the progress of polymerization from 1.8 s to 4.0 s (0.3 to 0.9 g-PP/g-cat), the particle surfaces became rather smooth by being covered by the formed polymer (Figure 3b: G). The cross-sectional view of the catalyst/polymer particle shows the smooth surface and indicates that many catalyst macropores were filled with polymer (Figure 3b: H,I). The cross-sectional images clarified a relatively great part of macropores along the periphery were remained unfilled (pointed with arrows). This fact indicated that the polymer was rather selectively formed on the surfaces, and retards the monomer and/or activator diffusion inside the particles and slows the pores filling process. The lowest magnitude of build-up type polymerization kinetics can be attributed to the vacant macropores, which might be considered as a consequence of mass transfer limitations inside the catalyst particle.

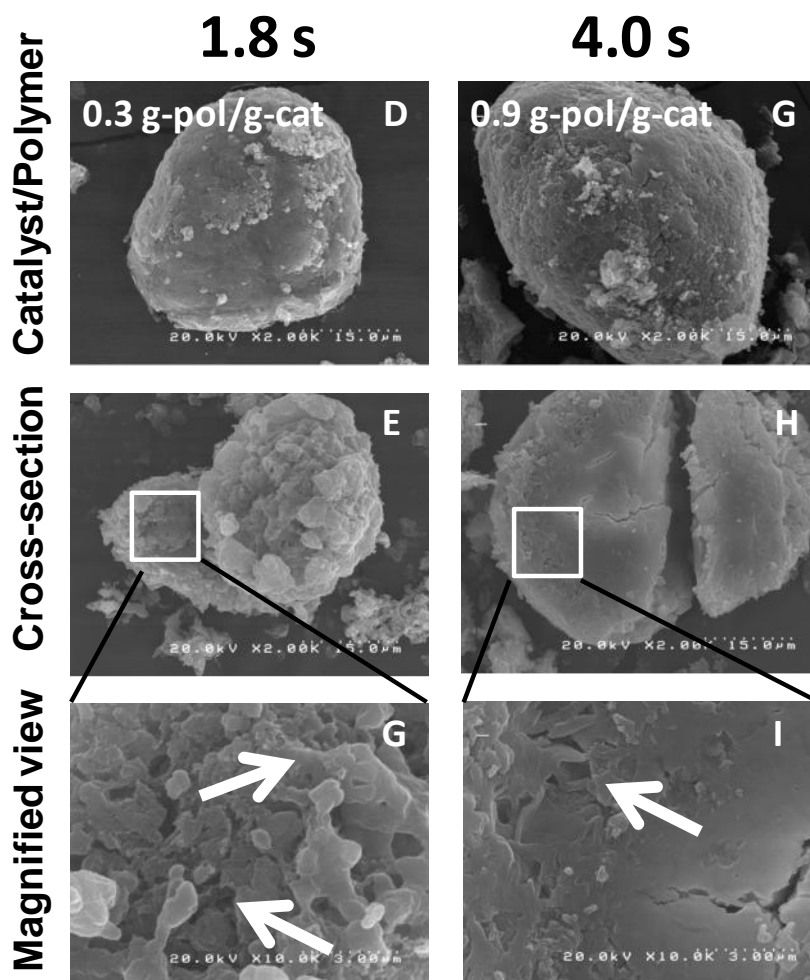


Figure 3b Catalyst polymer images for propylene polymerization at *ca.* 1.8 s and 4.0 s. The yield was mentioned in g-PP/g-cat to show the macroscopic phenomena of catalyst/polymer particle morphology development with polymerization kinetics.

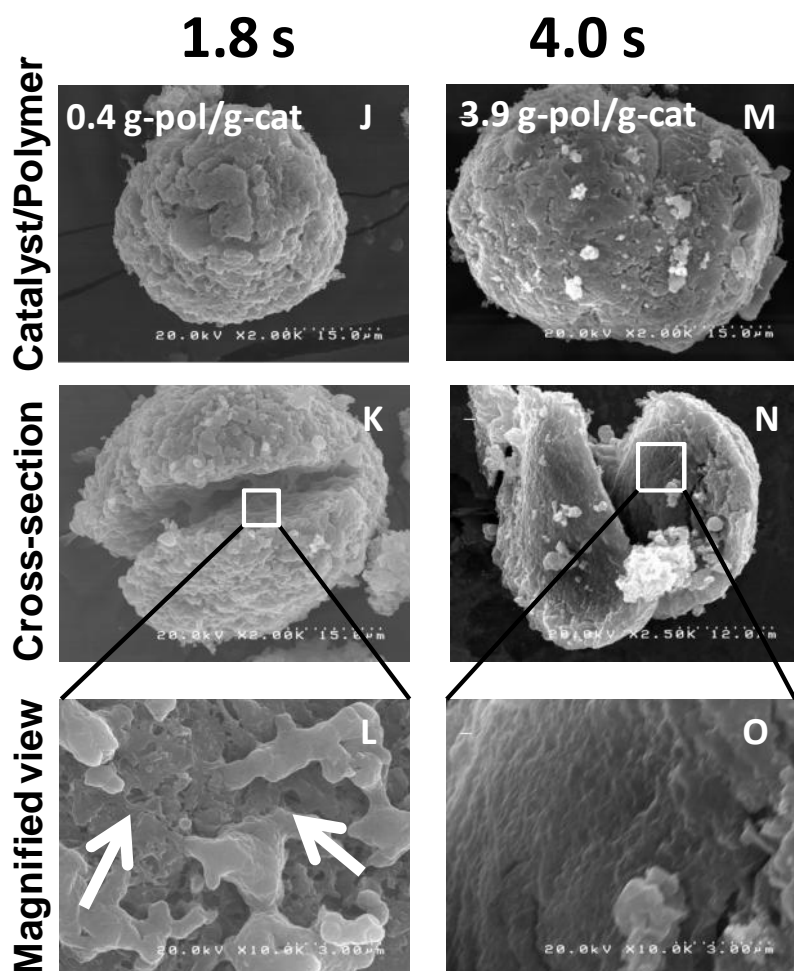


Figure 3b Catalyst polymer images for ethylene/propylene copolymerization at *ca.* 1.8 s and 4.0 s.

In ethylene/propylene copolymerization the morphological developments for 1.8 s (Figure 3c: J,K and L) were quite similar to those observed for propylene polymerization (Figure 3b) Rough particle surfaces with partial macropores filling and some fibrillar structures were visible (pointed with arrows). It is widely accepted that such fibrillar structures result from the stretching of the formed polymer during the fragmentation of

Chapter 4

Initial morphology and kinetics development in Ziegler-Natta catalyst studied through stopped-flow ethylene/propylene and 1-hexene/propylene copolymerization

catalyst particles. On the other hand, significant differences were observed at 4.0 s (Figure 3c, M). Even producing a sufficient amount of polymer (3.9 g-PP/g-cat), the particle surfaces were not smooth but even became rougher than those at 1.8 s. With the progress of polymerization from 1.8 s to 4.0 s (0.4 to 3.9 g-PP/g-cat), the cross-sectional view of the catalyst/polymer particle shows the smooth surface and indicates that most of the catalyst macropores were filled with polymer (Figure 3c: N,O). With progress of polymerization, the macropores filling process seems to be continued in smooth manner. These results exemplify the filtering effect: better monomer and activator diffusion through copolymer layer into the catalyst particles for pores filling process. The macropores filling process was found to be faster for ethylene/propylene copolymerization most probably due to the lower crystallinity of the copolymer shell formed over the catalyst particle which offers lower mass transfer limitation. The larger curvature of build-up region in ethylene/propylene polymerization kinetics can be attributed to the generation of inner hidden potential active sites induced by faster macropores filling and fragmentation.

The morphological developments in 1-hexene/propylene copolymerization at *ca.* 1.8 s (Figure 3d: P,Q and R) were seems to be similar to those observed for ethylene/propylene polymerization with thick polymer shell around the catalyst particle (Figure 3c). However, noticeable differences were observed at 4.0 s (Figure 3d: S). The particle surfaces appear smoother than at 1.8 s. The cross section view of the catalyst/polymer particle shows a thick copolymer layer around the catalyst particle and many of the catalyst macropores were still partially unfilled (Figure 3c: N,O). The slower development of build-up kinetics curvature can be attributed to the mass transfer limitations induced by the thick polymer shell around the catalyst particle.

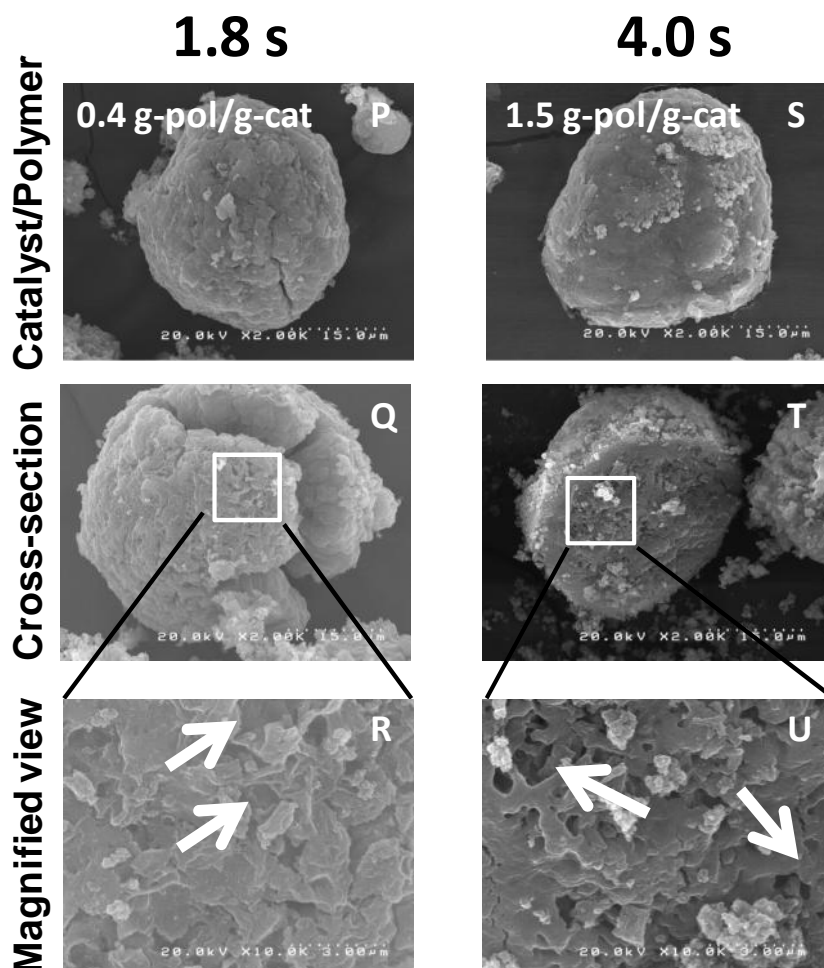


Figure 3b Catalyst polymer images for 1-hexene/propylene copolymerization at *ca.* 1.8 s and 4.0 s.

It is widely known that the formation of the polymer layer over the catalyst particle play crucial role for the mass transfer of (co)monomer and activator in the catalyst particle. It is obvious to suppose the role of polymer crystallinity for regulating the mass transfer issues. As observed that *ca.* 1.8 s exists as a transition point for the yield enhancement, it seems that the polymer crystallinity at *ca.* 1.8 s play major role for deciding the fate of subsequent

Chapter 4

Initial morphology and kinetics development in Ziegler-Natta catalyst studied through stopped-flow ethylene/propylene and 1-hexene/propylene copolymerization

polymerization kinetics. The polymer crystallinity was measured by XRD as represented in

Table 1.

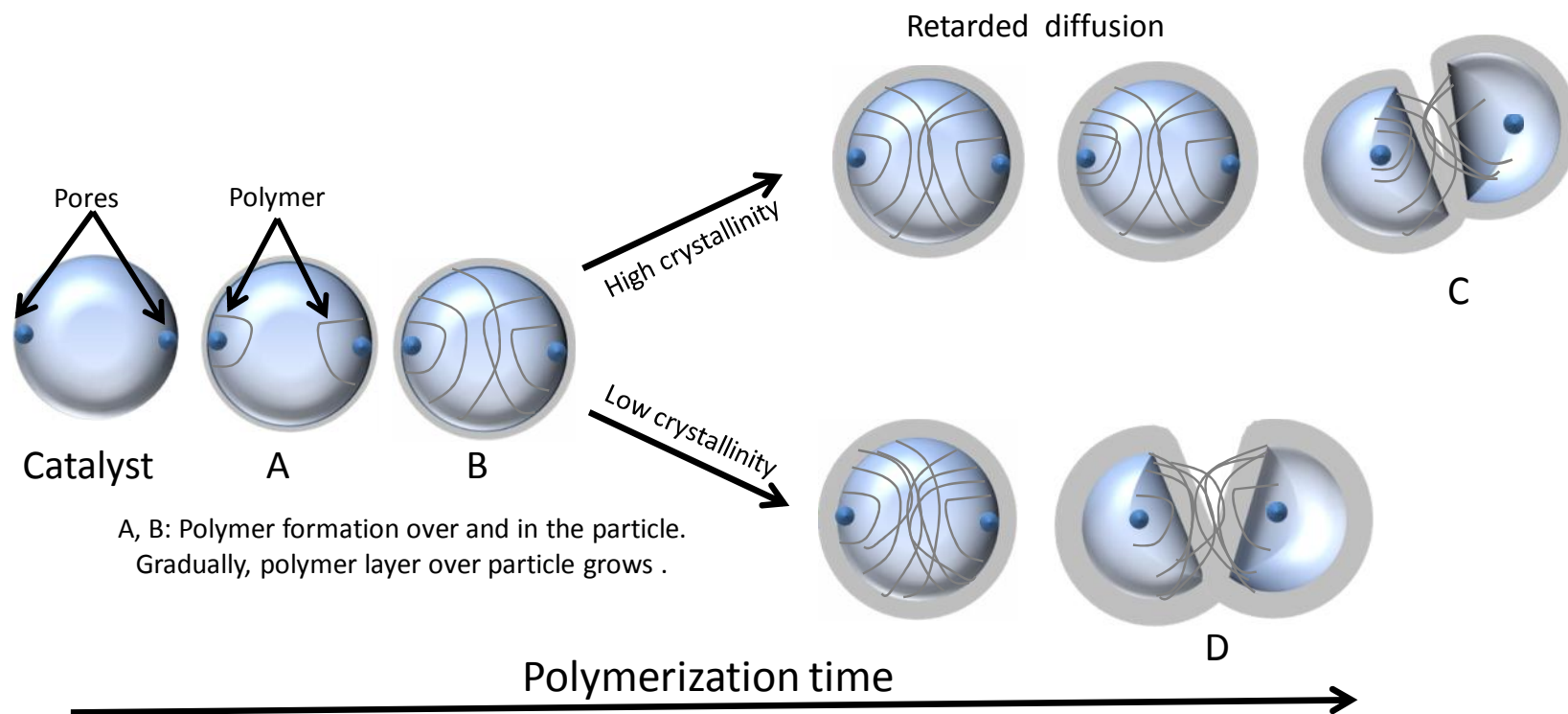
Table 1 Polymer crystallinity at *ca.* 1.8 s of polymerization

Sample	Crystallinity ^a (%)
C3	58.9
C2/C3	39.7
C6/C3	48.1

^a Determined by GPC-IR.

^b Determined by XRD.

It was observed that the crystallinity ethylene/propylene copolymer was lower (39.7 %) than the corresponding 1-hexene copolymer (48.1 %) and polypropylene (58.9 %). It suggests that the lower crystalline polymer allow easier mass transfer through the polymer layer around the catalyst particle to give higher degree of yield enhancement. These results clearly infer that the comonomer content and polymer crystallinity play important role for modulating the mass transfer inside the catalyst particle for catalyst fragmentation and subsequent polymerization kinetics.



Scheme 1 Catalyst/polymer particle fragmentation dependence on polymer crystallinity.

Chapter 4

Initial morphology and kinetics development in Ziegler-Natta catalyst studied through stopped-flow ethylene/propylene and 1-hexene/propylene copolymerization

Scheme 1 has been proposed for greater comprehension of the catalyst/polymer fragmentation process on the basis of polymer crystallinity. It is known that the macropores are important for triggering the fragmentation process in the catalyst. It is widely acknowledged that the hydraulic stress development beyond the critical stress (depends on material and/or architecture) in the catalyst pores causes the particle disintegration. The process can be envisaged that the initial polymer formation takes place on the highly exposed catalyst surfaces and lead to the formation of layer around the particle (Scheme 1: A). Depending up on the kind of polymer and its crystallinity the (co)monomer and activator diffusion inside the particle occur through the polymer layer (Scheme 1: B). If the polymer crystallinity will be higher more mass transfer limitations would exist. The polymer shell of higher crystallinity around the catalyst particles retards the reagent diffusion inside the particle and consequently slows the fragmentation process (Scheme 1: C). On the other hand, mass transfer limitations substantially reduced for the polymer layer of lower crystallinity. Furthermore, inside the catalyst particle the polymer having lower crystallinity offers greater mobility (or lower stress) and consequently need greater amount of polymer to generate requisite hydraulic stress for the catalyst particle disintegration as shown in Scheme 1: D). In other words, the polymer of lower crystallinity offers lower mass transfer limitations and faster catalyst/polymer growth through facile fragmentation of catalyst particle or *vice-versa*.

4.4 Conclusion

In current study the connection between initial constant activity and macroscopic build-up type of copolymerization kinetics has been established for the first time using stopped-flow technique. The transition from linear to non-linear (build-up) yield enhancement was considered to be mainly due to fragmentation of the catalyst polymer particle. The filter effect by polymer layer was explained on the basis of polymer crystallinity. It was found that the polymer crystallinity play important role for modulating the mass transfer inside the catalyst particle for catalyst fragmentation and subsequent polymerization kinetics. A model has been proposed and shows the catalyst fragmentation process with polymer crystallinity along polymerization time. It was proposed that the polymer of lower crystallinity offers lower mass transfer limitations and faster catalyst/polymer growth through facile fragmentation of catalyst particle.

Chapter 4

Initial morphology and kinetics development in Ziegler-Natta catalyst studied through stopped-flow ethylene/propylene and 1-hexene/propylene copolymerization

References

- [1] (a) J. Boor, *Ziegler Natta Catalyst and Polymerization*; Academic Press New York, **1979**. (b) P. J. T. Tait, I. G. Berry, *Catalyst Design for Tailor-Made Polyolefins*, Eds., K.Soga, M. Terano, Elsevier, Amsterdam, **1994**, p 55.
- [2] (a) P. Galli, P. C. Barbe, L. Noristi, *Angew. Makromol. Chem.* **1984**, 120, 73. (b) G. Cecchin, E. Marchetti, G. Baruzzi, *Macromol. Chem. Phys.* **2001**, 202, 1987.
- [3] P. Galli, G. Vecellio, *J. Polym. Chem.* **2004**, 42, 396.
- [4] M. Smit, X. Zheng, R. Brull, J. Loos, J. C. Chadwick, C. Koning, *J. Polym. Sci. Part A: Polym. Chem.* **2006**, 44, 2883.
- [5] S. Jungling, S. Koltzenburg, R. Mulhaupt, *J. Polym. Sci. Part A: Polym. Chem.* **1997**, 35, 1.
- [6] (a) V. Busico, P. Corradini, A. Ferraro, A. Proto, *Makromol. Chem.* **1986**, 187, 1125. (b) R. Spitz, R. Masson, C. Bobichon, A. Guyot, *Makromol. Chem.* **1988**, 189, 1043. (c) V. Pasquet, R. Spitz, *Makromol. Chem.* **1993**, 194, 451. (d) I. Kim, J. H. Kim, H. K. Choi, M. C. Chung, S. I. Woo, *J Appl Polym Sci.* **1993**, 48, 721. (e) N. Kashiwa, J. Yoshitake, T. Tsutsui, *Polym Bull.* **1988**, 19, 339. (f) J. C. W. Chien, T. Nozaki, *J. Polym. Sci. Part A: Polym. Chem.* **1993**, 31, 227. (g) T. Taniike, S. Takahashi, T. Wada, I. Kouzai, M. Terano, *Macromol. Res.* **2010**, 18, 834.
- [7] V. Busico, R. Cipullo, C. Polzone, G. Talarico, J. C. Chadwick, *Macromol.* **2003**, 36, 2616.

- [8] X. Zheng, M. S. Pimplapure, G. Weickert, J. Loos, *Macromol. Rapid Commun.* **2006**, 27, 15.
- [9] (a) M. T. J. Pater, G. Weickert, M. P. W. van Swaaji, *AlChE*, **2003**, 49, 180. (b) M. T. J. Pater, G. Weickert, M. P. W. van Swaaji, *J. Appl. Polym. Sci.* **2003**, 87, 1421.
- [10] X. Zheng, M. Pimplapure, G. Weickert, J. Loos, *Macromol. Rapid Commun.* **2006**, 27, 15.
- [11] (a) M. Kakugo, H. Sadatoshi, M. Yokoyama, K. Kojima, *Macromol.* **1989**, 22, 547. (b) L. Noristi, E. Marchetti, G. Baruzzi, P. Sgarzi, *J. Polym. Sci., Part A: Polym. Chem.* **1994**, 32, 3047.
- [12] K. Soga, H. Yanagihara, D. Lee, *Makromol. Chem.* **1989**, 190, 995.
- [13] G. Cecchin, E. Marchetti, G. Baruzzi, *Macromol. Chem. Phys.* **2001**, 202, 1987.
- [14] C. Przbyla, B. Tesche, G. Fink, *Macromol Rapid Commun.* **1999**, 20, 328.
- [15] A. D. Martino, J. P. Broyer, D. Schweich, C. D. Bellefon, G. Weickert, T. F. L. McKenna, *Macromol. React. Eng.* **2007**, 1, 284.
- [16] T. Keii, M. Terano, K. Kimura, K. Ishii, *Makromol. Chem. Rapid Commun.* **1987**, 8, 583.
- [17] B. Liu, H. Matsuoka, M. Terano, *Macromol. Rapid. Commun.* **2001**, 22, 1.
- [18] T. Keii, K. Soga, “*Catalytic Olefin Polymerization*”, Elsevier, Tokyo, **1989**, p. 166.
- [19] A. D. Martino, J. P. Broyer, D. Schweich, C. D. Bellefon, G. Weickert, T. F. L. McKenna, *Macromol. React. Eng.* **2007**, 1, 284.

Chapter 4

Initial morphology and kinetics development in Ziegler-Natta catalyst studied through stopped-flow ethylene/propylene and 1-hexene/propylene copolymerization

- [20] (a) M. Kaminaka, K. Soga, *Polym.* **1992**, 33, 1105. (b) M. Kaminaka, K. Soga, *Macromol. Chem. Phys. Rapid. Commun.* **1991**, 12, 367.
- [21] A. D. Martino, G. Weickert, T. F. L. Mckenna, *Macromol. React. Eng.* **2007**, 1, 165.
- [22] V. Q. Thang, T. Taniike, M. Umemori, M. Ikeya, Y. Hiraoka, N. D. Nghia, M. Terano, *Macromol. React. Eng.* **2009**, 3, 467.
- [23] T. Taniike, V. Q. Thang, N. T. Binh, Y. Hiraoka, T. Uozumi, M. Terano, *Macromol. Chem. Phys.* **2011**, 212, 723.
- [24] T. Taniike, B. T. Nguyen, S. Takahashi, V. Q. Thang, M. Ikeya, M. Terano, *J. Polym. Sci. Part A: Polym. Chem.* **2011**, 49, 4005.
- [25] T. Taniike, S. Sano, M. Ikeya, V. Q. Thang, M. Terano, *Macromol. React. Eng.* **2012**, 6, 275.
- [26] M. Terano, K. Kimura, A. Murai, M. Inoue, K. Miyoshi, *JP Patent S62-158704*, **1987**.
- [27] A. Dashti, A. Ramazani, Y. Hiraoka, S. Y. Kim, T. Taniike, M. Terano, *Polym. Int.* **2008**, 58, 40.
- [28] S. Dwivedi, T. Taniike, M. Terano, *Macromol. Chem. Phys.* **2014**, submitted.

Chapter 5

General Conclusions

This dissertation discussed the chemical and/or physical transformations occurring in Ziegler-Natta (ZN) catalyst from the view point of elucidating the origin of polymerization kinetics by stopped-flow (SF) method.

The chapter 1 includes the historical background of olefin polymerization on scientific and industrial aspects, and present understanding of ZN catalyst was introduced owing to lead the objective of this dissertation as general introduction.

In chapter 2 the chemical and physical transformations of Ziegler-Natta catalyst at initial stage of propylene polymerization kinetics was studied in the terms of elucidating the key role of alkylaluminium in catalyst activation process. An improved stopped-flow (SF) technique was employed to clarify the origin of kinetics in propylene polymerization with $\text{Mg}(\text{OEt})_2$ -based Ziegler-Natta catalyst. Polymerization in the range of 0.1-5 s exhibited kinetic transition from a linear development to a build-up-type development of the yield. It was found that a lower alkylaluminum concentration led to a lower yield in the linear regime, while the extent of the activation became greater in the build-up regime. The origin of these kinetic behaviors was studied using scanning electron microscopy (SEM) for catalyst/polymer particles and cross-fractionation analyses for polymer structures. It was found that the kinetic transition mainly arose from the fragmentation of the catalyst particles and resultant increase in the active-site concentration. The fragmentation manner strongly depended on the alkylaluminum concentration, which affected not only the amount but also the placement of initial polymer formation. The nature of active sites varied as a result of an aging effect with alkylaluminum: their stereospecificity, propagation rate constant and tolerance for chain transfer reactions increased as the polymerization

progressed.

Chapter 3 discussed the role of external donor and hydrogen at the initial stage of Ziegler-Natta propylene polymerization. The bridge between the initial constant activity region and build-up regime of the polymerization kinetics was firstly established for propylene polymerization in the presence of external donor and/or H₂ using an improved SF technique. The yield development degree in the presence of external donor was found to be lowest and attributed to the active site poisoning. With the progress of polymerization, especially in the build-up region, active sites were found to be dominantly isospecific with higher chain propagation capabilities. On the other hand, in the presence of H₂, significant chain transfer behaviour appears to be active between *ca.* 1.0 to 1.8 s of polymerization. Thereafter, the nature of active sites was nearly similar with the active sites at *ca.* 1.8 s. However, in the presence of H₂ and external donor the active sites were found to be in synergism between the active sites with the external donor and H₂ and expressed retarded polymer chain propagation.

Chapter 4 demonstrates the initial morphology and kinetics development in Ziegler-Natta catalyst studied through stopped-flow ethylene/propylene and 1-hexene/propylene copolymerization. In current study the connection between initial constant activity and macroscopic build-up type of copolymerization kinetics has been established for the first time using stopped-flow technique. The transition from linear to non-linear (build-up) yield enhancement was considered to be mainly due to fragmentation of the catalyst polymer particle. The filter effect by polymer layer was explained on the basis of polymer crystallinity. It was found that the polymer crystallinity play important role for modulating

the mass transfer inside the catalyst particle for catalyst fragmentation and subsequent polymerization kinetics. A model has been proposed and shows the catalyst fragmentation process with polymer crystallinity along polymerization time. It was proposed that the polymer of lower crystallinity offers lower mass transfer limitations and faster catalyst/polymer growth through facile fragmentation of catalyst particle.

In this dissertation the origin of macroscopic polymerization kinetics has been observed and explained in the terms of chemical and/or physical transformations in the ZN catalyst through stopped-flow polymerization.

It is widely known that industry employ prepolymerization step at mild conditions to facilitate the controlled activation of the catalyst for obtaining good polymer morphology and kinetics. However the reason for the origin of overwhelming build-up polymerization kinetics and/or morphology has been scarcely addressed in a systematic manner. In this dissertation the kind of changes occurring in the catalyst at active site level and/or catalyst/polymer particle morphological growth have been successfully discussed to find the origin of build-up type of polymerization kinetics.

This dissertation unfolds the huge potential of SF technique for deeper understanding of ZN olefin polymerization mechanism by exploiting the large-scale stopped-flow (LSF) apparatus. Prolonged SF polymerization seems to be very promising for the said purpose. The obtained results can be employed for in industry for the improvement in the design of ZN catalyst architecture and/or to optimize polymerization conditions to facilitate better activator and/or monomer diffusion inside the catalyst particle for obtaining the superior

Chapter 5
Conclusions

controlled catalyst activation. In academia, the strategy of prolonged olefin polymerization can be employed for 1) understanding the ZN mechanism from various perspectives such as initiation of polymer chain degradation etc., 2) understanding the mechanism of other heterogeneous catalysts, especially for olefin polymerization.

Achievements

Publications

1. S. Dwivedi, S. S. Gujral, T. Taniike, M. Terano, *Pure Appl. Chem.* **2013**, 85(3), 533.
2. Y. Zeng, A. Matta, S. Dwivedi, T. Taniike, M. Terano, *Macromol. React. Eng.* **2013**, 7, 668.
3. T. Taniike, S. Takahashi, T. Wada, K. Tonosaki, S. Dwivedi, M. Terano, *Macromol. Symp.* **2012**, 313, 1.
4. S. Dwivedi, T. Taniike, M. Terano, Understanding chemical and physical transformations of Ziegler-Natta catalyst at initial stage of propylene polymerization kinetics: Key role of alkylaluminium in catalyst activation process, *Macromol. Chem. Phys.* DOI 10.1002/macp.201400124.
5. S. Poonpong, S. Dwivedi, T. Taniike, M. Terano, Structure-Performance Relationship for dialkyldimethoxysilane as an external donor in stopped-flow propylene polymerization using a Ziegler-Natta catalyst, *Macromolecular Chemistry and Physics*, published, **2014**, DOI 10.1002/macp.201400157.
6. S. Dwivedi, T. Taniike, M. Terano, Role of external donor and hydrogen at the initial stage of Ziegler-Natta propylene polymerization, in preparation.
7. S. Dwivedi, T. Taniike, M. Terano, Initial morphology and kinetics development in Ziegler-Natta catalyst studied through stopped-flow ethylene/propylene and 1-hexene/propylene copolymerization, in preparation.

Achievements

Conferences

8. S. Dwivedi, T. Taniike, M. Terano, Synthesis of Phillips catalyst by chemical modification of support to control the catalyst activity and branching in polyethylene, 8th *International Ziegler-Natta Colloquium 2012* March 27-30, Kanazawa, Japan.
9. S. Dwivedi, T. Taniike, M. Terano, Chemical modification of silica support to improve the branching ability of Phillips catalyst, *Polym. Soc. Jpn.* **2012** May 29-31, Yokohama, Japan.
10. S. Dwivedi, T. Taniike, M. Terano, Effects of alkyl-Al on the active site nature of heterogeneous Ziegler-Natta catalyst studied by stopped-flow propylene polymerization, *Polym. Soc. Jpn.* **2012** September 19-21, Nagoya, Japan
11. S. Dwivedi, T. Taniike, M. Terano, Physical and chemical transformations of active sites in heterogeneous Ziegler-Natta catalyst during initial stage of propylene polymerization, *International Conference on the Reaction Engineering of Polyolefins (INCOREP) 2013* September 2-5, Ferrara, Italy.
12. S. Dwivedi, T. Taniike, M. Terano, Activity enhancement mechanism of heterogeneous Ziegler-Natta catalyst studied by large-scale stopped-flow propylene polymerization, *International Symposium on Advanced Materials, JAIST 2013* October 17-18, Ishikawa, Japan.

Achievements

Acknowledgements

It is a pleasure to convey my gratitude to all who contributed to the successful completion of the minor research project in my humble acknowledgment.

I would like to convey my deepest gratitude to my supervisor, Professor Minoru Terano, for this opportunity, his constant guidance, motivation and straight involvement in this the research project. The studies would never been performed without the great help of Professor Dr. Minoru Terano. I would like to thank Associate Professor Toshiaki Taniike for his crucial constructive comments at various stages of this research.

I am grateful to Professor Dr. Masayuki Yamaguchi, Professor Dr. Kohei Nitta and Associate Professor Dr. Tatsuo Kaneko for his positive comments during reviewing the dissertation and valuable suggestions. I would like to express my sincere gratitude to Professor Kohki Ebitani, minor research supervisor, for providing support in this research in various ways.

I would like to record my gratefulness to Dr. Phairat Phiriyawirut, Dr. Sumate Charoenchaidet and Dr. Supanan Patthamasang for the supervision, advice, and guidance from the very early stage of the minor research project as well as giving me extraordinary experiences throughout the work in the field of polyolefins through the well equipped laboratory at the SCG Chemicals, Thailand.

I pay sincere gratitude to all the members of Terano laboratory for their kind assistance at the various stages of this research. I pay my heartiest thanks to all the persons who were important to the successful realization of this project work.

Acknowledgements

I am grateful to Japan Advanced Institute of Science and Technology for their financial support. I want to acknowledge Sumitomo Chemical Co., Japan Polypropylene Co., and Tosoh FineChem Co. for their great support in this research work.

Finally I am grateful to my parents for their great support and blessings during this work.

Sumant Dwivedi

Terano Laboratory
School of Materials Science,
Japan Advanced Institute of Science and Technology
Ishikawa, Japan

Effect of External Electron Donors on Microstructure of Hetero Phase

Poly(ethylene-*co*-propylene) prepared using MgCl₂-supported Ziegler-Natta catalysts

1 Introduction

In Ziegler-Natta (ZN) olefin polymerization desired polymer characteristics can be achieved by modifying the supported titanium catalyst systems used for the polymerization with structurally different external donor added during the polymerization. Since the structure of alkylaluminium is changed upon being complexed with alkoxy silane.^[1] Therefore, the nature of the external donor influences the microstructure structure of the formed polymer.^[2] The objective of this research is to systematically investigate the effect of individual and mixed silane-based external donor on the microstructure distribution in heterophasic ethylene-propylene copolymer prepared by sequential polymerization.

2 Experimental

Commercial 4th generation ZN catalyst containing di-*n*-butyl phthalate (DBP) was employed. Propylene and ethylene were used as monomers, H₂ was used as chain transfer agent, triethyl aluminium was used as cocatalyst. Dicyclopentyl dimethoxysilane (DCPDMS, D-donor), Cyclohexylmethyl dimethoxysilane (CHMDMS, C-donor), Tetra ethoxysilane (TEOS, T-donor), Diethylamino-trimethoxysilane (U-donor) were employed as alkoxy silane based external donors. The D-donor was mixed with the T-donor at four concentrations (mol/mol), *ca.* D-donor 90 % and 10 % T-donor (D10T) and similarly D7.5T, D5T and D2.5T were prepared.

A series of homo- and sequential polymerizations were performed. Firstly propylene bulk polymerization was performed (catalyst = *ca.* 10 mg, Al/Si = 4 and H₂ was varied either 10 bar or 30 bar) at 70 °C and 30 bar for 1 h followed by ethylene/propylene gas phase copolymerization at 70 °C, 12 bar for 30 min to obtain impact copolymer.

The molecular weight of homopolymer was determined gel permeation chromatography. The chain microstructure and isotacticity was determined by ¹³C-nuclear magnetic resonance (NMR) operated at 100 MHz using Bruker 400 MHz NMR spectrometer.

3 Results and discussion

A series of polymerizations were conducted with various individual silane-based external donors. It was found that T donor expressed lowest activity which can be considered as an effect due to the active site poisoning with the Lewis basic free alkoxy groups. The performance of C and D donor was found to be nearly similar. The performance by U-donor was found to be most superior. The trend for activity was kept at both the H₂ concentration.

In the case of mixed electron donors it was observed that the trend for the catalyst activity is different with variation in the H₂ concentration. At lower H₂ concentration trend for catalyst productivity was similar with the individual donor. On the contrary at the higher hydrogen concentration the phenomenon is quite complex. An increment in the catalyst activity has been observed by increasing the T-donor content up to D7.5T and thereafter it decreases. It shows that mixed donors shows quite complex behavior as compared to the performance of individual donors at two hydrogen concentration. The

hydrogen response can be clearly observed with the increment of hydrogen concentration in polymerization with the various donors. The molecular weight distribution of the polymers obtained from the mixed donors were found to be broadened as expected due to the formation of larger heterogeneity in the catalytic active sites.

The average ethylene content was found to be in the around 10-15 % in the impact copolymer. The rubber content was nearly same (*ca.* 30 wt%) among all impact copolymers. Diad and triad sequences were measured for all impact copolymers. Correlation for the microstructure sequence distribution between individual and mixed donors was absent.

4 Conclusions

The impact copolymerization successfully carried out in the sequential polymerization process by using variety of external donors. The catalytic performance of mixed donors was found to be synergistic. It has been observed that mixed donors offer precise tuning of polymer properties, while the behavior of mixed donor was not obvious to exist between the two extreme polymer properties by individual donors. The mechanistic details are highly complex to be determined with the given set of data.

References

- [1] J. Koivumaki, J. V. Seppala, L. Kutti, *Polym. Bull.* **1992**, 29, 185.
- [2] M.C. Sacchi, Z. Q. Fan, F. Forlini, I. Tritto, P. Locatelli, *Macromol. Chem. Phys.* **1994**, 195, 2805.

Supporting information

Table 1 Homopolymerization results

Donor	H ₂ ^{homo} (bar)	Activity (Kg-polymer/g-cat/h)	M _n	M _w /M _n	
C	10	13.54	6.9	7.5	
D		12.80	17.2	6.8	
U		16.22	5.6	9.5	
T		5.13	5.7	12.1	
D2.5T		16.35	10.9	10.2	
D5T		13.43	6.0	11.2	
D7.5T		11.21	8.5	9.7	
D10T		9.58	6.3	9.8	
C		30	19.80	6.4	7.7
D			18.83	17.3	6.3
U	22.38		4.6	7.8	
T	12.00		2.3	6.6	
D2.5T	20.00		6.1	11.1	
D5T	21.64		4.0	9.4	
D7.5T	29.38		6.5	11.0	
D10T	21.00		5.9	9.0	

M_n and M_w/M_n has been determined by GPC.

Table 2 Impact copolymerization results

Set	Donor	^a H ₂ ^{homo} (bar)	Activity (Kg-polymer/g-cat/h)	^b PER	^c PER-C2
I	C	10	15.06	8.68	40.76
	D		14.90	23.91	46.72
	U		20.71	28.70	37.05
	T		6.76	10.02	40.78
	D2.5T		20.73	23.39	42.77
	D5T		15.00	11.73	32.29
	D7.5T		12.56	20.56	35.06
	D10T		10.57	11.95	28.83
II	C	30	21.95	9.38	34.48
	D		20.60	22.90	38.71
	U		28.00	24.34	44.89
	T		16.36	13.86	38.96
	D2.5T		22.12	6.38	25.19
	D5T		26.56	22.21	46.56
	D7.5T		34.00	14.47	42.88
	D10T		24.44	9.75	25.71

^a represents amount of hydrogen added during propylene bulk polymerization,

^b represents total amount of rubber content in the impact copolymer,

^c represents amount of ethylene in rubber content.

Table 3 ICP (Set I) chain microstructure distribution determined by ^{13}C NMR

	(P)	(E)	PP	PP*	PE	EE	PEP	PEE	EEE	PPP	PPE	EPE
C	0.952	0.048	0.940	0.003	0.044	0.013	0.072	0.013	0.015	0.129	0.257	0.514
D	0.928	0.072	0.877	0.006	0.062	0.056	0.072	0.070	0.078	0.255	0.175	0.350
U	0.884	0.116	0.774	0.015	0.198	0.013	0.061	0.015	0.004	0.158	0.254	0.508
T	0.964	0.036	0.954	0.003	0.035	0.008	0.079	0.010	0.014	0.278	0.206	0.413
D2T	0.767	0.233	0.602	0.017	0.225	0.156	0.075	0.024	0.175	0.220	0.169	0.337
D5T	0.916	0.084	0.861	0.002	0.094	0.043	0.065	0.031	0.037	0.155	0.237	0.475
D7T	0.898	0.102	0.837	0.006	0.123	0.034	0.109	0.045	0.016	0.218	0.204	0.408
D10T	0.892	0.108	0.853	0.007	0.102	0.038	0.148	0.061	0.021	0.142	0.209	0.418
	P₁	P₂	P₃	E₁	E₂	E₃	x₁	x₂	x₃	x₄	x₅	x₆
C	0.514	0.025	0.461	0.222	0.144	0.634	0.919	0.005	0.042	0.020	0.014	0.003
D	0.350	0.025	0.625	0.126	0.022	0.852	0.915	0.012	0.037	0.033	0.003	0.013
U	0.508	0.059	0.433	0.150	0.027	0.823	0.805	0.032	0.073	0.084	0.006	0.001
T	0.413	0.015	0.572	0.230	0.099	0.671	0.940	0.006	0.033	0.014	0.007	0.002
D2T	0.337	0.079	0.584	0.071	0.004	0.926	0.740	0.042	0.077	0.139	0.002	0.060
D5T	0.475	0.040	0.485	0.161	0.038	0.801	0.891	0.003	0.055	0.044	0.007	0.010
D7T	0.408	0.042	0.550	0.235	0.037	0.728	0.845	0.013	0.097	0.037	0.008	0.005
D10T	0.418	0.045	0.536	0.243	0.038	0.719	0.817	0.013	0.103	0.059	0.008	0.005

P and E represent propylene and ethylene. (P) and (E) has been designated for the propylene and ethylene content respectively. PP, EE and PE represent diads distribution. PP* used to represent the propylene inversion (head to tail-tail to head). E_i or P_i (i=1 to 3) represents the distribution of uninterrupted *i* monomers of E and P units. The distribution of uninterrupted *i* methylene units are designated as x_i (i=1 to 6).

Table 4 ICP (Set II) chain microstructure distribution determined by ^{13}C NMR

	(P)	(E)	PP	PP*	PE	EE	PEP	PEE	EEE	PPP	PPE	EPE
C	0.952	0.048	0.904	0.003	0.081	0.011	0.020	0.009	0.008	0.075	0.296	0.592
D	0.920	0.080	0.833	0.005	0.148	0.014	0.027	0.008	0.011	0.120	0.278	0.556
U	0.905	0.095	0.790	0.008	0.179	0.023	0.026	0.020	0.006	0.069	0.293	0.586
T	0.928	0.072	0.879	0.008	0.090	0.023	0.057	0.018	0.023	0.136	0.255	0.510
D2T	0.939	0.061	0.919	0.005	0.048	0.028	0.095	0.038	0.030	0.087	0.250	0.500
D5T	0.919	0.081	0.849	0.004	0.125	0.022	0.053	0.031	0.006	0.094	0.272	0.543
D7T	0.908	0.092	0.811	0.007	0.157	0.025	0.035	0.023	0.008	0.069	0.288	0.577
D10T	0.945	0.055	0.909	0.003	0.069	0.018	0.042	0.016	0.009	0.053	0.293	0.586
	P₁	P₂	P₃	E₁	E₂	E₃	x₁	x₂	x₃	x₄	x₅	x₆
C	0.592	0.029	0.379	0.099	0.055	0.846	0.926	0.006	0.019	0.044	0.005	0.002
D	0.556	0.045	0.399	0.080	0.014	0.906	0.876	0.010	0.027	0.084	0.002	0.004
U	0.586	0.056	0.359	0.101	0.013	0.885	0.856	0.018	0.041	0.082	0.003	0.003
T	0.510	0.037	0.453	0.140	0.106	0.754	0.884	0.015	0.041	0.045	0.016	0.006
D2T	0.500	0.030	0.470	0.219	0.079	0.703	0.903	0.009	0.053	0.025	0.009	0.006
D5T	0.543	0.044	0.413	0.166	0.015	0.819	0.870	0.008	0.055	0.065	0.002	0.002
D7T	0.577	0.053	0.370	0.121	0.031	0.848	0.857	0.015	0.046	0.075	0.006	0.004
D10T	0.586	0.032	0.381	0.202	0.024	0.774	0.917	0.007	0.045	0.028	0.003	0.003

P and E represent propylene and ethylene. (P) and (E) has been designated for the propylene and ethylene content respectively. PP, EE and PE represent diads distribution. PP* used to represent the propylene inversion (head to tail-tail to head). E_i or P_i (i=1 to 3) represents the distribution of uninterrupted *i* monomers of E and P units. The distribution of uninterrupted *i* methylene units are designated as x_i (i=1 to 6).